Title
THE THEORY OF NUCLEAR MAGNETIC RESONANCE DETECTED BY NUCLEAR RADIATIONS

Authors
Matthias, E.
Olsen, B.
Shirley, D.A.
et al.

Publication Date
1971

Submitted to Physical Review

UCRL-18413
Preprint

THE THEORY OF NUCLEAR MAGNETIC RESONANCE DETECTED BY NUCLEAR RADIATIONS

E. Matthias, B. Olsen, D. A. Shirley,
J. E. Templeton and R. M. Steffen

January 1971

AEC Contract No. W-7405-eng-48

LAWRENCE RADIATION LABORATORY
UNIVERSITY of CALIFORNIA BERKELEY

UCRL-18413

DISCLAIMER

UCRL-18413

THE THEORY OF NUCLEAR MAGNETIC RESONANCE DETECTED BY NUCLEAR RADIATIONS

E. Matthias, B. Olsen, D. A. Shirley, and J. E. Templeton

Lawrence Radiation Laboratory
University of California
Berkeley, California 94720

and

R. M. Steffen

Department of Physics
Purdue University
Lafayette, Indiana 47907

THE THEORY OF NUCLEAR MAGNETIC RESONANCE DETECTED BY NUCLEAR RADIATIONS*

E. Matthias†, B. Olsen††, D. A. Shirley, and J. E. Templeton‡

Lawrence Radiation Laboratory
University of California
Berkeley, California 94720

and

R. M. Steffen

Department of Physics
Purdue University
Lafayette, Indiana 47907

January 1971

ABSTRACT

A comprehensive theoretical description is given for the effects of magnetic resonance on the angular distribution of radiation emitted from oriented nuclear states. The formulation is made in a general way. It may be applied to an ensemble of nuclei oriented by any method: for example, nuclear reactions, angular correlations, and low-temperature nuclear orientation may be treated.

---

*Work performed under the auspices of the U. S. Atomic Energy Commission.

†Present Address: I. Physikalisches Institut, Freie Universität Berlin, Boltzmannstrasse 20, 1 Berlin 33, West Germany.

††Present Address: Institute of Physics, University of Uppsala, Thunbergsvägen 7, Uppsala 12, Sweden.

‡Present Address: Oxford Instrument Corporation, 100 Cathedral Street, Annapolis, Maryland, U. S. A. 21401.

In fact the theory can also be applied to optical double resonance experiments. Statistical tensors are defined to describe nuclear orientation in the "resonant" state. Interactions of the oriented ensemble with extranuclear fields are then considered, and the effect of a radio-frequency (rf) field on the angular distribution of radiation is given.

Two formulations are given for the "pure magnetic" case, for which numerical calculations were done. One employs angular correlation formalism, following the evolution of the density matrix in the laboratory frame S, while the other is more closely related to conventional NMR. In the latter approach the transformation into the frame S''', wherein the statistical tensors are time-invariant, is described in terms of a "Generalized Torque Equation" governing the motion of a unit vector along the symmetry axis in S'''. Both formulations are exact.

Time-dependent distribution functions are worked out in detail, both with fixed and random phase angle between the rf field and the initial symmetry direction. Fast oscillations due to the constant magnetic field are modulated by slow oscillations due to the rf field. Time-integral curves were calculated. These show great sensitivity to the rank of the relevant statistical tensor, to geometry, and to the phase of the rf field. Multipole structure is predicted for certain geometries, with the resonance line showing a number of maxima equal to the rank of the statistical tensor. Under certain conditions two types of asymmetry are observable. A "transient" asymmetry appears for low rf field values: this symmetry is sensitive to the sign of the nuclear moment, but it disappears in high rf fields. Odd-rank statistical tensors can also give response functions with "persistent" asymmetry that remains at high rf fields. This is a parity effect and is not sensitive to the sign of the nuclear moment. Effects of relaxation are also discussed briefly.

I. INTRODUCTION

Recent progress[1-7] in nuclear radiation detection of NMR (NMR/RD) has stimulated us to develop a theoretical description of this method, which is presented here. We have two principal aims: (1) to provide a description that is sufficiently exact and complete as to be immediately useful to anyone planning experiments in this area, and (2) to give a unified description that stresses the essential similarities in the various experimental techniques that may be combined with NMR. The three such techniques that we shall consider are nuclear orientation, perturbed angular correlations, and angular distributions following nuclear reactions. We denote the combinations of these with NMR as NMR/ON, NMR/PAC, and NMR/NR, respectively. Experiments of these types have typical double resonance character, with the "effect" being observed by the spatial multipole intensity pattern of the nuclear transition rather than by its energy absorption. For all experiments of this type it is desirable to achieve a sizeable degree of polarization or alignment of the nuclear state such that it exhibits a non-isotropic radiation pattern of the general form

$$W(\Theta) = \sum_{\lambda} B_{\lambda} G_{\lambda} A_{\lambda} P_{\lambda} (\cos \Theta) \quad .$$

Here, B_{λ} is the orientation parameter, G_{λ} is the perturbation factor, and A_{λ} is a parameter that depends only on the nuclear transition. The three methods mentioned above each apply to a certain lifetime range:

1. NMR/PAC will involve states with 10^{-8} sec $< T_{1/2} < 10^{-5}$ sec;
2. NMR/NR applies to isomeric states in the range 10^{-8} sec $< T_{1/2} <$ minutes;

3. NMR/ON requires $T_{1/2} \geq$ hours, except for reorientation in intermediate states with $T_{1/2} \geq T_1$, where T_1 is the nuclear spin lattice relaxation time.

The origins of the NMR/RD field are diverse: this fact has probably delayed its development. Indeed, the basic knowledge and technology for experiments of the types cited above were available in 1960 or earlier: they only awaited being put together. In 1952 Deutsch and Brown[8] used annihilation radiation to detect NMR in positronium. Already in 1951 Brossel and Bitter[9] had calculated NMR lineshapes for optical double-resonance lines, in which atomic excited states were oriented by optical pumping and resonance absorption was detected by depolarization of de-exciting dipole radiation. Guichon, Blamont, and Brossel[10] reported the effect in atomic mercury in 1956. These experiments are very similar to the NMR/RD methods, and it can be shown that our theoretical description is sufficiently general to include the optical double resonance work.

Two papers appeared in 1953 in which Bloembergen and Temmer suggested NMR/ON[11] and Abragam and Pound suggested NMR/PAC.[12] Neither of these suggestions was quite specific enough to lead directly to a successful experiment,[13] but they laid the theoretical groundwork for the two methods. Between 1953 and 1966 several very interesting experiments were reported[14-20] in the general area of NMR/RD. Unfortunately, they all depended on rather special properties (such as beta asymmetry, gaseous samples, special lattices, etc.), and in any case none of them was very close to the 1953 proposals. Thus the applicability of NMR/RD was rather limited.

With the success of recent experiments on both solutes in host metal lattices and free atoms,[1-7] the scope of NMR/RD has become much broader. The NMR/PAC, NMR/ON, and NMR/NR methods have all been shown to work. An impressive number of resonances have already been observed.[21-26] Although several discussions have appeared in which theoretical aspects of NMR/RD were treated,[27-30] it is clear that the growth of the field calls for a more general and thorough treatment, as given below. In particular, the following points will be carefully considered: lineshape, power dependence, rf-phase, favorable geometries, and time-differential effects.

Before considering the theory of NMR/RD, it is useful to consider its range of application, and particularly to define the limits of its applicability. NMR/RD and conventional NMR are complementary rather than competitive. In fact it is inconceivable with present technology to do both conventional NMR and NMR/RD on the same nuclear state. It appears that NMR/RD alone is applicable to most nuclear states of lifetime less than years. At the other end of the stability spectrum the NMR/RD methods might be able to produce observable effects for states having lifetimes down to 10^{-9} sec or perhaps even shorter. It would, however, be pointless to study such very short-lived states (i.e., $\tau \leq 10^{-8}$ sec) by NMR/RD, because the natural linewidths would preclude measurements of higher accuracy than that obtainable with time-integral PAC. For slightly longer-lived states, in the $\tau \gtrsim 10^{-8}$ sec range, time-differential PAC becomes applicable. Using, for example, the stroboscopic observation technique,[31] time-differential PAC can be made not only as accurate as NMR/PAC, but actually a little better. This advantage arises because the stroboscopic method yields the Fourier transform of the time spectrum, which is essentially equivalent to an NMR line, but with

no rf broadening. To do NMR/PAC efficiently on the same state would require, as we show later, a radiofrequency field of sufficient intensity to increase the linewidth by about a factor of two. Therefore NMR/RD offers no a priori advantage of accuracy for states in the 10^{-3} to 10^{-8} sec range. It may, however, be applied to cases in which the resonant frequency is so high as to preclude fast timing, as for ^{100}RhFe.[21] In any event NMR/RD is unlikely to be of much value for states of lifetime $\tau < 10^{-8}$ sec because of natural line-width, or for states with $\tau > 10^{6}$ years for intensity reasons. For nuclear states in the range (10^{-8} sec) $< \tau <$ (years), NMR/RD combines the advantages of NMR with the extremely high sensitivity of single-quantum detection. In comparison with conventional NMR, NMR/RD has much higher sensitivity.

The essential equivalence of the three NMR/RD methods is established and discussed in Sec. II, and the density matrix formalism is introduced. General equations for perturbation of an angular distribution by an rf field are derived in Sec. III. In Sec. IV the "pure" magnetic resonance case is treated by another geometrical approach more familiar in the NMR field. Section V presents a discussion of several properties of the perturbation factor. In Sec. VI the resonance behavior for specific geometries is discussed. In Sec. VII the influence of relaxation is treated briefly.

II. PERTURBATION OF ORIENTED STATES

II.1. Description of Oriented States

An ensemble of oriented nuclei may be prepared in several ways. The absorption or emission of unpolarized radiation in a direction $\underset{\sim}{k}_1$ by a randomly oriented ensemble (ordinary source or target) produces an oriented ensemble of nuclei which is axially symmetric about $\underset{\sim}{k}_1$. Orientation of nuclei can also be achieved through the interaction of external fields with either the (static) magnetic dipole moment or the (static) electric quadrupole moments at low temperatures. Dynamic microwave or optical methods of nuclear orientation, which depend on the emission and absorption of radiation in the electronic environment of the nuclei, can also be used.

It is assumed here that the oriented ensemble of nuclei possesses an axis of cylindrical symmetry, which we shall denote by the unit vector $\underset{\sim}{k}_1$. The state of the oriented ensemble at the time of formation $t = 0$ will be represented by the density matrix $\rho(0)_{\underset{\sim}{z}}$ with matrix elements $\langle Im'|\rho(0)|Im\rangle$ in the representation $|Im\rangle$, where I is the angular momentum quantum number of the individual nuclear states and m and m' are eigenvalues of I_z with respect to the quantization axis $\underset{\sim}{z}$. If $\underset{\sim}{z}$ is parallel to the symmetry axis $\underset{\sim}{k}_1$, the density matrix is diagonal in the $|Im\rangle$ representation at $t = 0$.

It is convenient to expand the density matrix $\rho(0)_{\underset{\sim}{z}}$ in terms of irreducible spherical tensors $\rho^{\lambda}_{q}(0)_{\underset{\sim}{z}}$ of rank λ, the so-called "statistical tensors".[32] The statistical tensors are defined by

$$\rho^{\lambda}_{q}(0)_{\underset{\sim}{z}} = \sum_{m} (-1)^{I+m'} \langle I-m'Im|\lambda q\rangle \langle Im'|\rho(0)|Im\rangle \qquad (1)$$

Using the orthogonality relation of the Clebsch-Gordan coefficients $\langle I-m'Im|\lambda q\rangle$ this definition leads to the multipole expansion of $\rho(0)_{\underset{\sim}{z}}$:

$$\langle Im'|\rho(0)|Im\rangle = \sum_{\lambda} (-1)^{I+m'} \langle I-m'Im|\lambda q\rangle \rho_q^{\lambda}(0)_{\underset{\sim}{z}} \quad . \tag{2}$$

The tensors $\rho_q^{\lambda}(0)_{\underset{\sim}{z}}$ are hermitian in the sense that

$$\rho_q^{\lambda}(0)^*_{\underset{\sim}{z}} = (-1)^q \rho_{-q}^{\lambda}(0)_{\underset{\sim}{z}} \quad . \tag{3}$$

Under a rotation R of the quantization coordinate system by the Euler angles α, β, γ which carries the z axis into a new z' axis, $\underset{\sim}{z} \rightarrow \underset{\sim}{z}'$, the statistical tensors transform according to the irreducible representation $D^{(\lambda)}_{qq'}(\underset{\sim}{z} \rightarrow \underset{\sim}{z}')$ of the three-dimensional rotation group R^{33}:

$$\rho_{q'}^{\lambda}(0)_{\underset{\sim}{z}'} = \sum_{q} \rho_q^{\lambda}(0)_{\underset{\sim}{z}} \cdot D^{\lambda}_{qq'}(\underset{\sim}{z} \rightarrow \underset{\sim}{z}') \quad , \tag{4}$$

where the indices $\underset{\sim}{z}$ and $\underset{\sim}{z}'$ represent the quantization coordinate systems. If the symmetry axis $\underset{\sim}{k}_1$ is chosen as the quantization axis, $\rho_q^{\lambda}(0)_{\underset{\sim}{k}_1}$ is invariant under a rotation about $\underset{\sim}{k}_1$, i.e. under the transformation $D^{\lambda}_{qq'}(\alpha,0,0) = \delta_{qq'} e^{-iq\alpha}$. Hence, in this representation we have after the transformation

$$\rho_{q'}^{\lambda}(0)_{\underset{\sim}{k}_1} = \rho_0^{\lambda}(0)_{\underset{\sim}{k}_1} \delta_{0q'} \quad , \tag{5}$$

and the orientation of the ensemble of nuclei of spin I is completely described by the $2I$ parameters $\rho_0^{\lambda}(0)_{\underset{\sim}{k}_1}$. Even values of λ mean alignment of the nuclear ensemble. The $\rho_0^{\lambda}(0)_{\underset{\sim}{k}_1}$ are identical (except for a trivial factor) to the

orientation parameters $B_\lambda(I)$ which are employed in the theory of nuclear orientation.[34,35] Different sign conventions are used in nuclear orientation theory. We shall adopt the relation

$$B_\lambda(I) = (2I + 1)^{1/2} \rho_{0}^{\lambda}(0)_{\underset{\sim}{k}_1} \quad , \tag{6a}$$

or

$$B_\lambda(I) = (2I + 1)^{1/2} \sum_m (-1)^{I+m} \langle I-m\ Im | \lambda 0 \rangle\ P(m) \quad . \tag{6b}$$

Here P(m) is just ρ_{mm}, a diagonal element of the density matrix. The orientation parameters are normalized such that

$$B_0(I) = 1 \quad \text{if} \quad \sum_m P(m) = 1 \quad .$$

The orientation parameters can be computed from Eqs. (6) if the populations P(m) of the axially symmetric m - substates are known from the method of orientation (e.g. low temperature orientation, Coulomb excitation, nuclear reactions, etc.).

For an ensemble that is oriented by observing, in the direction $\underset{\sim}{k}_1 = \underset{\sim}{z}$, a preceding (unpolarized) nuclear radiation X emitted from a (random) state I_0, the orientation parameters are similar (but not identical) to the directional distribution parameters $A_\lambda(X)$ as defined in directional correlation problems.[36] Consider a state of spin I oriented by the observation of a preceding gamma radiation of multipole components (π,L) (π = E (electric) or π = M (magnetic)) emitted in the decay $I_0 \rightarrow I$. The orientation parameters are given in terms of reduced <u>emission</u> matrix elements $\langle I \| \underset{\sim}{j}_N\ \underset{\sim}{A}_L^{(\pi)} \| I_0 \rangle$,

$$B_\lambda(I) = \frac{\sum_{L\pi L'\pi'} (-1)^{L+L'+\lambda} F_\lambda(LL'I_0I) \langle I\| j_{N\sim L}^{A(\pi)} \| I_0 \rangle \langle I\| j_{N\sim L'}^{A(\pi')} \| I_0 \rangle^*}{\sum_{L,\pi} |\langle I\| j_{N\sim L}^{A(\pi)} \| I_0 \rangle|^2} , \quad (7a)$$

where $F_\lambda(LL'I_0I)$ are the F-coefficients as defined e.g. in reference 36. For a pure multipole gamma radiation (πL) the $B_\lambda(I)$ are simply

$$B_\lambda(I) = (-1)^\lambda F_\lambda(LLI_0I) \quad . \quad (7b)$$

The quantization (symmetry) axis for the $B_\lambda(I)$ is of course, the observation direction $\underset{\sim}{k}_1$.

The orientation parameters of a state I that is oriented by the observation of radiation X other than gamma radiation is given by

$$B_\lambda(I) = \frac{(-1)^\lambda \sum_{L,L'} (-1)^{L+L'} b_\lambda(LL';X) F_\lambda(LL'I_0I) \langle I\| XL\| I_0 \rangle \langle I\| XL'\| I_0 \rangle^*}{\sum_{L} b_0(LL;X) |\langle I\| XL\| I_0 \rangle|^2} , \quad (8)$$

where the $b_\lambda(LL',X_1)$ and $\langle I\| XL\| I_0 \rangle$ are the particle parameters and the reduced matrix elements, respectively, for the emission of the particle X with multipolarity L and L'. The particle parameters for β-transitions usually include the reduced matrix elements and the factor $(-1)^{\lambda+L+L'}$.[36]

In nuclear orientation experiments the parent nucleus, a long-lived isotope, is oriented, and the $B_\lambda(I)$ may be calculated from knowledge of the ambient temperature and the Hamiltonian describing the interaction of the nuclear moments with extranuclear fields.

Nuclear reactions produce an ensemble of nuclei oriented relative to the beam direction. The orientation is axially symmetric if the incoming particles are unpolarized and if the outgoing particles are observed at 180° or not at all. The $B_\lambda(I)$ parameters thus depend upon the detailed reaction mechanisms. Often the assumption is made that the population distribution in magnetic substates is Gaussian, with maximum population in the substate(s) that have minimum spin projection in the beam direction.

II.2. General Description of the Perturbation of an Oriented State

The central problem in calculating the influence of an extranuclear perturbation on angular distributions or correlations is the computation of the time-evolution of the density matrix $\rho(t)$ from a given initial state $\rho(0)$ for a specific perturbation Hamiltonian $\mathcal{H}$:

$$\rho(0) \xrightarrow{\mathcal{H}} \rho(t) \quad .$$

The time-evolution of a density operator is given by the von Neumann equation[32]

$$i\hbar\,\dot{\rho} = [\mathcal{H}, \rho] = \mathcal{H}\rho - \rho\mathcal{H} \quad . \tag{9}$$

The operators ρ and $\mathcal{H}$ must be defined in the same reference frame.

Solutions of Eq. (9) are found by introducing the time-evolution operator $\Lambda(t)$, which represents a time-dependent unitary transformation of the density matrix ρ:

$$\rho(t) = \Lambda(t)\,\rho(0)\,\Lambda(t)^\dagger \quad . \tag{10}$$

can be derived. A comparison with Eqs. (3) and (16) shows that the $G^{q\bar{q}}_{\lambda\bar{\lambda}}(t)$ are actually the expansion coefficients of the hermitian adjoint statistical tensors $\rho^{\lambda\ \dagger}_{q}$.

An ensemble of nuclei formed at the time t = 0 with a symmetry axis $\underset{\sim}{k}_1$ changes under an extranuclear perturbation into an ensemble that is given at time t by the statistical tensor

$$\rho^{\bar{\lambda}}_{\bar{q}}(t)_{\underset{\sim}{z}} = \sum_{\lambda,q} G^{q\bar{q}}_{\lambda\bar{\lambda}}(t)^{*}_{\underset{\sim}{z}} \cdot \rho^{\lambda}_{0}(0)_{\underset{\sim}{k}_1} \cdot D^{(\lambda)}_{0q}(\underset{\sim}{k}_1 \longrightarrow \underset{\sim}{z}) \quad , \tag{19}$$

where Eqs. (4), (5), and (16) have been used. For the representation axis $\underset{\sim}{z}$ of $\rho^{\bar{\lambda}}_{\bar{q}}(t)_{\underset{\sim}{z}}$ and $G^{q\bar{q}}_{\lambda\bar{\lambda}}(t)^{*}_{\underset{\sim}{z}}$ a symmetry axis of the perturbing interaction can be chosen in order to have a particularly simple form of the attenuation coefficient (Eq. (17)). If the statistical tensor $\rho^{\bar{\lambda}}_{\bar{q}}(t)$ that describes the perturbed ensemble is to be represented in the original $\underset{\sim}{k}_1$ representation, one has

$$\begin{aligned} \rho^{\bar{\lambda}}_{\bar{q}}(t)^{*}_{\underset{\sim}{k}_1} &= \sum_{\bar{q}'} \rho^{\bar{\lambda}}_{\bar{q}'}(t)^{*}_{\underset{\sim}{z}} D^{(\bar{\lambda})^{*}}_{\bar{q}'\bar{q}}(\underset{\sim}{z} \longrightarrow \underset{\sim}{k}_1) \\ &= \sum_{q\bar{q}'\lambda} \rho^{\lambda}_{0}(0)^{*}_{\underset{\sim}{k}_1} D^{(\lambda)^{*}}_{0q}(\underset{\sim}{k}_1 \longrightarrow \underset{\sim}{z}) G^{q\bar{q}'}_{\lambda\bar{\lambda}}(t)_{\underset{\sim}{z}} D^{(\bar{\lambda})^{*}}_{\bar{q}'\bar{q}}(\underset{\sim}{z} \longrightarrow \underset{\sim}{k}_1) \ . \end{aligned} \tag{20}$$

II.3. Perturbation by a Static Magnetic Field

The Hamiltonian that describes the interaction of a static magnetic field $\underset{\sim}{H}_0$ with the magnetic moment $\underset{\sim}{\mu} = g\ \underset{\sim}{I}\ \frac{\mu_N}{\hbar}$ of a nuclear state has the form

$$\mathcal{H} = - \underset{\sim}{\mu} \cdot \underset{\sim}{H}_0 \quad . \tag{21}$$

It is diagonal if the direction of $\underset{\sim}{H}_0$ is chosen as quantization axis $\underset{\sim}{z}$, i.e. $\underset{\sim}{H}_0 = H_0 \underset{\sim}{e}_z$, where $\underset{\sim}{e}_z$ is a unit vector. Thus

$$\langle Im' | \mathcal{H} | Im \rangle = -H_0 \langle Im' | \mu_z | Im \rangle = -H_0 (-1)^{I-m'} \begin{pmatrix} I & 1 & I \\ -m' & 0 & m \end{pmatrix} \langle I \| \mu \| I \rangle$$

$$= -H_0 \frac{m}{[(2I+1)(I+1)I]^{1/2}} \langle I \| \mu \| I \rangle \delta_{mm'} \quad , \tag{22}$$

where the Wigner-Eckart theorem and the explicit expression for the 3-j symbol have been used. With the conventional definition of the magnetic moment

$$\mu = \langle I\ I | \mu_z | I\ I \rangle = \frac{I}{[(2I+1)(I+1)I]^{1/2}} \langle I \| \mu \| I \rangle \quad , \tag{23}$$

the energy eigenvalues are given by the well-known expression

$$E_m = \langle Im | \mathcal{H} | Im \rangle = -H_0 \mu \frac{m}{I} = -g \mu_N H_0 m = \omega_0 \hbar m \quad , \tag{24}$$

where g is the g-factor of the nuclear state and μ_N is the nuclear magneton. In this equation we have introduced the Larmor frequency

$$\omega_0 = -g H_0 \mu_N / \hbar \quad . \tag{25}$$

In the $\{Im\}$ representation, i.e. $\underset{\sim}{H}_0 = H_0 \underset{\sim}{e}_z$, the evolution operator is diagonal;

$$\langle \bar{m}|\Lambda(t)|m \rangle = e^{-i\omega_0 mt}\, \delta_{\bar{m}m} \quad , \tag{26}$$

and after summing over m' and $\bar{m}$ and using the orthogonality property of the Clebsch-Gordan coefficients, the perturbation coefficient (Eq. (17)) takes the simple form

$$G^{q\bar{q}}_{\lambda\bar{\lambda}}(t)_{\underset{\sim}{H}_0} = e^{-iq\omega_0 t}\, \delta_{q\bar{q}}\, \delta_{\lambda\bar{\lambda}} \quad . \tag{27}$$

The time-evolution equation (16) for a static magnetic interaction thus becomes

$$\rho^{\lambda}_{q}(t)_{\underset{\sim}{H}_0} = e^{+iq\omega_0 t}\, \rho^{\lambda}_{q}(0)_{\underset{\sim}{H}_0} \quad . \tag{28}$$

This equation is equivalent to the equation that describes a rotation of the quantization coordinate axes about $\underset{\sim}{H}_0$ through an angle $\alpha = -\omega_0 t$:

$$D^{(\lambda)}_{qq'}(\alpha,0,0) = e^{-iq\alpha}\, \delta_{qq'} = e^{+iq\omega_0 t}\, \delta_{qq'} \quad . \tag{29}$$

Hence, if one writes the statistical tensor $\rho^{\lambda}_{q}(t)$ in a representation with respect to a coordinate system $S'_0(t)$ that rotates about $\underset{\sim}{H}_0 = H_0 \underset{\sim}{e}_z$ with the angular velocity $-\omega_0$ (i.e., in a left-hand sense) one obtains

$$\rho^{\lambda}_{q}(0)_{S'_0(t)} = \sum_{q'} \rho^{\lambda}_{q'}(t)_{\underset{\sim}{H}_0}\, e^{-iq'\omega_0 t}\, \delta_{q'q} = \rho^{\lambda}_{q}(0)_{\underset{\sim}{H}_0} \quad . \tag{30}$$

This equation is the quantum-mechanical equivalent of the Larmor theorem, which states that the influence of a uniform static magnetic field $\underset{\sim}{H}_0$ on an ensemble of magnetic dipoles $\underset{\sim}{\mu}$ can be expressed by using the description of the ensemble for $\underset{\sim}{H}_0 = 0$ but with reference to a coordinate system that rotates with the Larmor frequency ω_0 about $\underset{\sim}{H}_0$.

If the ensemble has a symmetry axis $\underset{\sim}{k}_1$ the effect of a magnetic field $\underset{\sim}{H}_0$ can be described by a rotation of the symmetry axis $\underset{\sim}{k}_1$ about $\underset{\sim}{H}_0$ with the Larmor frequency ω_0. This interpretation will be useful in later discussions.

II.4. Perturbation by Radiofrequency Fields

II.4.1. The Time-Dependent (Differential) Perturbation Coefficient

The presence of a static magnetic field H_0 causes a splitting of the energy levels of the nuclear states (Eq. (24)):

$$E_m = \hbar\omega_0 m \quad , \tag{31}$$

where the quantization axis is parallel to $\underset{\sim}{H}_0$. A radiofrequency (rf) field of proper frequency and polarization direction will induce transitions between the magnetic substates and will alter the degree of orientation of the ensemble of nuclei.

An rf field, $\underset{\sim}{H}_1(t)$, is considered whose magnetic vector is perpendicular to $\underset{\sim}{H}_0$, i.e., it lies in the x-y plane. A circularly polarized electromagnetic field is represented by the magnetic vector

$$\underset{\sim}{H}_{\pm}^{rf}(t) = H_1 [\underset{\sim}{e}_x \cos(|\omega|t + \Delta) \pm \underset{\sim}{e}_y \sin(|\omega|t + \Delta)]; \tag{32}$$

where the index + or - indicates right or left circular polarization, respectively. The phase Δ accounts for the fact that the radiofrequency field has a particular direction at $t = 0$, when the nuclear state is formed. If continuous rf is used with no "phase-locking" one has to average over the phase Δ. The necessity to introduce a phase angle distinguishes radiative detection methods from continuous-wave NMR in stable nuclei, where no time scale is defined by either creation or decay of a nuclear state, although an analogous time scale exists in pulsed NMR experiments. Thus, for short-lived isomeric states the lifetime represents a minimum "time window", which results in a characteristic line width even for very long nuclear relaxation times.

For a linearly polarized (ℓp) field along the x-axis one has

$$\underset{\sim}{H}^{rf}_{\ell p}(t) = 2\, H_1\, \underset{\sim}{e}_x \cos\left(|\omega| t + \Delta\right) \quad . \tag{33}$$

Following the usual practice we may regard $\underset{\sim}{H}^{rf}_{\ell p}(t)$ as being composed of right- and left-circularly polarized components $\underset{\sim}{H}^{rf}_{\pm}(t)$ (see Eq. (32)). Only the component rotating with the same sense as the nuclear Larmor precession can induce resonance. This component is determined by the sign of the nuclear g-factor. Allowing for ω to have the sign defined by $\omega = -\frac{g}{|g|}|\omega|$ we may write the resultant magnetic field acting on the nuclear state as

$$\underset{\sim}{H}(t)_{cp} = H_0 \underset{\sim}{e}_z + H_1 [\underset{\sim}{e}_x \cos\left(\omega t + \Delta\right) + \underset{\sim}{e}_y \sin\left(\omega t + \Delta\right)] \quad . \tag{34}$$

The interaction Hamiltonian in the laboratory system S is:

$$\mathcal{H}(t) = -\underset{\sim}{\mu} \cdot \underset{\sim}{H}(t) \quad , \tag{35}$$

e.g. for a circularly polarized rf field:

$$\mathcal{H}(t) = -g \frac{\mu_N}{\hbar} \{H_0 I_z + H_1 [I_x \cos(\omega t + \Delta) + I_y \sin(\omega t + \Delta)]\} \quad . \qquad (36)$$

This expression follows from the fact that the effective magnetic moment operator $\underset{\sim}{\mu}$ is proportional to the total angular momentum operator $\underset{\sim}{I}$

$$\underset{\sim}{\mu} = g \frac{\mu_N}{\hbar} \underset{\sim}{I} \quad . \qquad (37)$$

By using the operator identity[37]

$$I_x \cos\theta + I_y \sin\theta = e^{-iI_z\theta/\hbar} I_x e^{+iI_z\theta/\hbar} \quad , \qquad (38)$$

the Hamiltonian (Eq. (36)) can be written in the form:

$$\mathcal{H}(t) = -g \frac{\mu_N}{\hbar} [H_0 I_z + H_1 e^{-iI_z(\omega t + \Delta)/\hbar} I_x e^{+iI_z(\omega t + \Delta)/\hbar}] \quad . \qquad (39)$$

The Hamiltonian (Eq. (39)) is expressed with respect to the laboratory system S.

For the computation of the perturbation coefficient $G^{q\bar{q}}_{\lambda\bar{\lambda}}(t)_{\underset{\sim}{z}}$ of Eq. (17) the matrix elements of the evolution operator $\Lambda(t)$ (Eq. (12)) in the $\{Im\}_{\underset{\sim}{z}}$ representation with respect to the laboratory frame S are required. In order to apply Eq. (12) the Hamiltonian $\mathcal{H}(t)$ of Eq. (39) must first be transformed to a frame of reference S' such that H' does not contain the time t explicitly. This transformation is accomplished by introducing a system S' that rotates with the angular frequency ω about the z-axis of the laboratory system. This transformation is represented by the time-dependent unitary transformation operator

$$U(t) = e^{-iI_z(\omega t + \Delta)/\hbar} \quad , \tag{40}$$

and the Hamiltonian $\mathcal{H}'$ in S' is

$$\mathcal{H}' = U^{\dagger}(t)\mathcal{H}(t)\, U(t) - i\,\hbar U^{\dagger}(t)\,\frac{\partial U(t)}{\partial t} \quad . \tag{41}$$

The term $-i\hbar U^{\dagger}\partial U/\partial t$, which must be added because the transformation is time-dependent, corresponds to the classical Coriolis force.

The execution of the transformation (Eq. (41)) leads to

$$\mathcal{H}' = -g\,\frac{\mu_N}{\hbar}\,[(1 - \frac{\omega}{\omega_0})\, H_0 I_{z'} + H_1 I_{x'}] \quad . \tag{42}$$

This "time-independent" Hamiltonian is not diagonal. It describes an interaction of the nuclear ensemble with an effective magnetic field $\underset{\sim}{H}_e$ in the x'-z' plane of S':

$$H_e = [(1 - \frac{\omega}{\omega_0})^2\, H_0^{\,2} + H_1^{\,2}]^{1/2} \quad . \tag{43}$$

The direction $\underset{\sim}{z}''$ of $\underset{\sim}{H}_e$ is given by the angle β with respect to the $\underset{\sim}{z}'$-axis (see Figs. 1 and 2)

$$\tan\beta = \frac{H_1}{(1 - \frac{\omega}{\omega_0})H_0} \quad . \tag{44}$$

Hence, by a further rotation $V(\beta)$ of the coordinate system S'(t) about the $\underset{\sim}{y}'$ axis through the Euler angle β the new $\underset{\sim}{z}''$ axis is made to coincide with the direction of $\underset{\sim}{H}_e$:

$$\mathcal{H}'' = V(\beta)^{\dagger}\, \mathcal{H}'\, V(\beta) = e^{iI_y\beta/\hbar}\, \mathcal{H}'\, e^{-iI_y\beta/\hbar} \quad . \tag{45}$$

The explicit evaluation of $\mathcal{H}''$ by using operator identities similar to Eq. (38) gives

$$\mathcal{H}'' = -g\,\frac{\mu_N}{\hbar}\,[(1 - \frac{\omega}{\omega_0})^2\, H_0^{\,2} + H_1^{\,2}]^{1/2}\, I_{z''} \quad . \tag{46}$$

This Hamiltonian is diagonal and has the matrix elements in the angular momentum representation $\{In\}_{\underset{\sim}{z}''}$

$$\langle n|\mathcal{H}''|n'\rangle = E_n \delta_{nn'} = \hbar\, \omega_e n \delta_{nn'}$$

with
$$\omega_e = -g\,\frac{\mu_N}{\hbar}\,[(1 - \frac{\omega}{\omega_0})^2\, H_0^{\,2} + H_1^{2}]^{1/2} \quad . \tag{47}$$

At resonance $\omega = \omega_0$, the energy splittings are given by

$$\Delta E = -g\,\mu_N\, H_1 = \omega_1\, \hbar \tag{48}$$

They are independent of H_0. The solution of the Schrödinger equation (Eq. (11)) in the system S'' is now given by

$$\Lambda''(t) = e^{-\frac{i}{\hbar}\mathcal{H}''t} \quad . \tag{49}$$

Since we want to find an expression for the matrix elements $\langle \bar{m}|\Lambda(t)|m\rangle$, the time-evolution operator $\Lambda''(t)$ must be transformed back to the laboratory system S :

$$\Lambda(t) = [U(t)\ V(\beta)]\ \Lambda''(t)\ \ [U(t)\ V(\beta)]^{\dagger}$$

$$= U(t)\ e^{-iI_y\beta/\hbar}\ \Lambda''(t)\ e^{iI_y\beta/\hbar}\ U^{\dagger}(t = 0) \quad . \tag{50}$$

The operator $U^{\dagger}$ acts on the initial state and hence must be evaluated at $t = 0$. The evolution operator is now expressed in the angular momentum representation $\{Im\}_{\underset{\sim}{z}}$:

$$\langle \bar{m}|\Lambda(t)|m \rangle = \langle \bar{m}|e^{-iI_z(\omega t + \Delta)/\hbar}\ e^{-iI_y\beta/\hbar}\ \Lambda''(t)\ e^{iI_y\beta/\hbar}\ e^{iI_z\Delta/\hbar}$$

$$= e^{-i[\bar{m}\ \omega t + (\bar{m} - m)\Delta]}\ \langle \bar{m}|e^{-iI_y\beta/\hbar}\ \Lambda''(t)\ e^{iI_y\beta/\hbar}|m \rangle \quad . \tag{51}$$

Using the closure relation $\sum_n |n\rangle\langle n| = 1$ twice, one obtains

$$\langle \bar{m}|\Lambda(t)|m \rangle = \sum_{\bar{n}n} e^{-i[\bar{m}\omega t + (\bar{m} - m)\Delta]}\ \langle \bar{m}|e^{-iI_y\beta/\hbar}|\bar{n} \rangle\langle \bar{n}|\Lambda''(t)|n \rangle$$

$$\times \langle n|e^{iI_y\beta/\hbar}|m \rangle \quad . \tag{52}$$

Since $\mathcal{H}''$ is diagonal in the representation $\{In\}_{\underset{\sim}{z}''}$, the evolution operator $\Lambda''(t)$ is diagonal:

$$\langle \bar{n}|\Lambda''(t)|n \rangle = e^{-\frac{i}{\hbar}E_n t}\ \delta_{n\bar{n}} \quad . \tag{53}$$

Introducing the D-functions (Ref. 33, p. 22)

$$D^{(I)}_{mn}(0,\beta,0) = d^{(I)}_{mn}(\beta) = \langle m|e^{-iI_y\beta/\hbar}|n\rangle \quad , \tag{54}$$

eq. (52) can be expressed in the explicit form:

$$\langle \bar{m}|\Lambda(t)|m\rangle = e^{-i[\bar{m}\omega t + (\bar{m} - m)\Delta]} \sum_n d^{(I)}_{\bar{m}n}(\beta)\, d^{(I)}_{mn}(\beta)\, e^{-iE_n t/\hbar} \quad . \tag{55}$$

Here, the relation $d^{(I)*}_{mn}(\beta) = d^{(I)}_{mn}(\beta)$ has been used.

The perturbation coefficient that describes the interaction of a circularly polarized radio-frequency field plus a static magnetic field with an ensemble of nuclei with spin I is now easily constructed from Eqs. (17) and (55):

$$G^{q\bar{q}}_{\lambda\bar{\lambda}}(t)_{\underset{\sim}{z}} = \sum_{m,\bar{m},n,n'} (-1)^{2I + m' + \bar{m}'} \langle I\ -\bar{m}'\ I\bar{m}|\bar{\lambda}\bar{q}\rangle \langle I\ -m'\ Im|\lambda q\rangle$$

$$\times\, d^{(I)}_{\bar{m}n}(\beta)\, d^{(I)}_{mn}(\beta)\, d^{(I)}_{m'n'}(\beta)\, d^{(I)}_{\bar{m}'n'}(\beta)\, e^{-i(\bar{q}-q)\Delta}\, e^{-i[(E_n - E_{n'}) + \bar{q}\omega\hbar]t/\hbar} \quad . \tag{56}$$

For a further reduction of this expression the perturbation coefficient is written in terms of the Wigner 3-j symbols instead of Clebsch-Gordan Coefficients:

$$G^{q\bar{q}}_{\lambda\bar{\lambda}}(t)_{\underset{\sim}{z}} = [(2\lambda + 1)(2\bar{\lambda} + 1)]^{1/2} \sum_{m,\bar{m},n,n'} (-1)^{2I + m + \bar{m} + \lambda + \bar{\lambda}} \begin{pmatrix} I & I & \lambda \\ m' & -m & q \end{pmatrix} \begin{pmatrix} I & I & \bar{\lambda} \\ \bar{m}' & -\bar{m} & \bar{q} \end{pmatrix}$$

$$\times\, d^{(I)}_{\bar{m}n}(\beta)\, d^{(I)}_{mn}(\beta)\, d^{(I)}_{\bar{m}'n'}(\beta)\, d^{(I)}_{m'n'}(\beta)\, e^{-i(\bar{q}-q)\Delta}\, e^{-i[(E_n - E_{n'}) + \bar{q}\omega\hbar]t/\hbar} \quad . \tag{57}$$

The summations over m and $\bar{m}$ can now be performed by using $d^{(I)}_{mn}(\beta) = (-1)^{m-n} d^{(I)}_{-m-n}(\beta)$ and the contraction relation for the D-functions (Ref. 33, p. 123):

$$\sum_{m} \begin{pmatrix} I & I & \lambda \\ m' & -m & q \end{pmatrix} D^{(I)}_{m'n'}(\beta)\, D^{(I)}_{-m-n}(\beta) = \begin{pmatrix} I & I & \lambda \\ n' & -n & p \end{pmatrix} D^{(\lambda)*}_{qp}(\beta) \quad , \tag{58}$$

and similarly for the sum over $\bar{m}$. The result is:

$$G^{q\bar{q}}_{\lambda\bar{\lambda}}(t)_{\underset{\sim}{z}} = [(2\lambda + 1)(2\bar{\lambda} + 1)]^{1/2} \sum_{n,n'} (-1)^{\lambda+\bar{\lambda}} \begin{pmatrix} I & I & \lambda \\ n' & -n & p \end{pmatrix} \begin{pmatrix} I & I & \bar{\lambda} \\ n' & -n & p \end{pmatrix} d^{(\lambda)}_{qp}(\beta)\, d^{(\bar{\lambda})}_{\bar{q}p}(\beta)$$

$$\times e^{-i(\bar{q}-q)\Delta}\, e^{-i[(E_n - E_{n'}) + \bar{q}\omega\hbar]t/\hbar} \quad . \tag{59}$$

It is important to recognize that the perturbation coefficient (Eq. (59)) is given in a representation where the quantization axis $\underset{\sim}{z}$ is chosen in the direction of $\underset{\sim}{H}_o$. A similar approach applies to <u>any</u> perturbation that is described by a Hamiltonian of the form:

$$\mathcal{H} = \mathcal{H}_{\text{static}} - \underset{\sim}{\mu} \cdot \underset{\sim}{H}_{rf}(t) \quad , \tag{60}$$

where $\mathcal{H}_{\text{static}}$ is symmetrical about the $\underset{\sim}{z}$-axis and $\underset{\sim}{H}_{rf}(t)$ is periodic and in the xy plane. For static quadrupole interactions with axially symmetric field gradients, however, each transition frequency must be treated individually.

Throughout this discussion it was assumed that relaxation interactions are negligible, i.e., it was assumed that all relaxation times are long compared with the lifetime of the state of interest. The influence of relaxation phenomena will be discussed in Chapter VII.

It should be noted that the perturbation coefficient (Eq. (59)) describes the situation in which the circularly polarized rf component is rotating in a plane perpendicular to the static field $\underset{\sim}{H}_0$. The sign of ω refers to the circular polarization of the rf field that induces resonance. For a linearly polarized rf field the sign remains undetermined. The ensemble responds primarily to only one of the two circular polarization components that constitute the linearly polarized rf field, but it is only possible to determine which component is responsible by using the phase Δ. The effects of the other component have been considered by Lewis.[38]

II.4.2. The Time-Integrated Perturbation Coefficient

If the nuclear states under consideration have a finite lifetime τ, the observation of the influence of extranuclear perturbations on the ensemble is limited to time-intervals of a few τ after formation of the states at $t = 0$. If all nuclear states are observed, independent of the actual time when they happen to decay, the weighted average is observed, with the decay factor $e^{-t/\tau}$ as weighting factor. Such a "time-integrated" observation is described by the integral perturbation coefficient:

$$\hat{G}^{q\bar{q}}_{\lambda\bar{\lambda}} = \frac{1}{\tau} \int_0^\infty G^{q\bar{q}}_{\lambda\bar{\lambda}}(t)\, e^{-t/\tau} dt \quad . \tag{61}$$

After performing the integration over the differential perturbation coefficient (Eq. (59)) one obtains:

$$\hat{G}^{q\bar{q}}_{\lambda\bar{\lambda}} = [(2\lambda+1)(2\bar{\lambda}+1)]^{1/2} \sum_{n,n'} (-1)^{\lambda+\bar{\lambda}} \begin{pmatrix} I & I & \lambda \\ n' & -n & p \end{pmatrix} \begin{pmatrix} I & I & \bar{\lambda} \\ n' & -n & p \end{pmatrix} d^{(\lambda)}_{qp}(\beta)\, d^{(\bar{\lambda})}_{\bar{q}p}(\beta)$$

$$\times e^{-i(\bar{q}-q)\Delta} \frac{1 - i[(E_n - E_{n'}) + \bar{q}\omega\hbar]\tau/\hbar}{1 + [(E_n - E_{n'}) + \bar{q}\omega\hbar]^2 (\frac{\tau}{\hbar})^2} \quad . \tag{62}$$

II.4.3. The Role of Phases in the Differential Perturbation Coefficient

The phase Δ that was introduced by Eq. (32) defines the state of the radiofrequency field at the time of the creation of the nuclear state, $t = 0$. The phase angle Δ appears in the transformation (Eq. (40)) from the laboratory frame S to the rotating frame S'(t) as the angle between $\underset{\sim}{x}$ and $\underset{\sim}{x}'$ at $t = 0$ (see Fig. 1).

Two cases of phase relationships must be distinguished:

a) Random Phase Distribution

When the rf field is completely unrelated to the formation of the nuclear state the phase distribution is random. This situation corresponds to continuous wave rf experiments with radioactive sources and accelerator beams, where the nuclear states are produced continuously and without any time-relation to the rf field.

Since all phase angles Δ are equally probable, the corresponding perturbation coefficients (Eqs. (59) or (62)) must be integrated over the phase angle. The phase Δ appears only in the factor $e^{-i(\bar{q}-q)\Delta}$. Hence the integration over Δ reduces to the integral

$$\frac{1}{2\pi}\int_0^{2\pi} e^{-i(\bar{q}-q)\Delta}\, d\Delta = \delta_{q\bar{q}} \quad . \tag{63}$$

Thus in random phase observations only terms with $q = \bar{q}$ occur.

b) Fixed Phase Angle

The fixed phase angle situation can be realized in NMR/RD observations because of the possibility of synchronizing the origin of time $t = 0$ with $\underset{\sim}{H}_1(t)$ by for example, phase-locking rf trains of proper length to accelerator pulses in NMR/NR, or by sensing the phase and sorting the data into bins in NMR/PAC experiments. In these cases no restrictions apply to the general form of the perturbation coefficient in Eqs. (59) and (62) and the particular value of Δ that describes the experimental conditions must be used.

II.4.4. The Perturbation Coefficient for Magnetic Interactions

For equidistant splittings caused by a static magnetic field H_0 the perturbation coefficients $G^{q\bar{q}}_{\lambda\bar{\lambda}}(t)$ are independent of the spin I of the nuclear states and terms with $\lambda \neq \bar{\lambda}$ vanish. A proof of this statement will be given and an analytical expression for $G^{q\bar{q}}_{\lambda\bar{\lambda}}(t)$ will be derived.

For a pure magnetic interaction one has (see Eq. (47))

$$E_n - E_{n'} = (n - n')\,\omega_e \hbar = p\omega_e \hbar \quad , \tag{64}$$

and the summations over n and n' in Eq. (59), can be performed keeping p fixed. The orthogonality property of the 3-j symbols results then in $(2\lambda + 1)^{-1}\,\delta_{\lambda\bar{\lambda}}$. Hence, only terms with $\lambda = \bar{\lambda}$ remain and the final result for the differential $G^{q\bar{q}}_{\lambda\lambda}(t)$ can be written in the form:

$$G_{\lambda\lambda}^{q\bar{q}}(t) = e^{-i\bar{q}\omega t}\, e^{-i(\bar{q}-q)\Delta} \sum_{p} e^{-ip\omega_e t}\, d_{qp}^{(\lambda)}(\beta)\, d_{\bar{q}p}^{(\lambda)}(\beta) \quad . \tag{65}$$

This expression for $G_{\lambda\lambda}^{q\bar{q}}(t)$ describes a periodic pattern in which a fast oscillation $e^{-i\bar{q}\omega t}$ is amplitude-modulated by slowly-varying components $e^{-ip\omega_e t}$.

For the time-integrated perturbation coefficient one obtains

$$\hat{G}_{\lambda\lambda}^{q\bar{q}}(\omega) = \sum_{p} \frac{1 - i(p\omega_e + \bar{q}\omega)\tau}{1 + [p\omega_e + \bar{q}\omega]^2\tau^2}\, e^{-i(\bar{q}-q)\Delta}\, d_{qp}^{(\lambda)}(\beta)\, d_{\bar{q}p}^{(\lambda)}(\beta) \quad . \tag{66}$$

From this equation it can be seen that the perturbation coefficient $\hat{G}_{\lambda\lambda}^{q\bar{q}}$ is independent of the nuclear spin I. This is true because no interference terms with $\lambda \neq \bar{\lambda}$ occur. The physical reason for this is that one deals here with pure magnetic interactions which always give an equidistant splitting, i.e. one basic frequency. Interference terms with $\lambda \neq \bar{\lambda}$ would occur for quadrupole and combined magnetic-plus-quadrupole interactions.

In the case of a <u>random</u> rf phase, the formula for the perturbation coefficient is appreciably simplified. Averaging over all phase angles Δ leaves only terms with $q = \bar{q}$ and Eq. (65) reduces to

$$G_{\lambda\lambda}^{qq}(t) = e^{-iq\omega t} \sum_{p=-\lambda}^{+\lambda} e^{-ip\omega_e t}\, [d_{qp}^{(\lambda)}(\beta)]^2 \quad . \tag{67}$$

In the following we note some useful symmetry properties of $G_{\lambda\lambda}^{q\bar{q}}(t)$ that apply for $\Delta = 0$.

The symmetry about resonance is to terms of order $\frac{\omega-\omega_0}{\omega_0} \ll 1$

$$\hat{G}^{q\bar{q}}_{\lambda\lambda}(\omega-\omega_0 < 0) \cong (-1)^{q+\bar{q}}\, \hat{G}^{q\bar{q}^*}_{\lambda\lambda}(\omega-\omega_0 > 0) \quad . \tag{68}$$

The symmetry of $\hat{G}^{q\bar{q}}_{\lambda\lambda}$ with respect to a sign change in q and $\bar{q}$ is

$$\hat{G}^{q\bar{q}}_{\lambda\lambda} = (-1)^{q+\bar{q}}\, G^{-q-\bar{q}^*}_{\lambda\lambda} \quad . \tag{69}$$

III. ANGULAR DISTRIBUTION OF RADIATION EMITTED FROM PERTURBED ORIENTED STATES

III.1. General Expression

In this chapter we consider the angular distribution of some nuclear radiation X_2 that is emitted from a perturbed oriented ensemble of nuclei. The emitting oriented state at the time t is represented by the statistical tensors of Eqs. (19) or (20). The quantization axis $\underset{\sim}{z}$ for the representation of $\rho^{\bar{\lambda}}_{\bar{q}}(t)_{\underset{\sim}{z}}^{*}$ in Eq. (19) is the quantization axis for the representation in which the perturbation coefficients $G^{q\bar{q}}_{\lambda\bar{\lambda}}(t)$ are most conveniently expressed.

The emission and observation of the radiation X_2 in the direction $\underset{\sim}{k}_2$ is described by an efficiency matrix $\varepsilon(\underset{\sim}{k}_2)$ or an efficiency tensor $\varepsilon^{\lambda}_{q}(\underset{\sim}{k}_2)$, which is defined in terms of $\varepsilon(\underset{\sim}{k}_2)$ by Eq. (1). The result of this observation, i.e. the angular distribution or correlation of the radiation X_2 with respect to the symmetry axis $\underset{\sim}{k}_1$ of the unperturbed ensemble is given by the trace:

$$W(\underset{\sim}{k}_1, \underset{\sim}{k}_2; t) = \mathrm{Tr}\left(\rho(\underset{\sim}{k}_1;t)_{\underset{\sim}{z}} \cdot \varepsilon(\underset{\sim}{k}_2)_{\underset{\sim}{z}}\right) , \tag{70}$$

where $\rho(\underset{\sim}{k}_1)$ and $\varepsilon(\underset{\sim}{k}_2)$ must be expressed in the same representation, e.g. in the $\underset{\sim}{z}$-coordinate system. Using Eq. (2) and the orthogonality of the Clebsch-Gordan coefficients, Eq. (70) can also be expressed in the form:

$$W(\underset{\sim}{k}_1,\underset{\sim}{k}_2;t) = \sum_{\bar{q},\bar{\lambda}} \rho^{\bar{\lambda}}_{\bar{q}}(\underset{\sim}{k}_1;t)^{*}_{\underset{\sim}{z}}\, \varepsilon^{\bar{\lambda}}_{\bar{q}}(\underset{\sim}{k}_2)_{\underset{\sim}{z}} \quad . \tag{71}$$

The efficiency tensors $\varepsilon^{\bar{\lambda}}_{\bar{q}}(\underset{\sim}{k}_2)$ are particularly simple if a representation is chosen with respect to the observation direction k_2 of the radiation X_2. For directional observations, i.e. for polarization-insensitive detectors, $\varepsilon^{\bar{\lambda}}_{\bar{q}}(\underset{\sim}{k}_2)_{\underset{\sim}{k}_2}$ vanishes for $\bar{q} \neq 0$ (axial symmetry about $\underset{\sim}{k}_2$) and the $\varepsilon^{\bar{\lambda}}_{0}(\underset{\sim}{k}_2)_{\underset{\sim}{k}_2}$ are simply the

angular distribution parameters $A_{\bar{\lambda}}(X_2)$ for the radiation X_2 as defined in angular correlation problems.[36] E.g., for gamma radiation we have

$$A_{\bar{\lambda}}(\gamma_2) = \frac{\sum_{\pi_2 L_2 \pi_2' L_2'} F_{\bar{\lambda}}(L_2 L_2' I_2 I) \langle I_2 \| j_{\underset{\sim}{N}} A_{L_2}^{(\pi_2)} \| I \rangle \langle I_2 \| j_{\underset{\sim}{N}} A_{L_2'}^{(\pi_2')} \| I \rangle}{\sum_{\pi_2 L_2} | \langle I_2 \| j_{\underset{\sim}{N}} A_{L}^{(\pi_2)} \| I \rangle |^2} \quad . \tag{72}$$

The efficiency tensors in the $\underset{\sim}{z}$-representation are:

$$\varepsilon_{\bar{q}}^{\bar{\lambda}}(\underset{\sim}{k}_2)_{\underset{\sim}{z}} = A_{\bar{\lambda}}(X_2)\, D_{0\bar{q}}^{(\bar{\lambda})}(\underset{\sim}{k}_2 \to \underset{\sim}{z}) \quad . \tag{73}$$

The angular distribution or correlation function is now easily constructed from Eqs. (71), (19), and (73):

$$W(\underset{\sim}{k}_1, \underset{\sim}{k}_2; t) = \sum_{q,\lambda,\bar{q},\bar{\lambda}} \rho_0^{\lambda}(0)^*_{\underset{\sim}{k}_1} A_{\bar{\lambda}}(X_2)\, G^{q\bar{q}}_{\lambda\bar{\lambda}}(t)_{\underset{\sim}{z}}\, D^{(\lambda)}_{q0}(\underset{\sim}{z} \to \underset{\sim}{k}_1)\, D^{(\bar{\lambda})*}_{\bar{q}0}(\underset{\sim}{z} \to \underset{\sim}{k}_2) \quad , \tag{74}$$

where the unitary property of the D-function has been used.

If the D-functions are replaced by the corresponding spherical harmonics:[33]

$$D^{(\lambda)}_{q0}(\phi,\theta,0) = \left(\frac{4\pi}{2\lambda+1}\right)^{1/2} Y^*_{\lambda,q}(\theta,\phi) \quad , \tag{75}$$

and if the orientation parameters (Eq. (6a)) are used Eq. (74) takes the well known form:[36]

$$W(\underset{\sim}{k}_1,\underset{\sim}{k}_2;t) = \frac{4\pi}{\sqrt{2I+1}} \sum_{\substack{\lambda\bar{\lambda} \\ q\bar{q}}} \frac{B_\lambda(I)}{\sqrt{(2\lambda+1)(2\bar{\lambda}+1)}} A_{\bar{\lambda}}(X_2)\, G^{q\bar{q}}_{\lambda\bar{\lambda}}(t)_{\underset{\sim}{z}}\, Y^*_{\lambda q}(\theta_1,\phi_1)\, Y_{\bar{\lambda}\bar{q}}(\theta_2,\phi_2) \quad . \quad (76)$$

The angles θ_i and ϕ_i characterize the directions $\underset{\sim}{k}_i$ with respect to the quantization axis $\underset{\sim}{z}$ in system S in which the perturbation coefficient $G^{q\bar{q}}_{\lambda\bar{\lambda}}(t)_{\underset{\sim}{z}}$ is represented (see Fig. 3).

For vanishing perturbation Eq. (17) reduces to

$$G^{q\bar{q}}_{\lambda\bar{\lambda}}(0)_{\underset{\sim}{z}} = \delta_{q\bar{q}}\, \delta_{\lambda\bar{\lambda}} \quad , \quad (77)$$

and the summation over $q = \bar{q}$ in Eq. (74) results in $D^{(\lambda)}_{00}(\underset{\sim}{k}_1 \rightarrow \underset{\sim}{k}_2) = P_\lambda(\cos\Theta)$, where Θ is the angle between $\underset{\sim}{k}_1$ and $\underset{\sim}{k}_2$. Hence the unperturbed directional correlation is given by the usual expression (after dropping the irrelevant factor $(2I+1)^{-1/2}$):

$$W(\theta) = \sum_\lambda B_\lambda(I)\, A_\lambda(X_2)\, P_\lambda(\cos\theta) \quad . \quad (78)$$

III.2. The Response Function $\Gamma_\lambda(t)$

In order to facilitate the planning and analysis of NMR/RD experiments the "angular distribution functions" $W(\underset{\sim}{k}_1,\underset{\sim}{k}_2;\underset{\sim}{H}_0,t)$ for some typical and useful experimental arrangements will be given. The formulae are restricted to pure magnetic dipole interactions, i.e. $\bar{\lambda} = \lambda$ and to directional distributions.

For a specific choice of the angles θ_1,ϕ_1 and θ_2,ϕ_2 (see Fig. 3) the directional distribution or correlation function (Eq. (76)) can be written in the form:

$$W(\theta_1\phi_1\theta_2\phi_2;\underset{\sim}{H}_0 t) = \sum_\lambda B_\lambda(I)\, A_\lambda(X_2)\, \Gamma_\lambda(t) \quad . \tag{79}$$

Terms with $\lambda > 4$ are of no practical interest. The coefficients Γ_λ are given by (see Eq. (76)):

$$\Gamma_\lambda(t) = \frac{4\pi}{2\lambda+1} \sum_{q,\bar{q}} G^{q\bar{q}}_{\lambda\lambda}(t)\, Y^*_{\lambda,q}(\theta_1,\phi_1)\, Y_{\lambda,\bar{q}}(\theta_2,\phi_2) \quad , \tag{80}$$

and a corresponding equation for $\hat{\Gamma}_\lambda$, describing time-integrated experiments. For random phases $q = \bar{q}$; hence the terms with $q \neq \bar{q}$ vanish. The definition of Γ_λ is chosen in such a way that it contains the perturbation and the geometry. In the unperturbed case Γ_λ reduces to $P_\lambda(\cos\Theta)$.

Of particular interest is the geometry in which $\underset{\sim}{k}_1$ and $\underset{\sim}{k}_2$ are parallel to H_0, because it leads to a simple expression for the angular distribution. In addition, since $q = \bar{q} = 0$ for geometrical reasons, there is no difference between the random and fixed phase case. The $\Gamma_\lambda(t)$ coefficients are for this geometry identical with the perturbation factor:

$$\Gamma_\lambda(\theta_1 = \theta_2 = 0;t) = G^{00}_{\lambda\lambda}(t) \quad . \tag{81a}$$

In the case of "antiparallel geometry" the odd terms change sign according to

$$\Gamma_\lambda(\theta_1 = 0;\theta_2 = \pi;t) = (-1)^\lambda\, G^{00}_{\lambda\lambda}(t) \quad . \tag{81b}$$

For more complicated geometrical arrangements explicit expressions for the Γ_λ-coefficients are given in Tables I-III.

III.3. Geometrical Interpretation of the Perturbation Formula

III.3.1. Static Magnetic Interaction

For a static magnetic interaction with a field $\underset{\sim}{H}_0$ the perturbation coefficients are given by Eq. (27) for $\underset{\sim}{z} = \underset{\sim}{H}_0$ and the angular distribution function (Eq. (74)) is of the form:

$$W(\underset{\sim}{k}_1,\underset{\sim}{k}_2,t) = \sum_{\lambda,q} A_\lambda(X_2)\ \rho_0^\lambda(0)^*_{\underset{\sim}{k}_1}\ D_{0q}^{(\lambda)*}(\underset{\sim}{k}_1 \to \underset{\sim}{H}_0)\ e^{-iq\omega_0 t}\ D_{q0}^{(\lambda)*}(\underset{\sim}{H}_0 \to \underset{\sim}{k}_2) \quad , \quad (82)$$

where the unitary property of the D-functions has been used. Using Eq. (29) the distribution function (Eq. (82)) can be expressed in the form

$$W(\underset{\sim}{k}_1,\underset{\sim}{k}_2;t) = \sum_{\lambda,q,q'} A_\lambda(X_2)\ \rho_0^\lambda(0)^*_{\underset{\sim}{k}_1}\ D_{0q}^{(\lambda)*}(\underset{\sim}{k}_1 \to \underset{\sim}{H}_0)\ D_{qq'}^{(\lambda)*}(-\omega_0 t,0,0)\ D_{q'0}^{(\lambda)*}(\underset{\sim}{H}_0 \to \underset{\sim}{k}_2)$$

$$= \sum_\lambda A_\lambda(X_2)\ \rho_0^\lambda(t)^* \quad , \quad (83)$$

where

$$\rho_0^\lambda(t)^* = \rho_0^\lambda(0)^*_{\underset{\sim}{k}_1} \sum_{qq'} D_{0q}^{(\lambda)*}(\underset{\sim}{k}_1 \to \underset{\sim}{H}_0)\ D_{qq'}^{(\lambda)*}(-\omega_0 t,0,0)\ D_{q'0}^{(\lambda)*}(\underset{\sim}{H}_0 \to \underset{\sim}{k}_2) \quad . \quad (84)$$

The statistical tensor $\rho_0^\lambda(t)$ is the same as $\rho_0^\lambda(0)_{\underset{\sim}{k}_1}$, but in a representation with respect to the coordinate system that is obtained by the application of three successive rotations to the coordinate system with $\underset{\sim}{z}_1 = \underset{\sim}{k}_1$: first $\underset{\sim}{k}_1 \to \underset{\sim}{H}_0$, then a rotation by $\alpha = -\omega_0 t$ about $\underset{\sim}{H}_0$

This statement is equivalent to the discussion following Eq. (30), i.e. that the effect of a static magnetic field on an oriented ensemble can be described by a rotation of the symmetry axis $\underset{\sim}{k}_1$ of the ensemble about $\underset{\sim}{H}_0$ by an angle $\alpha' = \omega t$.

To reduce Eq. (84) the group property of the D-functions can be used. The successive application of two rotations R_1 and R_2, in that order, can be expressed in terms of one rotation R by using the group property of the D-matrices:

$$\sum_q D^{(\lambda)}_{q_1 q}(R_1)\, D^{(\lambda)}_{q q_2}(R_2) = D^{(\lambda)}_{q_1 q_2}(R) \quad . \tag{85}$$

Hence, the summation over q and q' in Eq. (83) results in:

$$W(\underset{\sim}{k}_1, \underset{\sim}{k}_2; t) = \sum_\lambda \rho_0^\lambda(0)^*_{\underset{\sim}{k}_1} A_\lambda(X_2)\, P_\lambda[\cos \eta(t)] \quad .. \tag{86}$$

A comparison with Eqs. (79) and (80) shows that $P_\lambda[\cos \eta(t)] \equiv \Gamma_\lambda(t)$. The angle $\eta(t)$ is the angle between $K(t)$ and $\underset{\sim}{k}_2$, where $\underset{\sim}{K}(t)$ is the symmetry axis of the ensemble at the time t. The symmetry axis is represented by a unit vector $\underset{\sim}{K}(t)$ that is obtained by rotating the original symmetry axis $\underset{\sim}{k}_1$ about $\underset{\sim}{H}_0$ through $+\omega_0 t$. That is,

$$\cos \eta(t) = \underset{\sim}{K}(t) \cdot \underset{\sim}{k}_2 \qquad (|k_2| = 1)$$

$$= \cos\theta_1 \cos\theta_2 + \sin\theta_1 \sin\theta_2 \cos(\Theta - \omega_0 t) \quad , \tag{87}$$

where $\Theta = \phi_2 - \phi_1$. Using this expression it is simple to derive the angular correlation function for <u>any</u> direction of the magnetic field with respect to the

detectors. The two most common special cases are:

(1) If $\underset{\sim}{k}_1$ and/or $\underset{\sim}{k}_2$ is parallel or antiparallel to $\underset{\sim}{H}_0$ the time-dependent term vanishes and the angular correlation is unperturbed :

$\cos \eta = \cos\theta_1 \cos\theta_2$.

(2) If $\underset{\sim}{k}_1$ and $\underset{\sim}{k}_2$ are both perpendicular to $\underset{\sim}{H}_0$, a geometry that is commonly used for the measurement of unidirectional magnetic perturbations, the angle $\eta(t)$ is given by

$$\eta(t) = \theta - \omega_0 t \quad . \tag{88}$$

III.3.2. Static Magnetic Interaction in the Presence of a Radiofrequency Field

The angular distribution of radiation X_2 emitted from an oriented ensemble that interacts with a static magnetic field $\underset{\sim}{H}_0$ and a radiofrequency field $\underset{\sim}{H}_1(t)$ is given by Eq. (74) with the perturbation coefficient of Eq. (65).

$$W(\underset{\sim}{k}_1,\underset{\sim}{k}_2;t) = \sum_{\lambda,q,\bar{q},p} \rho_0^{\lambda}(0)^*_{\underset{\sim}{k}_1} A_\lambda(X_2)\, D^{(\lambda)^*}_{0q}(\underset{\sim}{k}_1 \to \underset{\sim}{H}_0)\, e^{iq\Delta}\, D^{(\lambda)^*}_{qp}(0,\beta,0)$$

$$\times e^{-ip\omega_e t}\, D^{(\lambda)^*}_{p\bar{q}}(0,-\beta,0)\, e^{-i\bar{q}(\omega t+\Delta)}\, D^{(\lambda)^*}_{\bar{q}0}(\underset{\sim}{H}_0 \to \underset{\sim}{k}_2) \tag{89}$$

$$= \sum_{\lambda} A_\lambda(X_2)\, \rho_0^{\lambda}(0)^*_{\underset{\sim}{k}_1}\, \Gamma_\lambda(t)$$

$$= \sum_{\lambda} A_\lambda(X_2)\, \rho_0^{\lambda}(t)^* \quad .$$

By making use of Eq. (29), $\rho_0^{\lambda}(t)^*$ can be written in the form

$$\rho_0^{\lambda}(t)^* = \rho_0^{\lambda}(0)^*_{\underset{\sim}{k}_1} \sum_{\substack{qq'pp' \\ \bar{q}\bar{q}'}} D_{0q}^{(\lambda)^*}(0,-\theta_1,-\phi_1)\, D_{qq'}^{(\lambda)^*}(\Delta,0,0)$$

$$\times D_{q'p}^{(\lambda)^*}(0,\beta,0)\, D_{pp'}^{(\lambda)^*}(-\omega_e t,0,0)\, D_{p'\bar{q}}^{(\lambda)^*}(0,-\beta,0)\, D_{\bar{q}\bar{q}'}^{(\lambda)^*}(-\omega t-\Delta,0,0)$$

$$\times D_{\bar{q}'0}^{(\lambda)^*}(\phi_2,\theta_2,0) \quad . \tag{90}$$

Again the summations over q, q', p, p', $\bar{q}$, and $\bar{q}'$ can be performed and the result is

$$D_{00}^{(\lambda)^*}(0,\eta(t),0) = P_\lambda[\cos\,\eta(t)] = \Gamma_\lambda(t) \quad .$$

Thus the angular correlation function can formally be written as

$$W(\underset{\sim}{k}_1,\underset{\sim}{k}_2;t) = \sum_\lambda \rho_0^{\lambda}(0)^*_{\underset{\sim}{k}_1} A_\lambda(X_2)\, P_\lambda[\cos\,\eta(t)] \quad . \tag{91}$$

This means that, as in the static case, the influence of the perturbation can be described by a time-dependent angle $\eta(t)$.

Before leaving this section, let us recapitulate, with emphasis on the physical meaning of the above results.

Referring to Eq. (90), we can understand the effect of the rotation matrices $D^{(\lambda)}$ in the following way. At time t = 0 the ensemble has symmetry about $\underset{\sim}{k}_1$, and only statistical tensors with q = 0 are nonzero in a frame with z axis along $\underset{\sim}{k}_1$, i.e., only tensors of the form $\rho_0^{\lambda}(0)^*_{\underset{\sim}{k}_1}$ are nonzero (the complex

conjugate notation is used to retain consistency with Eq. (71)). Now in the pure magnetic case it is possible, using successive time-independent rotations, to express $\rho_0^\lambda(0)^*$ in a frame S''' wherein the Hamiltonian vanishes. For $t > 0$ the frame S''' rotates relative to the S frame. It is thus necessary to transform back into the S frame using the (now time-dependent) rotation matrices in reverse order, and finally to transform into a frame with z-axis along $\underset{\sim}{k}_2$, in order to obtain the desired $\rho_0^\lambda(t)^*_{\underset{\sim}{k}_2}$. To express the symmetry axis at time $t = 0$ (i.e., the $\underset{\sim}{k}_1$ axis) in the S''' frame the following operations must be performed:

1. Rotation of the $\underset{\sim}{k}_1$ frame through the angles $(0,-\theta_1,-\phi_1)$, to express $\underset{\sim}{k}_1$ in the S frame at $t = 0$.
2. Rotation of the S (or xyz) frame about $\underset{\sim}{H}_0$ through angle Δ in order to adjust the rf phase. This operation defines the new x' axis as being along $\underset{\sim}{H}_1$ at time $t = 0$, and $\underset{\sim}{k}_1$ is then expressed in the S' (or x'y'z') frame at $t = 0$ (Fig. 1).
3. Rotation of the S' frame about the y' axis (see Fig. 2a) through the angle β. The new z" axis then falls along $\underset{\sim}{H}_e$, and $\underset{\sim}{k}_1$ is expressed in the S" frame, at $t = 0$. Now at $t = 0$ the S" frame coincides with a rotating frame S''' that rotates about z" = z''' with frequency ω_e, and in which the magnetic field disappears altogether (see Fig. 2b). Thus $\underset{\sim}{k}_1$ is also expressed in S''' at $t = 0$.

The remaining rotations in Eq. (90) describe the time-evolution of the symmetry axis, and express it in the laboratory frame. Since the direction of this axis will no longer coincide with $\underset{\sim}{k}_1$, we shall now call it $\underset{\sim}{K}(t)$. Thus after the above operations the vector that we have is $\underset{\sim}{K}(0)'''$. We must now:

4. Rotate the S''' frame about $\underset{\sim}{H}_e$ (i.e., about z" = z''') through the angle $-\omega_e t$. This gives $\underset{\sim}{K}(t)"$.
5. Rotate the S" frame about the y" = y' axis through the angle $-\beta$ to give $\underset{\sim}{K}(t)'$.
6. Rotate the S' frame about $\underset{\sim}{H}_0$ (i.e., about z' = z) through the angle $-\omega t-\Delta$, thereby obtaining $\underset{\sim}{K}(t)$ expressed in the S frame.

The resulting vector $\underset{\sim}{K}(t)$ must be related to the emission direction $\underset{\sim}{k}_2$ in order to obtain the angular distribution in the $\underset{\sim}{k}_2$ direction at time t. This is accomplished by the last rotation, $D^{(\lambda)*}_{\bar{q}'0}(\phi_2,\theta_2,0)$, which expresses $\underset{\sim}{K}(t)$ in the $\underset{\sim}{k}_2$ frame.

The two ways of computing the angular distribution from a state that is perturbed by static and radiofrequency magnetic fields, as given by Eqs. (79) and (80) on one hand and by Eqs. (90) and (91) on the other, are identical. The rotations which are contained in $\Gamma_\lambda(t)$ (see Eq. (80)) in a rather implicit manner were discussed one by one in Eq. (90) only to provide the reader with a physical understanding of the rather formal derivation of the perturbed angular correlation function. In the next chapter the same approach will be made to describe the behavior of the symmetry axis of an ensemble under the influence of static and periodic magnetic fields, in complete analogy to the behavior of the magnetization vector in conventional NMR (Bloch equations).

IV. THE GENERALIZED TORQUE EQUATION: AN ALTERNATE APPROACH FOR MAGNETIC INTERACTIONS

The theory developed above is exact and complete. It may be used to describe any NMR/RD experiment involving magnetic and quadrupole interactions, etc. However, for pure magnetic interactions, the most important single case, we have also found another approach to be valuable. This second formulation, which owes its origins to NMR theory, is derived below.

The transformations, described by Eqs. (89) and (90) and the discussion following, are simply successive rotations in space. Equation (90) was formulated to display their spin-independence, for the magnetic case. It is also useful, however, to eliminate specific reference to the ranks of the statistical tensors. To do so we exploit the symmetry of the system by transforming into the reference frame S''' wherein ρ is time-independent (except for nuclear decay) and axially symmetric (i.e., $\rho_q^\lambda = 0$ for $q \neq 0$). Of course this means that we must express $\underset{\sim}{k}_1$, the direction of axial symmetry at $t = 0$, in the reference frame S''' wherein the part of the Hamiltonian that describes the interaction of the nuclei with the time-dependent magnetic field, which can be written in the laboratory frame as

$$H_S(t) = H_1(\underset{\sim}{e}_x \cos(\omega t+\Delta) + \underset{\sim}{e}_y \sin(\omega t+\Delta)) + H_0 \underset{\sim}{e}_z \quad , \tag{92}$$

is always zero. This is accomplished by three successive rotations,

$$R_1(S \rightarrow S') = \begin{pmatrix} \cos(\omega t+\Delta) & \sin(\omega t+\Delta) & 0 \\ -\sin(\omega t+\Delta) & \cos(\omega t+\Delta) & 0 \\ 0 & 0 & 1 \end{pmatrix}$$

$$R_2(S' \to S'') = \begin{pmatrix} \cos\beta & 0 & -\sin\beta \\ 0 & 1 & 0 \\ \sin\beta & 0 & \cos\beta \end{pmatrix}$$

$$R_3(S'' \to S''') = \begin{pmatrix} \cos\omega_e t & \sin\omega_e t & 0 \\ -\sin\omega_e t & \cos\omega_e t & 0 \\ 0 & 0 & 1 \end{pmatrix} \quad .$$

The S and S' frames were defined in Sec. II.4.1. and illustrated in Fig. 1. The S" frame introduced above, has axis z" along $\underset{\sim}{H}_e$ with $\beta = \cos^{-1} \sphericalangle(\underset{\sim}{z}', \underset{\sim}{z}'')$. Finally S''' is a rotating frame relative to S": the purpose of R_3 is to "transform out" the remaining magnetic field $\underset{\sim}{H}_e$ so that

$$\underset{\sim}{H}_{S'''}(t) \equiv 0 \quad . \tag{93}$$

Figure 2 illustrates S" and S'''. For $\Delta = 0$ there is a one to one correspondence between (S''', S", ω_e, $\underset{\sim}{H}_e$) and (S', S, ω, $\underset{\sim}{H}_0$), as a comparison of R_1 and R_3 will show.

We now denote a unit vector along the symmetry axis of ρ as $\underset{\sim}{K}(t)$, without reference to the frame in which it is written (see Eq. (87)). Clearly it must satisfy the boundary condition

$$\underset{\sim}{K}(t=0) = \underset{\sim}{k}_1 \quad , \tag{94}$$

and it may be written in S''' at t = 0 as

$$\underset{\sim}{K}_{S'''}(t=0) = R_3(t=0)\, R_2 R_1(t=0) \underset{\sim}{k}_1 \quad , \tag{95}$$

where k_1 is referred to the S frame.

To express $\underset{\sim}{K}(t)$ in S we need only transform back, obtaining

$$\underset{\sim}{K}_S(t) = R_1^{-1}(t)\, R_2^{-1}\, R_3^{-1}(t)\, R_3(0)\, R_2\, R_1(0)\, \underset{\sim}{k}_1 \quad . \tag{96}$$

The explicit form for $\underset{\sim}{K}_S(t)$ is

$$\underset{\sim}{K}_S(t) =$$

$$\begin{aligned}
&= \{[(\cos^2\beta \cos(\omega t+\Delta) \cos\omega_e t + \sin^2\beta \cos(\omega t+\Delta) - \cos\beta \sin(\omega t+\Delta) \sin\omega_e t)\cos\Delta \\
&+ (\cos\beta \cos(\omega t+\Delta) \sin\omega_e t + \sin(\omega t+\Delta) \cos\omega_e t)\sin\Delta]k_{1x} \\
&+ [(-\cos\beta \cos(\omega t+\Delta) \sin\omega_e t - \sin(\omega t+\Delta) \cos\omega_e t)\cos\Delta \\
&+ (\cos^2\beta \cos(\omega t+\Delta) \cos\omega_e t - \cos\beta \sin(\omega t+\Delta) \sin\omega_e t + \sin^2\beta \cos(\omega t+\Delta))\sin\Delta]k_{1y} \\
&+ [\sin\beta \cos\beta \cos(\omega t+\Delta) - \sin\beta \cos\beta \cos(\omega t+\Delta) \cos\omega_e t + \sin\beta \sin(\omega t+\Delta) \sin\omega_e t]k_{1z}\}\underset{\sim}{e}_x \\
&+ \{[(\cos^2\beta \sin(\omega t+\Delta) \cos\omega_e t + \sin^2\beta \sin(\omega t+\Delta) + \cos\beta \cos(\omega t+\Delta) \sin\omega_e t)\cos\Delta \\
&+ (\cos\beta \sin(\omega t+\Delta) \sin\omega_e t - \cos(\omega t+\Delta) \cos\omega_e t)\sin\Delta]k_{1x} \\
&+ [(-\cos\beta \sin(\omega t+\Delta) \sin\omega_e t + \cos(\omega t+\Delta) \cos\omega_e t)\cos\Delta \\
&+ (\cos^2\beta \sin(\omega t+\Delta) \cos\omega_e t + \cos\beta \cos(\omega t+\Delta) \sin\omega_e t + \sin^2\beta \sin(\omega t+\Delta))\sin\Delta]k_{1y} \\
&+ [-\sin\beta \cos\beta \sin(\omega t+\Delta) \cos\omega_e t + \sin\beta \cos\beta \sin(\omega t+\Delta) - \sin\beta \cos(\omega t+\Delta) \sin\omega_e t]k_{1z}\}\underset{\sim}{e}_y \\
&+ \{[(\sin\beta \cos\beta - \sin\beta \cos\beta \cos\omega_e t) \cos\Delta + (-\sin\beta \sin\omega_e t) \sin\Delta]k_{1x} \\
&+ [(\sin\beta \sin\omega_e t) \cos\Delta + (\sin\beta \cos\beta - \sin\beta \cos\beta \cos\omega_e t)\sin\Delta]k_{1y} \\
&+ [\cos^2\beta + \sin^2\beta \cos\omega_e t]k_{1z}\}\underset{\sim}{e}_z \quad .
\end{aligned} \tag{97}$$

Observables in conventional NMR are related to the magnetization $\underset{\sim}{M}$, which obeys the Torque Equation,

$$\frac{d\underset{\sim}{M}}{dt} = \gamma \underset{\sim}{M} \times \underset{\sim}{H} \quad , \tag{98}$$

where $\gamma = g\mu_N/\hbar$. This property of $\underset{\sim}{M}$ is of great utility in visualizing the behavior of a spin ensemble in a conventional NMR experiment. We note that NMR theory is embodied in the previous sections: $\underset{\sim}{M}$ is collinear* with K(t) and its magnitude in S''' is proportional to ρ_0^1. In fact Eq. (98) is just a special case for $\lambda = 1$ of the more general transformation expressed by

$$\frac{d\underset{\sim}{K}}{dt} = \gamma \underset{\sim}{K} \times \underset{\sim}{H} \quad . \tag{99}$$

In many NMR/RD experiments $\underset{\sim}{M} \equiv \underset{\sim}{0}$ because of the parity symmetry of the experiment, which requires $\rho_0^\lambda = 0$ for odd λ. For these cases a "torque" equation still obtains, however, because, as inspection of Eq. (98) shows, the direction of $\underset{\sim}{M}$, rather than its magnitude, is important in the Torque Equation. Of course Eq. (99) depends on the states of the individual nuclei in the ensemble having gyromagnetic ratio γ, but it in no way requires a finite magnetization ensemble. Rather, the torque equation should be regarded as a transformation of coordinates that will eliminate $\underset{\sim}{H}(t)$ and allow the density matrix to remain time-independent in S'''. This is not a new result, of course, but our point of view is of necessity a little more crystallized than is common in the magnetic resonance literature, where $\underset{\sim}{M}$ is usually nonzero. The essential physical content of our approach is given in papers by Rabi, Ramsey, and Schwinger[39] and by Fano.[32] We may therefore write a Generalized Torque Equation,

---

*The case $\underset{\sim}{M} \| \underset{\sim}{z}$ in a continuous NMR experiment is analogous, then, to $\underset{\sim}{k}_1 \| \underset{\sim}{z}$ in an angular correlation experiment. Pulsed NMR experiments provide examples in which a natural time scale exists and for which $\underset{\sim}{k}_1$ is not parallel to the z-axis.

$$\frac{d\underset{\sim}{K}_S(t)}{dt} = \gamma\, \underset{\sim}{K}_S(t) \times \underset{\sim}{H}_S(t) \quad , \tag{100}$$

in a form that indicates explicitly its validity in the laboratory frame at any time t. Of course it is valid in any frame. This equation may be confirmed in detail by substituting the explicit expressions (92) and (97) into (100). Now $\eta(t)$, defined in Eq. (87) can be written in this notation as

$$\cos \eta(t) = \underset{\sim}{k}_2 \cdot \underset{\sim}{K}_S(t) \quad . \tag{101}$$

It is the angle between the $\underset{\sim}{k}_2$ direction, to the second detector, and the symmetry axis of the density matrix, as before. The multipole radiation pattern can be described by Legendre polynomials in the S''' frame,

$$W_{S'''}(t) = \sum_\lambda \rho_0^\lambda(0)^*_{\underset{\sim}{k}_1} A_\lambda(X_2)\, P_\lambda(\cos\theta_{S'''}) \quad .$$

To evaluate the counting rate in the laboratory frame, S, at time t, we need only know $\eta(t)$, the instantaneous angle between $\underset{\sim}{k}_2$ and $\underset{\sim}{K}(t)$. Thus

$$W(\underset{\sim}{k}_1, \underset{\sim}{k}_2, t) = \sum_\lambda \rho_0^\lambda(0)^*_{\underset{\sim}{k}_1} A_\lambda(X_2)\, P_\lambda(\cos\, \eta(t)) \quad . \tag{102}$$

But this result is identical to Eq. (91): only the point of view is different. For the time-integral functions

$$\hat{W}(\underset{\sim}{k}_1, \underset{\sim}{k}_2) = \sum_\lambda \rho_0^\lambda(0)^*_{\underset{\sim}{k}_1} A_\lambda(X_2)\, \hat{\Gamma}_\lambda(\underset{\sim}{k}_1, \underset{\sim}{k}_2) \quad , \tag{103}$$

we need only evaluate the time-integral Legendre Polynomials,

$$\hat{\Gamma}_\lambda(\underset{\sim}{k}_1,\underset{\sim}{k}_2) = \tau^{-1} \int_0^\infty e^{-t/\tau} P_\lambda(\cos \eta(t))\, dt \quad . \tag{104}$$

For any $\underset{\sim}{k}_1,\underset{\sim}{k}_2,\lambda$ these integrals can be written as linear combinations of integrals over powers of cos $\eta(t)$, of the form $\int_0^\infty e^{-t/\tau} [\cos \eta(t)]^n\, dt$, with $n \leqslant \lambda$. Now cos $\eta(t)$ is itself a linear combination of powers of sines and cosines of the angles $\omega_e t, \beta$, and $\omega t+\Delta$. After some trigonometric manipulation all the necessary integrals can be written in terms of integrals of the forms

$$\int_0^\infty e^{-t/\tau} \cos(\ell\omega_e t)\, dt \quad , \qquad \text{and} \qquad \int_0^\infty e^{-t/\tau} \sin(\ell\omega_e t)\, dt \quad ,$$

where ℓ is an integer.

As an example we shall work out the angular distribution for a specific geometry and relate it to the geometrical interpretation. We consider the case $\underset{\sim}{k}_1 \| +z, \underset{\sim}{k}_2 \| -z$ (Geometry no. 1 in Tables I and II), and calculate Γ_1 and Γ_2. From Eq. (97) we have $k_{1x} = k_{1y} = 0$; thus

$$\Gamma_1(t) = \cos \eta(t) = (\underset{\sim}{K}_S)_{-z} = -\sin^2\beta \cos\omega_e t - \cos^2\beta \quad ,$$

and

$$\Gamma_2(t) = P_2[\cos \eta(t)] = \tfrac{3}{2} \sin^4\beta \cos^2\omega_e t + 3\sin^2\beta \cos^2\beta \cos\omega_e t + \tfrac{3}{2} \cos^4\beta - \tfrac{1}{2} \quad .$$

The time-integral response function has the form

$$\hat{\Gamma}_2 = -\tfrac{1}{2} + \tfrac{3}{2} \cos^4\beta + \tfrac{3}{4} \sin^4\beta + 3\cos^2\beta \sin^2\beta\, [1+(\omega_e\tau)^2]^{-1}$$

$$+ \frac{3}{4} \sin^4\beta \, [1 + (2\omega_e\tau)^2]^{-1} \quad . \tag{105}$$

For the limiting case $\omega_1\tau \to \infty$ the last two terms approach zero and we have

$$\hat{\Gamma}_2 \, (\omega_1\tau \to \infty) = [P_2(\cos\beta)]^2 = \left(\frac{u^2 - 1/2}{u^2 + 1}\right)^2 \quad , \tag{106}$$

where u is the frequency in units of ω_1, $u = (\omega-\omega_0)/\omega_1 = \cot\beta$. The geometrical interpretation of this function is illustrated in Fig. 4. The $\hat{\Gamma}_2$ integral (Eq. (104)) is taken, for each value of ω, around a circle on the unit sphere. The circle must pass through $\underset{\sim}{k}_1$, where the path of integration starts ($\underset{\sim}{z}'$ in this case), and $\underset{\sim}{H}_e$ goes through the center of the circle. Far off resonance (top of Fig. 4) $\underset{\sim}{H}_e$ is near $\underset{\sim}{z}'$ and $P_2(\cos\eta(t))$ is near unity all around the circle. At resonance (bottom of Fig. 4) the integral is taken around a meridian, and $\hat{\Gamma}_2(\infty)$ has the hard-core value

$$\hat{\Gamma}_2(\infty) = \frac{1}{2\pi} \int_0^{2\pi} P_2(\cos\eta) \, d\eta = 1/4 \quad . \tag{107}$$

At intermediate values of u the integration path (Eq. (104)) heavily weights the "equatorial" regions, $\eta \sim \frac{\pi}{2}$, where P_2 is negative, and $\hat{\Gamma}_2$ drops to a single minimum in each direction around $u = 0$. Thus we have a complete geometrical interpretation of the curve. Similar arguments can be made for other geometries.

For the limiting case $\omega_1\tau \to \infty$, an expression for the $\hat{\Gamma}_\lambda$ functions defined in Eq. (80) is easily written down for any arbitrary geometry. We note that $\underset{\sim}{K}(t)$ precesses about $\underset{\sim}{H}_e$ until $\underset{\sim}{H}_e$ is the effective symmetry axis of the system. Thus $\rho^{\lambda}_{q\underset{\sim}{H}_e} = 0$ for $q \neq 0$, and only $\rho^{\lambda}_{0\underset{\sim}{H}_e}$ is left. But for any λ

only $\rho_0^\lambda(t=0)_{\underset{\sim}{K}}$ was nonzero, and thus only $\rho_0^\lambda(t)_{\underset{\sim}{K}}$ will be nonzero. Hence the general transformation equation for spherical statistical tensors (Eq. (4)) becomes

$$(\rho^\lambda_{0\underset{\sim}{H}_e}) = \rho_0^\lambda(t)_{\underset{\sim}{K}} \; D_{00}^{(\lambda)}(\alpha',\beta',\gamma') \quad . \tag{108}$$

Here $\alpha'\beta'\gamma'$ represent the rotation angles from the $\underset{\sim}{K}(t)$ frame to the $\underset{\sim}{H}_e$ frame. Now α' and γ' are time-dependent, but β' is not: it is the angle between $\underset{\sim}{H}_e$ and $\underset{\sim}{K}(t)$. But $D_{00}^{(\lambda)}$ is independent of α' and γ': in particular,[40]

$$D_{00}^{(\lambda)}(\alpha'\beta'\gamma') = P_\lambda(\cos\beta') \quad . \tag{109}$$

Thus

$$(\rho^\lambda_{0\underset{\sim}{H}_e}) = (\rho_0^\lambda)_{\underset{\sim}{k}_1} \; P_\lambda[\cos(\underset{\sim}{k}_1,\underset{\sim}{H}_e)] \quad , \tag{110}$$

where we have now used $\rho_0^\lambda(t)_{\underset{\sim}{K}} = \rho_0^\lambda(t=0)_{\underset{\sim}{k}_1}$. By similar arguments the rotation of $\underset{\sim}{H}_e$ about $\underset{\sim}{H}_0$ gives an analogous relation for statistical tensors in the S frame, namely

$$\rho^\lambda_{0\underset{\sim}{H}_0} = \rho^\lambda_{0\underset{\sim}{H}_e} \; P_\lambda[\cos(\underset{\sim}{H}_e,\underset{\sim}{H}_0)] = (\rho_0^\lambda)_{\underset{\sim}{H}_e} \; P_\lambda(\cos\beta) \quad . \tag{111}$$

Now the angular distribution of radiation from the oriented state varies in the limit, $\omega_0\tau \to \infty$ as

$$W(\underset{\sim}{k}_1,\underset{\sim}{k}_2,t) = \sum_\lambda (\rho_0^\lambda)_{\underset{\sim}{H}_0} \; A_\lambda(X_2) \; P_\lambda[\cos(\theta_2)] \quad . \tag{112}$$

Thus, for $\omega_1\tau \to \infty$,

$$\hat{W}(\underset{\sim}{k}_1,\underset{\sim}{k}_2,\omega_1\tau \to \infty) = \sum_\lambda (\rho_0^\lambda)_{\underset{\sim}{k}_1} A_\lambda(X_2)\, \hat{\Gamma}_\lambda(\infty) \quad , \tag{113}$$

and we have

$$\hat{\Gamma}_\lambda(\infty) = P_\lambda[\cos(\underset{\sim}{k}_1,\underset{\sim}{H}_e)]\, P_\lambda(\cos\beta)\, P_\lambda(\cos\theta_2) \quad , \tag{114}$$

as the limiting lineshape for any geometry and frequency as $\omega_1\tau \to \infty$.

In this "torque equation" approach the spin-independence is manifest from the beginning because we never use an $|\mathrm{Im}\rangle$ representation. There is only one response function, $\Gamma_\lambda(t)$, for each tensor rank, rather than the $G_{\lambda\lambda}^{q\bar{q}}(t)$. $\Gamma_\lambda(t)$ is always real. Of course the two theoretical approaches give identical results, and they require about the same amount of computational work. The chief advantage of the theory developed in Sec. III is its generality, which permits ready extension to more complicated $\mathcal{H}_e(t)$. An advantage of the present approach is the readily-grasped relationship between the experimental geometry and $\hat{\Gamma}_\lambda(\omega)$. With the functional forms of the Legendre polynomials in mind one can, with little or no actual calculation, predict the symmetry properties of $\hat{\Gamma}_\lambda(\omega)$ and even the qualitative shapes of the resonance curves for a given experiment.

The two theoretical approaches have been used interchangeably to obtain the results given in the following sections.

V. TIME-DEPENDENCE OF ANGULAR DISTRIBUTIONS

V.1. General Discussion

A time-differential observation shows the periodic motion of the nuclear magnetic moment under the influence of $\underset{\sim}{H}_0$ and $\underset{\sim}{H}_1$. The time-dependent perturbation coefficients $G_{\lambda\lambda}^{q\bar{q}}(t)$ are essentially the Fourier inverse of the time-integrated perturbation coefficients $\hat{G}_{\lambda\lambda}^{q\bar{q}}(\omega)$. Consequently the observation of the time-dependent perturbation factor does not lead to any additional information as compared to the time-integrated observation, but its discussion is instructive for the understanding of the resonance behavior.

The time-differential perturbation coefficient for a pure magnetic interaction is given by Eq. (65). Near resonance the time dependence of $G_{\lambda\lambda}^{q\bar{q}}(t)$ corresponds to a rapidly-oscillating function $e^{-i[\bar{q}\omega t + (\bar{q}-q)\Delta]}$ that is amplitude-modulated by the slowly-oscillating function

$$S_{\lambda\lambda}^{q\bar{q}}(t) = \sum_p e^{-ip\omega_e t} \, d_{qp}^{(\lambda)}(\beta) \, d_{\bar{q}p}^{(\lambda)}(\beta) \quad . \tag{115}$$

This low-frequency component can be interpreted as the rotation of the nuclear spin with frequency ω_e about the effective field $\underset{\sim}{H}_e$ in the Larmor frame that in turn rotates with frequency ω about $\underset{\sim}{H}_0$ (cf. Fig. 1). The high-frequency component originates from the transformation into this Larmor frame and represents physically the spin rotation with frequency ω. Of course $\underset{\sim}{H}_0$ and $\underset{\sim}{H}_1$ are the two magnetic fields actually present. Thus any experiment can alternatively be described in terms of the high and low frequencies ω_0 and ω_1 rather than ω and ω_e.

For frequencies far off resonance the modulation frequency increases as given by ω_e (Eq. (47)). Finally for $|\omega - \omega_e| >> |\omega_1|$ the perturbation coefficient approaches the form

$$G_{\lambda\lambda}^{q\bar{q}}(t) \simeq \sum_{P} e^{-i[(p+\bar{q})\omega t + (\bar{q}-q)\Delta]} \quad ,$$

and only the high-frequency component is left. Here the limits

$$\text{Lim}_{\left|\frac{\omega-\omega_0}{\omega_1}\right| \to 0} \beta = 0 \quad \text{(See Eq. (44))}$$

and

$$\text{Lim}_{\beta \to 0} [d_{qp}^{(\lambda)}(\beta)\, d_{\bar{q}p}^{\lambda}(\beta)] = 1 \quad ,$$

have been used.

It is possible to perform experiments in such a way that the rapid spin-rotation term vanishes for purely geometrical reasons. In Fig. 5 examples of the low-frequency oscillation are given for $\lambda = 1,2$. For $q = \bar{q} = 0$ (Fig. 5a) the oscillation can be observed directly in geometry no. 1 (Tables I and II) and the time-dependent angular correlation is determined by

$$\Gamma_\lambda(t) = S^{00}_{\lambda\lambda}(t) \quad . \tag{116}$$

The explicit forms at resonance, which can also be evaluated from Eq. (97), are

$$\Gamma_1(t) = -\cos \omega_e t \quad ,$$

$$\Gamma_2(t) = \frac{3}{2} \cos^2 \omega_e t - \frac{1}{2} \quad . \tag{117}$$

If $q \neq 0$ and $\bar{q} = 0$, as applies to geometries 5, 6, and 8 in Table I, then only the low frequency ω_e occurs in $\Gamma_\lambda(t)$. For geometry 5 (Fig. 5b) the explicit forms at resonance are

$$\Gamma_1(t) = \sqrt{\frac{1}{2}} \sin \omega_e t \, (\cos \Delta - \sin \Delta) \quad ,$$

$$\Gamma_2(t) = (3/8)(1 - \cos 2\omega_e t)\,(1 - \sin 2\Delta) - 1/2 \quad . \tag{118}$$

These functions are plotted in Fig. 5b for $\Delta = 3\pi/4$ and for random Δ. In the latter case $\Gamma_1(t)$ and $\Gamma_2(t)$ are obtained from the above expressions by replacing $\cos \Delta$, $\sin \Delta$, and $\sin 2\Delta$ by their ensemble-averaged values of 0. This causes $\Gamma_1(t, \text{random } \Delta)$ to vanish, while the oscillatory part of $\Gamma_2(t)$ is reduced by a factor of two in amplitude.

For those cases in which the experimental geometry is such that $\bar{q} \neq 0$ (no. 2, 3, 4, 7, 9 through 13), the oscillation with ω_e forms an envelope for the rapid oscillation of frequency ω (Fig. 5c). The phase factor $(q-\bar{q})\Delta$ which is added to the high-frequency term in Eq. (65) simply describes a constant shift of the periodic pattern $e^{-iq\omega t}$. The angular correlation can be calculated by the corresponding formula in Tables I and II.

For geometry 13 the specific expressions for $\lambda = 1$ and 2 at resonance are

$$\Gamma_1(t) = \underset{\sim}{k}_1 \cdot \underset{\sim}{k}_2 = \frac{1}{\sqrt{2}} \{[\cos(\omega t + \Delta) - \sin(\omega t + \Delta)]\cos \omega_e t \cos \Delta$$

$$+ [\sin(\omega t + \Delta) + \cos(\omega t + \Delta)]\sin \Delta\}$$

$$\Gamma_2(t) = \frac{3}{2}(\underset{\sim}{k}_1 \cdot \underset{\sim}{k}_2)^2 - \frac{1}{2} \quad . \tag{119a}$$

Choosing Δ as random, these expressions become

$$\bar{\Gamma}_1(t) = \frac{1}{2} \cos(\omega t + \pi/4)\ (1 + \cos \omega_e t) \quad ,$$

$$\bar{\Gamma}_2(t) = -\frac{1}{8} + \frac{3}{8} \cos^2 \omega_e t - \frac{3}{16} \sin 2\omega t\ (1 + \cos \omega_e t)^2 \quad . \tag{119b}$$

The behavior of $\bar{\Gamma}_1(t)$ is straightforward. It is simply the product of fast and slow terms. If such a curve were observed with time-resolution much slower than ω^{-1}, then $\bar{\Gamma}_1(t)_{obs}$ would simply vanish. By contrast, $\bar{\Gamma}_2(t)$ exhibits more interesting behavior. With poor time-resolution only the term in $\sin 2\omega t$ would vanish, leaving the slow component

$$\overline{\Gamma}_2(t)_{obs} = -\frac{1}{8} + \frac{3}{8}\cos^2\omega_e t \quad ,$$

as shown in Fig. 5(c).

Figure 6 shows the rapid oscillation ωt which, at resonance, near $t = 0$, represents the spin rotation in the field $\underset{\sim}{H}_0$ (the influence of $\underset{\sim}{H}_1$ is not yet evident). Examples are shown for two specific geometries (No. 9 and 11), with $H_1/H_0 = 10^{-3}$. A number of features are illustrated by this figure: (1) The shapes of the curves are identical for the two geometries chosen. (2) Near $t = 0$ only terms with $q = \bar{q}$ contribute since $\lim_{t\to 0} G^{q\bar{q}}_{\lambda\lambda}(t) = 1$. (3) Because of (2), the starting phase of the spin rotation is determined by the geometry alone. Although not shown in Fig. 6, the curves for $\omega/\omega_0 = 1.001$, 1.000, and 0.999 are practically indistinguishable on this scale near $t = 0$. The geometrical interpretation of this behavior is clear, since near $t = 0$ the limiting value of $\Gamma_\lambda(t)$ for these geometries is

$$\Gamma_\lambda(t) = P_\lambda[\cos\eta(t)] = P_\lambda\{\cos[\omega_0 t - (\phi_2 - \phi_1)]\} \quad . \tag{120}$$

To observe a resonance effect the condition $\omega_1\tau \geq 1$ must be fulfilled. Thus, for $H_1/H_0 = 10^{-3}$, as in Fig. 6, the amplitude of the rapidly oscillating functions will be appreciably affected only after $\approx \omega_0/\omega_1 = 10^3$ oscillations. An example of this behavior is given in Fig. 7 where a time segment of the differential perturbation factor $\Gamma_\lambda(t)$ near $\omega_1 t = 10^{-3}\ \omega_0 t = 1$ is shown. The following features are apparent: (1) The curves differ for different values of ω/ω_0, indicating the resonance effect. (2) Random and fixed-phase curves differ due to the contribution of factors with $q \neq \bar{q}$ in the case of fixed phases. (3) When passing through the resonance a change is observed for both amplitude and phase.

The behavior of the amplitude and phase near resonance depends crucially on the time segment selected and the specific geometry. For example, Fig. 7 represents a special case. In geometry 9 the rf field at t = 0 is parallel to $\underset{\sim}{k}_1$ at the resonant frequency ($\omega = \omega_0$) and therefore has no effect at all. In fact rather than inducing transitions it prevents them, acting thereby as a holding field. Thus the effect observed at $\omega = \omega_0$ for any geometry in which $\underset{\sim}{k}_1$ is parallel to $\underset{\sim}{H}_1(0)$ is really an "antiresonance". This effect will be discussed further in connection with Figs. 10 and 15.

The rapid oscillations shown in Figs. 6 and 7 represent spin rotations about the constant field H_0 which are conventionally measured with the field oriented perpendicular to the detector plane. They are only observable in levels with long lifetimes, and with reasonably low values of H_0. This means that in time-differential experiments one must take into account the envelope functions only if the time resolution is sufficiently good to resolve the high-frequency component. Should this fast oscillation be averaged out by the instrumental time resolution, only terms with $\bar{q} = 0$ contribute to the final perturbation factor (see Fig. 5c). An example can clarify this point. At room temperature the resonance for ^{100}Rh in Ni occurs at about 340 MHz.[1] The average period of the $\lambda = 2$ oscillations in Figs. 6 and 7 is $\delta = \pi/\omega_0$, or about 1.5 nsec in the case of ^{100}Rh in Ni. An observation of this fast oscillation requires a time resolution of about 1 nsec. The situation is still more difficult for ^{100}Rh in Fe which at room temperature has a resonance frequency of 883 MHz.[21] This frequency corresponds to a time period of about 0.57 nsec. Thus, it is difficult to observe the fast spin rotation of ^{100}Rh in Fe or Ni with present experimental techniques. However, this difficulty was

the very reason that led to the NMR/PAC method, which is not in any way restricted by the time-resolution of the equipment.

V.2. Random rf Phase

If the time of formation of the nuclear level is unrelated to the phase of the radiofrequency field, averaging over all phase angles Δ leads to $q = \bar{q}$ (Eq. (63)). For this situation the modulation function Eq. (115) at $\omega = \omega_0$ has the form

$$S^{qq}_{\lambda\lambda}(t)_{res} = \sum_p e^{-ip\omega_1 t} \left[d^{(\lambda)}_{qp}\left(\frac{\pi}{2}\right)\right]^2 \quad . \tag{121}$$

In the rotating frame $S'(t)$ at resonance the direction of $\underset{\sim}{H}_e$ coincides with $\underset{\sim}{H}_1$, which gives $\beta = \frac{\pi}{2}$ and $\omega_e = \omega_1$. Thus, the quantization axis of the representation in which $\mathcal{H}''$ is diagonal is parallel to $\underset{\sim}{H}_1$; the states $|In\rangle$ are stationary with respect to the x'-axis.

In experiments where the symmetry axis $\underset{\sim}{k}_1$ ($\underset{\sim}{k}_2$) of the oriented ensemble is parallel to the quantization axis $\underset{\sim}{z} = \underset{\sim}{H}_0$, with respect to which $G^{q\bar{q}}_{\lambda\lambda}(t)$ is given, only terms with $q = 0$ ($\bar{q} = 0$) contribute and Eq. (121) simplifies to

$$G^{00}_{\lambda\lambda}(\omega_1 t)_{res} = S^{00}_{\lambda\lambda}(t)_{res} = \sum_p e^{-ip\omega_1 t} \frac{(\lambda - p)!}{(\lambda + p)!}\left[P^p_\lambda(0)\right]^2$$

$$= \frac{(\lambda!)^2}{(\lambda!!)^4} + 2 \sum_{p>0} \frac{(\lambda - p)!(\lambda + p)!}{\left[(\lambda - p)!!(\lambda + p)!!\right]^2} \cos(p\omega_1 t) \quad , \tag{122}$$

where the explicit expression for $P^p_\lambda(0)$ has been used. The sum over p includes only terms with $\lambda + p$ = even.

In this specific case ($q = \bar{q} = 0$) the angular distribution of the radiation X_2 is given by (compare Eq. (76)):

$$W(\underset{\sim}{k}_1 \| \underset{\sim}{H}_0, \theta, t) = \sum_{\lambda} B_\lambda(I)\, A_\lambda\, (X_2)\, G^{00}_{\lambda\lambda}(t)_{res}\, P_\lambda(\cos\theta) \quad , \tag{123}$$

where θ is the angle between $\underset{\sim}{k}_1 (\| \underset{\sim}{H}_0)$ and $\underset{\sim}{k}_2$. Equation (123), with expression (Eq. (122)) for the perturbation coefficient $G^{00}_{\lambda\lambda}(t)_{res}$ inserted, describes a rotation of the angular distribution pattern about $\underset{\sim}{H}_1$ with a frequency ω_1. If the g-factor of the nuclear state is unknown, observation of the time-dependence of $G^{00}_{\lambda\lambda}(t)_{res}$ makes it possible to determine the effective amplitude, H_1^{eff}, of the radio-frequency field at the nucleus. In those cases where the externally applied rf field is enhanced by a paramagnetic or ferromagnetic coupling the enhancement factor $(1 + H_{int}/H_{ext})$ can be accurately determined. This possibility of a direct observation of H_1^{eff} is a valuable feature of the NMR/RD method.

VI. NMR BEHAVIOR OF TIME-INTEGRATED ANGULAR DISTRIBUTIONS

VI.1. General Considerations

In time-differential experiments the total perturbation factor is always periodic in time irrespective of the magnitudes of H_1 and H_0 provided only that these fields are sharply defined. However, time-integral measurements yield attenuation effects which depend sensitively on H_1, H_0 and the lifetime τ. In contrast to conventional NMR we find in NMR/RD a wide variety of line shapes. There are several reasons for this additional complexity, notably the extra vector $\underset{\sim}{k}_1$, higher multipole-order observables, and the natural time scale of the nuclear decay.

In planning an NMR/RD experiment one often wants the highest possible sensitivity consistent with the geometrical constraints, if any, imposed by the apparatus. Clearly there are many possible distinct sets of experimental conditions. The relative orientations of the four vectors $\underset{\sim}{k}_1$, $\underset{\sim}{k}_2$, $\underset{\sim}{H}_0$, and $\underset{\sim}{H}_1$, the magnitude of $\omega_1\tau$, and the option in some cases of fixed or random phase present an embarrassment of choice. With the observation of a few basic principles, however, selection of an optimum geometry is usually straightforward. There will be important symmetry considerations for a majority of experiments.

The formalism developed in Secs. II and III led to a general formula (see Eq. (62)) for the time-integrated perturbation coefficient that describes an axially symmetric static interaction in the presence of a radio-frequency (rf) field. For the special case of pure magnetic dipole interactions the perturbation factor has the form given in Eq. (66). This equation can be used to describe resonance experiments with various geometries and phase relations. In order to discuss resonance effects in time-integrated NMR/PAC measurements, a

few typical numerical results will be presented for some specific geometries and representative parameters. The discussion will distinguish between the resonance behaviors for random- and fixed-rf phase.

For some specific geometries the form of the angular correlation function can be obtained from Tables I ($\lambda = 1$), II ($\lambda = 2$), and III ($\lambda = 4$). In each table the response function $\Gamma_\lambda(t)$ is expressed in terms of the time-dependent perturbation factors $G_{\lambda\lambda}^{q\bar{q}}(\omega,t)$ (Eq. (80)). The time-integrated response function $\hat{\Gamma}_\lambda(\omega,t)$ bears the same functional relationship to the time-integral factors $\hat{G}_{\lambda\lambda}^{q\bar{q}}(\omega)$ (Eq. (61)). Since the phase angle Δ is included in $G_{\lambda\lambda}^{q\bar{q}}(\omega,t)$ and $\hat{G}_{\lambda\lambda}^{q\bar{q}}(\omega)$ (Eq. (65), (66)), the relations in these tables are valid for any Δ. The corresponding $\Gamma_\lambda(\omega,t)$ or $\hat{\Gamma}_\lambda(\omega)$ for random Δ may be obtained in each case by striking out the terms with $q \neq \bar{q}$ (Eq. (67)).

Also given in Table I are the explicit expressions for $\Gamma_\lambda(t) = P_1[\cos \eta(t)] = \underset{\sim}{K}(t)\cdot\underset{\sim}{k}_2$ that are found from Eq. (97) or by working out the $G_{\lambda\lambda}^{q\bar{q}}(\omega,t)$ factors in detail (Eq. (65)). Time-integral functions $\hat{\Gamma}_\lambda(\omega)$ may be obtained by integrating on $\tau^{-1}e^{-t/\tau}dt$ (Eq. (104)), while response functions for random Δ are obtained by integrating over $(2\pi)^{-1}\,d\Delta$. The corresponding expressions

$$\Gamma_2(t) = P_2[\cos \eta(t)] = \frac{3}{2}(\underset{\sim}{K}(t)\cdot\underset{\sim}{k}_2)^2 - \frac{1}{2} \quad ,$$

and

$$\Gamma_4(t) = P_4[\cos \eta(t)] = \frac{35}{8}(\underset{\sim}{K}(t)\cdot\underset{\sim}{k}_2)^4 - \frac{15}{4}(K(t)\cdot\underset{\sim}{k}_2)^2 + \frac{3}{8} \quad ,$$

are not given explicitly in Tables II and III, but they may be calculated, for each geometry, from the appropriate expression for $\underset{\sim}{K}(t)\cdot\underset{\sim}{k}_2$ as given in Table I.

Before starting we note that there are four natural frequency variables for any experiment: ω, ω_0, ω_1, and $1/\tau$. We can completely characterize any experimental situation by calculating $\hat{\Gamma}_\lambda$ as a function of the dimensionless variable $(\omega-\omega_0)/\omega_1$, with $\omega_1\tau$ held constant.* Let us make an observation at this point about linewidth. For low rf power ($\omega_1\tau \ll 1$) the natural linewidth $\hbar/\tau$ may be approached, but few nuclei will participate in rf transitions. For high power ($\omega_1\tau \gg 1$) most of the nuclei may experience rf transitions, but the linewidth will broaden to $\sim \hbar\omega_1$. Clearly maximum efficiency is achieved for $\omega_1\tau \sim 1$.

VI.2. Random rf Phase

VI.2.1. Resonance Line Shapes for $\underset{\sim}{k}_1$ and/or $\underset{\sim}{k}_2$ parallel to $\underset{\sim}{H}_0$

The general expression of the perturbation factor for random rf phase follows from Eq. (66) with $q = \bar{q}$:

$$\hat{G}^{qq}_{\lambda\lambda}(\omega) = \sum_p \frac{1 - i(p\,\omega_e + q\omega)\tau}{1 + [p\,\omega_e + q\omega]^2\tau^2} \left[d^{(\lambda)}_{qp}(\beta)\right]^2 \quad . \tag{124}$$

This equation can be used to calculate the various terms of $\hat{\Gamma}_\lambda$ in Tables I-III. An inspection of these tables shows that whenever $\underset{\sim}{k}_1$ or $\underset{\sim}{k}_2$ is parallel to the $\underset{\sim}{z}$-axis, as is the case in geometries no. 1 through 8, the response function Γ_λ contains only the one term $\hat{G}^{00}_{\lambda\lambda}$, since $q = \bar{q}$. Therefore the discussion will concern mainly these terms. Since the imaginary parts cancel for $q = 0$, we obtain from Eq. (124)

---

*The signs of ω_0 and ω_1 are defined consistently. Thus $(\omega-\omega_0)/\omega_1$ is always understood to mean $(\omega-|\omega_0|)/(|\omega_1|)$.

$$\hat{G}^{00}_{\lambda\lambda}(\omega) = \sum_{p} \frac{1}{1 + (p\ \omega_e \tau)^2} \left[d^{(\lambda)}_{0p}(\beta)\right]^2 \quad . \tag{125}$$

At resonance the perturbation coefficient becomes (compare Eq. (122))

$$\hat{G}^{00}_{\lambda\lambda}(\omega_1)_{res} = \sum_{p} \frac{(\lambda-p)!(\lambda+p)!}{[(\lambda-p)!!(\lambda+p)!!]^2} \left[\frac{1}{1 + (p\omega_1\tau)^2}\right] \qquad \text{for } (\lambda+p) \text{ even}$$

$$= 0 \qquad \text{for } (\lambda+p) \text{ odd} \quad . \tag{126}$$

An interesting feature of NMR/RD experiments is that a nonzero "hard-core" value of $\hat{G}^{00}_{\lambda\lambda}$ exists at resonance for λ even. In the limit of large rf amplitudes, i.e. large values of H_1, such that $\omega_1\tau \gg 1$ is satisfied, only the term with $p = 0$ in Eq. (126) remains:

$$\lim_{\omega_1\tau \to \infty} (\hat{G}^{00}_{\lambda\lambda})_{res} = \frac{[\lambda!]^2}{[\lambda!!]^4} \quad \text{for } \lambda \text{ even} \quad . \tag{127a}$$

Here, $\lambda!! = \lambda(\lambda-2)(\lambda-4)\cdots 2$ or 1. Using a more physical picture the hard core for $\beta = \pi/2$ comes about by integrating the Legendre polynomial around a meridian in the z' - y' plane.

$$\lim_{\omega_1\tau \to \infty} (\hat{G}^{00}_{\lambda\lambda})_{res} = \frac{1}{2\pi} \int_0^{2\pi} P_\lambda(\cos\eta)d\eta = \frac{[\lambda!]^2}{[\lambda!!]^4} \quad , \quad \lambda \text{ even}$$

$$= 0 \quad , \quad \lambda \text{ odd} \quad . \tag{127b}$$

The existence of this lower limit or hard core for λ = even implies that, at resonance, a fraction of the anisotropy always remains, no matter how large the imposed rf amplitude is. This hard-core behavior is illustrated in Fig. 8, in which $\hat{\Gamma}_\lambda = (\hat{G}^{00}_{\lambda\lambda})_{res}$ of Eq. (126) is plotted versus H_1/H_0 for some representative values of $\omega_0\tau$.

It is important to note, however, that at frequencies off resonance the perturbation coefficient $\hat{G}^{00}_{\lambda\lambda}(\omega)$ with λ = even can actually reach zero for sufficiently large amplitudes of H_1. The perturbation coefficient (Eq. (125)) vanishes, even for p = 0, if $d^{(\lambda)}_{00}(\beta) = P_\lambda(\cos\beta_\lambda) = 0$. This condition can be expressed in terms of the "maximum perturbation frequency" ω' by using Eq. (44):

$$\omega' = \omega_0 \left(1 - \frac{\cos\beta_\lambda}{\sqrt{1 - \cos^2\beta_\lambda}} \frac{H_1}{H_0}\right) . \qquad (128)$$

Here β_λ are the angles for which the Legendre polynomial $P_\lambda(\cos\beta_\lambda)$ vanishes, e.g. $\beta_{\lambda=1} = 90°$, $\beta_{\lambda=2} = 54.7°$, and $\beta_{\lambda=4} = 30.6°$ and $70.1°$. Since ω' in Eq. (128) is symmetric about resonance ω_0, $\hat{G}^{00}_{\lambda\lambda}$ behaves like a λ-fold split resonance line. This structure is demonstrated in Fig. 9 for λ = 1 through 4. It is a purely geometrical effect caused by the fact that multipole radiation with its characteristic intensity pattern is used to detect the resonance. This effect was first observed for the case λ = 2 in optical studies,[9,41] and all the formulae derived above apply to optical double-resonance experiments as well.

In connection with optical double resonance work it was pointed out[9] that the splitting of the resonance line allows a reliable determination of H_1. The distance between the points of maximum perturbation is obtained from Eq. (128)

$$(\omega_0 - \omega') = \frac{\cos \beta_\lambda}{\sqrt{1 - \cos^2 \beta_\lambda}} \omega_1 \quad . \tag{129}$$

For $\lambda = 2$, for example, $\cos \beta_2 = \pm 1/\sqrt{3}$ which gives $(\omega_0 - \omega') = \omega_1/\sqrt{2}$. Thus, with the frequency scale chosen in Fig. 9 the two minima occur at ± 0.71. Of course, the nuclear orientation is not destroyed at these minima, because of coherence exists among the substates. The nuclei are still oriented about $\underset{\sim}{H}_e$, and an adiabatic frequency shift will restore the orientation in the laboratory frame. By contrast, relaxation effects will destroy nuclear orientation in the $\underset{\sim}{H}_e$ frame (see Sec. VII).

The resonance behavior of $\hat{G}^{00}_{\lambda\lambda}(\omega)$ is shown for $\lambda = 1$ to 4 in Fig. 9. The frequency scale was chosen in such a way that the width of the curves is normalized with respect to H_1. The effect of power broadening of the resonance line which occurs for increasing rf amplitudes is readily deduced from this figure. It is apparent from the figure that for Δ random and any λ, $\hat{G}^{00}_{\lambda\lambda}$ is an even function of $(\omega-\omega_0)/\omega_1$, and hence is insensitive to the sign of ω_0. This statement also applies to any geometry with random Δ and $q = \bar{q} \neq 0$. For $q = 0$, this result is easily proved from Eq. (125) using the relation $[d^{(\lambda)}_{0p}(\beta)]^2 = [d^{(\lambda)}_{0p}(\pi-\beta)^2$ (see Eq. (68)).

If the angular distribution of allowed β-radiation emitted from a polarized nuclear state is used to detect the resonance, the line shape is determined by the term in $\lambda = 1$. In this case Eq. (125) reduces to

$$\hat{G}^{00}_{11} = \frac{1 + (\omega_0-\omega)^2\tau^2}{1 + (\omega_0-\omega)^2\tau^2 + (\omega_1\tau)^2} \quad . \tag{130}$$

Hence the line shape as a function of ω is a Lorentzian, as was pointed out by Sugimoto et al.[20]

VI.2.2. Resonance Line Shapes for $\underset{\sim}{k}_1$ and $\underset{\sim}{k}_2$ Non-Parallel to $\underset{\sim}{H}_0$

In the case of random phase these geometries lead to a response function which contains factors of the form given in Eq. (124). Examples are geometries 9 through 13 in Tables I-III. It can be inferred from Eq. (124) that the terms with $q \neq 0$ are considerably smaller than those with $q = 0$. Numerical calculations confirm this. Thus for complicated geometries the leading terms $\hat{G}^{00}_{\lambda\lambda}$ determine the shape of the resonance.

At resonance Eq. (124) takes the form

$$(\hat{G}^{qq}_{\lambda\lambda})_{res} = \sum_p \frac{1 - i(p\,\omega_1 + q\,\omega_0)\tau}{1 + (p\,\omega_1 + q\,\omega_0)^2\tau^2} [d^{(\lambda)}_{qp}\,(\pi/2)]^2 \quad . \tag{131}$$

For $\omega_1\tau \to \infty$ these perturbation terms show the same hard-core behavior discussed in connection with Eq. (126). In addition, a similar effect may be achieved even at modest rf amplitudes for large values of $\omega_0\tau$. Keeping $\omega_1\tau$ constant the perturbation term $(\hat{G}^{qq}_{\lambda\lambda})_{res}$ vanishes for $\omega_0\tau \to \infty$, unless $q = 0$. Large $\omega_0\tau$ and $\omega_1\tau$ values can be realized in experiments with large magnetic fields and long nuclear lifetimes.

In any NMR/RD experiment a natural symmetry axis about $\underset{\sim}{k}_1$ exists at $t = 0$. As $\underset{\sim}{K}(t)$ evolves there is no symmetry axis fixed in the laboratory frame until, as $\omega_0\tau \to \infty$, $\underset{\sim}{H}_0$ becomes a symmetry axis. For random-phase cases the symmetry is very simple. Whatever the position of $\underset{\sim}{k}_1$, $\underset{\sim}{K}(t)$ will precess until

ρ_0^λ, originally diagonal along $\underset{\sim}{k}_1$, becomes in the time-average diagonal along $\underset{\sim}{H}_0$, i.e., until the nuclei become oriented along $\underset{\sim}{H}_0$, in the ensemble average. Since $\underset{\sim}{k}_1$ and $\underset{\sim}{H}_0$ are in general not parallel, the magnitude of $\rho_0^\lambda(\underset{\sim}{H}_0)$ is usually less than that of $\rho_0^\lambda(\underset{\sim}{k}_1)$, because of averaging. If $\underset{\sim}{H}_0$ is the only magnetic field present, we have, for the limit $\omega_0\tau \to \infty$ (cf. Eq. (4))

$$(\rho_0^\lambda)_{\underset{\sim}{H}_0} = (\rho_0^\lambda)_{\underset{\sim}{k}_1} P_\lambda(\cos\theta_1) \quad . \tag{132}$$

If a strong radiofrequency field is also present, and $\omega_1\tau \to \infty$ with $\omega_0 >> \omega_1$ still, then $\underset{\sim}{K}(t)$ must be averaged around $\underset{\sim}{H}_e$ before being averaged around $\underset{\sim}{H}_0$. For this case Eqs. (110) and (111) give

$$(\rho_0^\lambda)_{\underset{\sim}{H}_0} = (\rho_0^\lambda)_{\underset{\sim}{k}_1} \overline{P_\lambda[\cos(\underset{\sim}{k}_1,\underset{\sim}{H}_e)]}\, P_\lambda(\cos\beta) \quad . \tag{133}$$

The line over $P_\lambda[\cos(\underset{\sim}{k}_1,\underset{\sim}{H}_e)]$ denotes an average over Δ. For frequencies far off resonance, $\beta \to 0$ and Eq. (133) reduces to Eq. (132).

Now $(\rho_0^\lambda)_{\underset{\sim}{H}_0}$ is simply a statistical tensor describing an ensemble of nuclei oriented relative to $\underset{\sim}{H}_0$. Thus the response function corresponding to Eqs. (132) and (133) can be written respectively

$$\hat{\Gamma}_\lambda = P_\lambda(\cos\theta_1)\, P_\lambda(\cos\theta_2) \quad , \tag{134}$$

for $\omega_0\tau \to \infty$ with no rf field present, and (cf. Eq. (114)):

$$\hat{\Gamma}_\lambda = \overline{P_\lambda[\cos(\underset{\sim}{k}_1,\underset{\sim}{H}_e)]}\, P_\lambda(\cos\beta)\, P_\lambda(\cos\theta_2) \quad , \tag{135}$$

for $\omega_1\tau \to \infty$ with $\omega_0 >> \omega_1$. In the average over Δ, the specific form

$$\cos(\underset{\sim}{k}_1,\underset{\sim}{H}_e) = \cos\beta\,\cos\theta_1 + \sin\beta\,\sin\theta_1\,\cos(\phi_1 - \Delta) \quad ,$$

should be used. Because $|P_\lambda(x)|$ has its maximum value of 1 at $x = \pm 1$, it is clear from this relation that the strongest angular correlations are obtained with parallel geometry, $\underset{\sim}{k}_1 \| \underset{\sim}{k}_2 \| \underset{\sim}{H}_0$. Inspection of Tables I-III shows that for each geometry the coefficient of $G^{00}_{\lambda\lambda}$ is $P_\lambda(\cos\theta_1)\,P_\lambda(\cos\theta_2)$.

Finally, for λ odd, random Δ, and $\underset{\sim}{k}_1$ in the x,y plane, we note that $\hat{\Gamma}_\lambda(\omega)$ vanishes identically for all $\omega_1\tau$ and ω because the ensemble average over Δ must be taken over odd powers of $\cos(\phi_1 - \Delta)$ (see Eq. (135)).

VI.2.3. Comparison with Spin-Rotation Measurements

A few observations can be made about the advantages and the applicability of time-integrated NMR/RD in comparison with time-differential PAC measurements in static fields oriented perpendicular to the detector plane. The latter, also known as the "spin rotation" method, measures the interaction frequency as a function of time. A Fourier analysis of these data yields the interaction frequency. An elegant derivative of the spin rotation method is the "stroboscopic" technique,[31] which compares the interaction frequency with a known frequency standard and in this way directly measures the frequency transform of the time spectrum.

An advantage of spin rotation or stroboscopic methods is that no energy is absorbed by the nuclear ensemble and thus no power broadening occurs. The width of the frequency transform is given by the nuclear lifetime and/or any relevant relaxation time. The applicability of these time-differential

techniques is, however, limited by the resolution time of the detection equipment. Hence for large interaction frequencies NMR/RD is the only method that can be applied. Notice that the conditions for the NMR technique to work effectively are $\omega_0\tau >> 1$ and $\omega_1\tau \geq 1$. Thus if a large effect is to be observed, the resonance line must be broadened by H_1. The extraction of any information about the lifetime τ or a possible relaxation time τ_{relax} by means of Eq. (125) then depends crucially on the knowledge of H_1.

VI.3. Fixed rf Phase (Pulsed rf)

VI.3.1. Symmetry Properties of $\hat{\Gamma}_\lambda$ for $\underset{\sim}{k}_2 \| \underset{\sim}{z}$:

Turning now to fixed-phase experiments, a wide range of behavior of $\hat{\Gamma}_\lambda$ is possible. It is worthwhile to discuss cases in which at least one of the vectors $\underset{\sim}{k}_1$, $\underset{\sim}{k}_2$ is along $\underset{\sim}{H}_0$ (these are the best cases in the sense of providing the largest effects). If the rf-phase has a well-defined value with respect to the time t = 0 when the nuclear level is formed, terms with $\bar{q} \neq q$ occur in the angular correlation function (see Eq. (66)). The general form of the response function as defined in Eq. (80) can be obtained from Tables I-III for a few interesting geometries. For fixed rf phase Δ the response functions depend strongly on phase angle and geometry and have little in common with the ones for random phase (Fig. 9). We wish to characterize the important symmetry properties of Γ_λ, for two reasons: (1) It is of practical value to know the relative sensitivities of $G_{\lambda\lambda}^{q\bar{q}}$ for different experimental configurations; and (2) we want explore the possibility of determining the sign of gH_0 without using a circularly-polarized rf field $\underset{\sim}{H}_1(t)$. We shall discuss the sign of gH_0 or that of ω_0 rather than that of g alone because for some important cases hyperfine

fields of unknown sign may play the role of H_0. The cases $\omega_1\tau \to \infty$ and $\omega_1\tau$ finite will be discussed separately.

From Eq. (66) it follows that for Δ fixed the cross-terms of the perturbation factor, $\hat{G}^{q\bar{q}}_{\lambda\lambda}$, with $q \neq \bar{q}$, have finite values as $\omega_1\tau \to \infty$. Thus even in the saturation limit $\hat{\Gamma}_\lambda(\infty)$ is strongly geometry-sensitive. We shall first discuss four cases in which $\underset{\sim}{k}_2$ is parallel to $\underset{\sim}{z}$, which gives $\bar{q} = 0$, since $Y_{\lambda\bar{q}}(0,\phi_2) = \delta_{\bar{q},0}\sqrt{\frac{2\lambda+1}{4\pi}}$. The limiting value for $G^{q0}_{\lambda\lambda}(\omega_1\tau \to \infty)$ consists only of the term for $p = 0$. Thus, from Eqs. (66) and (80) it follows that in this case the response function $\hat{\Gamma}_\lambda(\omega_1\tau \to \infty)$ can be written in the form:

$$\hat{\Gamma}_\lambda(\infty) = P_\lambda(\cos\beta) \sum_{q=-\lambda}^{+\lambda} \cos q(\Delta-\phi_1)\, d^{(\lambda)}_{q0}(\beta)\, d^{(\lambda)}_{q0}(\theta_1) \quad . \tag{136}$$

Figure 10 shows $\hat{\Gamma}_\lambda(\infty)$ for $1 \leq \lambda \leq 4$ for the cases ($\theta_1 = \pi/2$, $\phi_1 = \Delta$, i.e., $\underset{\sim}{k}_1 \| \underset{\sim}{x}'$ at $t = 0$), ($\theta_1 = \pi/2$, $\phi_1 = \pi/2 + \Delta$, i.e., $\underset{\sim}{k}_1 \| \underset{\sim}{y}'$ at $t = 0$), ($\theta_1 = \pi/2$, ϕ_1 random, i.e., $\underset{\sim}{k}_1$ random in the x'y' plane at $t = 0$), and, for comparison, ($\theta_1 = 0$, i.e., $\underset{\sim}{k}_1 \| \underset{\sim}{z}'$). The asymmetry that remains, for odd λ, as $\omega_1\tau \to \infty$ will be referred to as <u>persistent</u> asymmetry. It is insensitive to the sign of gH_0 since in the limit $\omega_1\tau \to \infty$, $\hat{\Gamma}_\lambda$ depends only on β, which is invariant against a sign change of gH_0 (compare Eq. (44)). A physical picture of this result would be the following: In the S' frame $\underset{\sim}{K}(t)$ precesses over a circular path (see Fig. 4); for $\omega_1\tau \to \infty$ the factor $e^{-t/\tau}$ approaches constancy and all segments of the circular path are weighted equally. Thus the sense of the precession is unimportant and the sign of gH_0 does not affect $\hat{\Gamma}_\lambda(\infty)$.

From Eq. (136) the following rules can be established:

(1) For Δ fixed and λ even, $\hat{\Gamma}_\lambda(\infty)$ is an even function of $(\omega-\omega_0)/\omega_1$, as in the case of random phase.

(2) For Δ fixed and λ odd, $\hat{\Gamma}_\lambda(\infty)$ is either an odd function of $(\omega-\omega_0)/\omega_1$, or else it does not depend on frequency at all, and vanishes for all frequencies.

The antiresonance phenomenon arises again in Fig. 10, in connection with the four curves labeled $\hat{\Gamma}_\lambda(x,z)$, because for this case, $\underset{\sim}{K}(t)$ and $\underset{\sim}{H}_1$ are both parallel to the x axis in the $S'(t)$ frame at resonance, and $\underset{\sim}{H}_1$ therefore acts as a holding field. Because $\underset{\sim}{H}_1$ induces no transitions at $\omega = \omega_0$, the perturbation factors have the same value at resonance as they have far off resonance; i.e., $\hat{\Gamma}_\lambda(\omega = \omega_0) = \hat{\Gamma}_\lambda(\omega = \pm\infty)$.

The remaining category of experiments, not covered by the above discussion, is that for which Δ is fixed and $\omega_1\tau$ is finite. In the limit $\omega_1\tau \to \infty$ the imaginary terms $i(p\,\omega_e\tau)$ vanish. (See Eq. (66).) For $\omega_1\tau \sim 1$, however, these imaginary terms are about the same size as the real components, and they can lead to asymmetries that are sensitive to the sign of gH_0. Since in this section we are concerned only with $\underset{\sim}{k}_2 \| \underset{\sim}{z}$, the discussion applies to geometries no. 1', 5, 6, and 8 in Tables I-III. For these geometries the response function $\hat{\Gamma}_\lambda$ (which is of course real) includes imaginary parts $\mathrm{Im}\{G_{\lambda\lambda}^{q0}\}$ which bring about an asymmetry. It should be remembered that $\mathrm{Re}\{G_{\lambda\lambda}^{q\bar{q}}\}$ and $\mathrm{Im}\{G_{\lambda\lambda}^{q\bar{q}}\}$ have opposite symmetries about resonance (see Eqs. (68)); for even (odd) q, the real (imaginary) part of $G_{\lambda\lambda}^{q0}$ is symmetric about the resonant frequency, while the imaginary (real) part is antisymmetric.

The response function $\hat{\Gamma}_\lambda$ can be affected in two ways. Both arise from the sense of precession about H_1 and both are <u>transient</u>, disappearing as $\omega_1\tau \to \infty$. It is not feasible to observe the sign of ω_0 <u>directly</u> in a time-integral experiment, as this sign will affect $\hat{\Gamma}_\lambda$ only in order ω_1/ω_0. Thus

all gH_0 sign determinations are made by measuring the sign of ω_1, as the geometries given below will indicate. We shall refer to the sign of ω_0 or ω_1 interchangeably. This implies that we know the sign of $\underset{\sim}{H}_0$ and also the phase Δ, which gives the sign of $\underset{\sim}{H}_1$ at $t = 0$. Maximum sensitivity in sign determinations can be attained by taking $\underset{\sim}{k}_2$ along $\underset{\sim}{H}_0$: this choice precludes any possibility of determining the sign of ω_0 directly, but (as discussed later) it offers the greatest variation of $\hat{\Gamma}_\lambda$ with ω.

The first way to infer the sign of the interaction is from asymmetry of the response function about the resonance. The sign of ω_0 can affect $\hat{\Gamma}_\lambda$ to render

$$\hat{\Gamma}_\lambda \left(\frac{\omega-\omega_0}{\omega_1} , \omega_0 > 0 \right) = (-1)^\lambda \hat{\Gamma}_\lambda \left(\frac{\omega_0-\omega}{\omega_1} , \omega_0 < 0 \right) \neq \hat{\Gamma}_\lambda \left(\frac{\omega-\omega_0}{\omega_1} , \omega_0 < 0 \right) . \quad (137)$$

Thus $\hat{\Gamma}_\lambda$ is neither an even nor an odd function of $\frac{\omega-\omega_0}{\omega_1}$, but $\hat{\Gamma}_\lambda(\omega_0 > 0)$ is $(-1)^\lambda$ times the reflection of $\Gamma_\lambda(\omega_0 < 0)$ through the resonant frequency.

As an example Fig. 11 shows the resonance curves which are to be expected with geometry no. 5. The marked feature of these curves is the asymmetry about $\omega = \omega_0$ for opposite signs of ω_1, or equivalently (for λ even) for the angles $\phi_1 = 45°$ (225°) and 135° (315°). This asymmetry can be used to determine the sign of ω_1 even when linearly-polarized rf is used. The difficulty in practice, however, is that the shift is small and can only be picked up in experiments that have great sensitivity and are free of additional broadening.

To understand the origin of the observable asymmetry, let us follow $\underset{\sim}{K}(t)$ as it evolves in the S' frame according to the torque equation (100). At

resonance, with $\underset{\sim}{H}_e \| x'$, $\hat{\Gamma}_\lambda$ is insensitive to the sign of ω_1 for even λ: this is a consequence of the even parity of P_λ. Off resonance this is no longer true. Suppose ω is slightly below ω_0, for example, and $\underset{\sim}{H}_e$ is thus in the (+ x', + z') quadrant of the x'z' plane. For $\theta_1 = \pi/2$, $\phi_1 = \pi/4$ as shown, and $\omega_1 > 0$, $\underset{\sim}{K}(t)$ will start up into the (+ x', + y', + z') octant, $\eta(t)$ will decrease rather abruptly from $\pi/2$, and $\Gamma_2(t)$ will increase rapidly from -1/2. For $\omega_1 < 0$, on the other hand, $\underset{\sim}{K}(t)$ will swing down into the (+ x', + y', - z') octant and $\eta(t)$ will increase rather slowly from $\pi/2$. Thus $\Gamma_2(t)$ will remain longer near -1/2. For $|\omega_1\tau| \sim 1$ a large fraction of the nuclei will decay while the effects of this transient asymmetry are still large, and they will affect $\hat{\Gamma}_\lambda$. For $|\omega_1\tau| >> 1$ this is no longer true and the line becomes symmetrical. Clearly experiments of the class illustrated in Fig. 11 are completely equivalent to time-integral PAC experiments in the S' frame, with precession taking place about $\underset{\sim}{H}_e$.

The second way in which the sign of ω_1 can affect $\hat{\Gamma}_\lambda$ is really very similar, though superficially quite different. In this case Γ_λ is an even function of $(\omega-\omega_0)/\omega_1$, but it is a <u>different</u> even function for $\omega_1 > 0$ than for $\omega_1 < 0$. Figure 12 illustrates this effect for geometry 8 ($\underset{\sim}{k}_1 = \sqrt{\frac{1}{2}}\,(\underset{\sim}{e}_y + \underset{\sim}{e}_z)$, $\underset{\sim}{k}_2 = \underset{\sim}{e}_z$, $\Delta = 0$). This is the exact equivalent, for NMR/PAC, of the most common arrangement for determining g-factors by time-integral PAC studies. In fact, for $\omega = \omega_0$ we find

$$\Gamma_\lambda(t) = P_\lambda[\cos(\theta_1 - \omega_1 t)] \quad , \tag{138}$$

$$\hat{\Gamma}_2 = \frac{1}{\tau} \int_0^\infty e^{-t/\tau} P_2[\cos(\theta_1 - \omega_1 t)]\, dt$$

$$\hat{\Gamma}_2 = \frac{1}{4} + \frac{3}{4} \frac{\cos 2(\theta_1 - \theta')}{\sqrt{1 + (2\omega_1\tau)^2}} \quad . \tag{139}$$

Here $\theta' = \frac{1}{2} \tan^{-1} 2\omega_1\tau$. The difference at resonance, due to the $\lambda = 2$ term, is

$$a_2 = 2 \frac{W(\omega_0 > 0) - W(\omega_0 < 0)}{W(\omega_0 > 0) + W(\omega_0 < 0)} \quad . \tag{140}$$

a_2 is maximum for $\theta_1 = \pi/4$, $\omega_1\tau = 1/2$: $(a_2)_{max} = \frac{-3A_2}{4 + A_2}$. These equations are familiar from angular-correlation theory. Maximum sensitivity is obtained in time-integral PAC by applying and reversing a DC magnetic field (the analogue of our H_1 at resonance) perpendicular to the correlation plane in which two detectors are placed at a relative angle of $\pi/4$ (or equivalent). The "attenuation factor" $[1 + (2\omega_1\tau)^2]^{-1/2}$ is well-understood: it leads to a vanishing difference when $\omega_1\tau$ becomes very large. In the NMR/PAC case this factor makes the effects of the sign of ω_1 on the lineshape transient.

For $\lambda > 2$, θ_1 should be smaller than $\pi/4$ for maximum a_λ, because the largest-amplitude, highest-frequency, component of $P_\lambda(\cos\theta)$ varies as $\cos\lambda\theta$. For example, $\hat{\Gamma}_4$ is relatively insensitive to the sign of ω_1 for $\theta_1 = \pi/4$, but is more sensitive for $\theta_1 = \pi/8$ (Fig. 13).

For λ odd, the odd parity of P_λ leads to more asymmetries in $\hat{\Gamma}_\lambda$. In general, however, these asymmetries can be divided into a transient type, that conveys information about the signs of ω_1 and/or A_λ, and a persistent type, that depends only on the sign of A_λ. In Fig. 14 we illustrate an experiment that is the $\lambda = 1$ counterpart of the one illustrated in Fig. 12.

Here $\theta_1 = \pi$ was chosen to maximize the difference

$$a_1 = 2\,\frac{W(\omega_0 > 0) - W(\omega_0 < 0)}{W(\omega_0 > 0) + W(\omega_0 < 0)} \quad ,$$

when

$$\hat{\Gamma}_1 = [1 + (\omega_1\tau)^2]^{-1/2} \cos(\theta_1 - \theta') \quad , \tag{141}$$

at $\omega = \omega_0$, with $\theta' = \tan^{-1} \omega_1\tau$ in this case. a_1 is maximum for $\omega_1\tau = 1$.

The persistent asymmetry in Fig. 14 happens to be zero. In Fig. 11 (top panel) we have a case in which both a nonzero persistent asymmetry and a transient asymmetry occur. As $|\omega_1\tau| \to \infty$ the transient part vanishes and no information is available about the sign of ω_1.

VI.3.2. Symmetry Properties of $\hat{\Gamma}_\lambda$ with $\underset{\sim}{k}_1$ and $\underset{\sim}{k}_2$ in the x-y Plane

It is evident from Table II that the magnitude of the resonance effects for $\lambda = 2$ drops by about another factor of two if neither $\underset{\sim}{k}_1$ nor $\underset{\sim}{k}_2$ is any longer parallel to the z-axis but both are instead perpendicular to it (geometries 9-13). This can easily be understood from Eq. (114), since $P_2(0) = -1/2$. A similar result is observed for $\lambda = 4$, but with a greater reduction in the effect. For odd λ, perpendicular geometry destroys the integral effect. This is easily deduced from Eqs. (97) and (101): the $(\underset{\sim}{k}_2)_{x,y} \cdot (\underset{\sim}{K}_s(t))_{xy}$ terms in $\cos \eta(t)$ are all linear in $\cos(\omega t+\Delta)$ or $\sin(\omega t+\Delta)$: thus all odd-rank Γ_λ have high-frequency factors with zero average value. They therefore average to zero in the transformation $S' \to S$. Hence we shall consider only even-λ cases further.

The response functions $\hat{\Gamma}_{\lambda=2,4}$ for geometries 9, 11, and 13 in Tables II and III are shown as examples in Figs. 15, 16, and 17. All these geometries are convenient for beam experiments, with the exception that no. 9 is not suitable for target foils where $\underset{\sim}{H}_1^{ext}$ and $\underset{\sim}{H}_0^{ext}$ have to be in the plane of the foil. They differ only by the angles ϕ_1 and ϕ_2 for $\underset{\sim}{k}_1$ and $\underset{\sim}{k}_2$. Through the factors $e^{-q\phi_1}$ and $e^{i\bar{q}\phi_2}$ (compare Eq. (76)) the choice of the angles sensitively affects the superposition of the various terms of the response function in Eq. (80). The phase angle Δ of the rf field and the angles ϕ_1 and ϕ_2 are equivalent in the sense that they occur in Eq. (76) in the form $\exp[-i\{q(\phi_1-\Delta) - \bar{q}(\phi_2-\Delta)\}]$. A particular value of Δ can be compensated by rotating the detector system by an angle Δ about the z-axis (cf. Figs. 1-3).

In Fig. 16 a <u>transient</u> asymmetry around the resonance frequency shows up for $\omega_1\tau \sim 1$: again it can be used to determine the sign of ω_1, provided that the phase angle Δ of H_1 at $t = 0$ is known. Since both detectors are located in a plane perpendicular to the z-axis, the rotation of $\underset{\sim}{K}(t)$ about the effective field can no longer be visualized as easily as in the foregoing section in which the system was invariant against rotations about the z-axis. Clearly, there is no rotational invariance with respect to the z-axis in geometries like the ones shown in Figs. 15-17. The general response function for these complicated geometries must either be calculated according to the formulae given in Tables I-III or by calculating $P_\lambda[\cos \eta(t)]$ with the proper vector $\underset{\sim}{K}(t)$ (see Eqs. (91) and (97)).

If we are not interested in a transient asymmetry effect like the one shown in Fig. 16 and the lifetime of the nuclear state is sufficiently long to permit reaching the asymptotic value $\omega_1\tau \to \infty$, a simple form for the response

function can be derived. For any "perpendicular" geometry with $\underset{\sim}{k}_1$ and $\underset{\sim}{k}_2$ in the x-y plane Eqs. (66) and (80) yield

$$\hat{\Gamma}_\lambda(\infty) = \frac{\lambda!}{(\lambda!!)^2} P_\lambda(\cos\beta) \sum_q (-1)^{q/2} e^{-iq(\phi_1-\Delta)} \frac{\sqrt{(\lambda-q)!(\lambda+q)!}}{(\lambda-q)!!(\lambda+q)!!} d^{(\lambda)}_{q0}(\beta)$$

$$\text{for } \lambda \text{ and } q \text{ even}$$

$$= 0 \qquad \text{for } \lambda \text{ and } q \text{ odd} \quad . \tag{142}$$

From Eq. (142) or Eq. (114), the limiting value of the $\lambda = 2$ response function at resonance can be obtained as

$$\hat{\Gamma}_2(\infty)_{res} = \frac{1}{16} + \frac{3}{16} \cos 2(\phi_1-\Delta) \quad . \tag{143}$$

For the particular geometries shown in Figs. 15-17 one finds $\hat{\Gamma}_2(\infty)_{res} = \frac{1}{4}, \frac{1}{16}$, and $-\frac{1}{8}$, respectively. The values of $\hat{\Gamma}_\lambda(\infty)$ off resonance are given by Eq. (114).

The resonance behavior of geometry no. 9 in Fig. 15 is the most obvious one for all perpendicular geometries since it has H_1 as symmetry axis in the rotating frame. The rotation ωt about the z-axis yields for $\omega_1\tau \to \infty$,

$$\hat{\Gamma}_\lambda(\infty)_{\omega_0} = [P_\lambda(0)]^2 \quad , \tag{144}$$

the same hard-core value that was obtained from random rf phase in parallel geometry. Slightly off resonance $\Gamma_2(\infty)$ dips to a minimum at a frequency between the zeros of $P_2[\cos(\underset{\sim}{k}_1,\underset{\sim}{H}_e)]$ and $P_2[\cos\beta]$, (see Eq. (114)). As we have noted before in discussing Figs. 7 and 10, geometry 9 is a special case because,

for $\omega = \omega_0$, $\underset{\sim}{H}_1$ acts as a holding field and the effect at this frequency is really an antiresonance. For cases in which the line is broadened by dipolar fields, the use of geometry 9 would serve to narrow the line, in analogy with similar applications in conventional NMR.[42-44] However in NMR/RD the $\underset{\sim}{k}_1$ vector can easily be taken along $\underset{\sim}{H}_1$ without using elaborate pulse techniques.

As mentioned above, it is considerably more difficult to visualize the spin motion in the case $\underset{\sim}{H}_0 \perp \underset{\sim}{k}_1 \perp \underset{\sim}{H}_1 \perp \underset{\sim}{H}_0 \perp \underset{\sim}{k}_2$, illustrated in Fig. 17 for $\phi_2 = \pi/4$ in geometry 13 (although for large $\omega_1\tau$ it becomes independent of ϕ_2). This geometry is important for accelerator experiments. Equations (66) and (80), or (114) are applicable here: Thus the "y-z" geometry of Fig. 10 gives a larger effect. For technical reasons it may, however, be impractical to count along $\underset{\sim}{H}_0$ (i.e., $\underset{\sim}{k}_2 \| \underset{\sim}{H}_0$). An interesting feature of this geometry is that the multipole structure of $\hat{\Gamma}_\lambda(\infty)$ is degraded, for even λ, to $\lambda/2$ minima, which gives this particular geometry the advantage that the resonance line for $\lambda = 2$ is considerably narrower compared with a normal width as shown in Fig. 10, perhaps allowing a more accurate frequency determination. The degradation of multipole structure is a consequence of $\hat{\Gamma}_\lambda(\infty)$ varying as $P_\lambda(\cos\beta)$ for this geometry, i.e.,

$$\hat{\Gamma}_\lambda(\infty) = P_\lambda(\cos \pi/2)\, P_\lambda(\cos\beta)\, P_\lambda(\cos\theta_2) \quad . \tag{145}$$

Variation of $\hat{\Gamma}_\lambda(\infty)$ as the square of $P_\lambda(\cos\beta)$ in parallel geometry (Eq. (106)) led to the complete multipole structure with λ components. For odd λ, $\hat{\Gamma}_\lambda(\infty)$ vanishes for all frequencies because the angle between $\underset{\sim}{H}_e$ and $\underset{\sim}{k}_1$ is $\pi/2$.

To provide the experimenter with an estimate of how large a resonance effect is to be expected for the easiest experimental setup, with $\underset{\sim}{H}_0 \perp \underset{\sim}{k}_1$, three

possibilities are summarized in Fig. 18. As a measure of the resonance effect at $\Delta = 0$, $\omega_1\tau \to \infty$, and $\underset{\sim}{k}_2$ along x, y, or z we define the quantity

$$\delta\hat{\Gamma}_\lambda(\infty) = \hat{\Gamma}_\lambda(\infty, |\omega-\omega_0| >> |\omega_1|) - \hat{\Gamma}_\lambda(\infty, \omega=\omega_0) \quad , \tag{146}$$

which gives the change in $\hat{\Gamma}_\lambda(\infty)$ at resonance for a given geometry. For odd λ, $\delta\hat{\Gamma}_\lambda = 0$ for all geometries, if $\underset{\sim}{k}_1 \perp \underset{\sim}{H}_0$. With even λ, either Eqs. (66) and (80) or (114) gives

$$\delta\hat{\Gamma}_\lambda(\infty) = P_\lambda(0)[1-P_\lambda(0)]\, P_\lambda(\cos\theta_2) \quad . \tag{147}$$

Again the advantages of parallel geometry are evident. Even if $\underset{\sim}{k}_1$ cannot be parallel to $\underset{\sim}{H}_0$, $\underset{\sim}{k}_2$ should still be chosen parallel.

Examples for various geometries and rf-phase relations given above served the purpose of pointing out experimental possibilities. A successful application of these ideas can be expected only for NMR experiments on long-lived isomers. Fixed-phase measurements are hardly feasible for NMR/PAC and NMR/ON and will probably be confined to accelerator experiments where it is technically possible to pulse the beam synchronously with the rf field.

VII. RELAXATION CONSIDERATIONS

A general discussion of the effects of relaxation on angular correlations is beyond the scope of this paper. Such a discussion has been given recently by Gabriel.[45] The purpose of this section is to discuss explicitly the single most important case of relaxation effects on NMR/RD, namely the influence of spin-lattice relaxation on line shapes and intensities. This case is especially important for NMR/NR experiments, in which nuclear lifetimes are often in the millisecond range and comparable to or longer than the spin-lattice relaxation time T_1.

The analysis in Secs. III and IV led to exact solutions for the time-dependence of radiation from an initially axially-symmetric distribution of nuclei subject to static and rotating magnetic fields. Now we shall introduce a random perturbation, $\mathcal{H}_R$, and show that the new solutions are similar to those that exist for the system in the absence of these fields. The time-dependence of the ensemble is now described by (compare Eq. (9))

$$i\hbar\dot{\rho} = [(\mathcal{H}_0 + \mathcal{H}_R), \rho] \quad . \tag{148}$$

The density matrix in a field-free frame may be written

$$\rho'''(t) = U^{\dagger}(t)\, \rho(t)\, U(t) \quad , \tag{149}$$

where U(t) is the transformation into a coordinate frame in which $\mathcal{H}_0$ vanishes. In the case of magnetic interactions U(t) represents the transformation into the S''' frame: it is given by the series of rotations described by Eq. (90) or Eq. (96). After substitution of Eq. (149) into Eq. (148) and comparison with Eq. (9), we have

$$i\hbar\dot{\rho}''' = [U^{\dagger}\mathcal{H}_R U, \rho''']\quad . \tag{150}$$

This equation is exact. Its validity does not depend on the relative sizes of $\mathcal{H}_0$ and $\mathcal{H}_R$. It describes the time-evolution of ρ''' under the influence of only a relaxation Hamiltonian $\mathcal{H}_R''' = U^{\dagger}\mathcal{H}_R U$. In many cases, however, $\mathcal{H}_R$ is invariant to rotation and we can write

$$\mathcal{H}_R''' = \mathcal{H}_R\quad . \tag{151}$$

Combining Eqs. (150) and (151), we get

$$i\hbar\dot{\rho}''' = [\mathcal{H}_R, \rho''']\quad . \tag{152}$$

Let us examine the conditions under which Eq. (151) is valid. For $\mathcal{H}_R$ to be invariant to rotation of only the nuclear coordinates, the interaction responsible for relaxation must be <u>isotropic</u>. This means that the extranuclear environment, or lattice, must meet certain conditions. The basic requirement is that, in the ensemble, the lattice states available for participation in the relaxation process must not be associated with a particular direction in space. When the static Hamiltonian $\mathcal{H}_0$ is associated with a particular direction in space, this condition requires $\Delta E \ll kT$, where ΔE is the energy quantum transferred in the relaxation process. For example, the problem in the magnetic case is that ΔE is implicitly associated with a direction defined by $\underset{\sim}{H}_0$. From the principle of detailed balance any microscopic relaxation process must be related to its inverse by a proportionality factor $e^{\Delta E/kT}$ that thereby relates the process to $\underset{\sim}{H}_0$. Thus unless $\Delta E \ll kT$ and $e^{\Delta E/kT} \cong 1$, the relaxation process cannot be approximated as being isotropic, regardless of other details of the system.

An additional requirement is that the product of the characteristic strength and the correlation time of the random fluctuations be small,[12]

$$\omega_p \tau_c << 1 \quad . \tag{153}$$

This insures that $\mathcal{H}_R$ is small enough to be treated as a perturbation. The correlation time of the perturbation must also be small enough that the system remains substantially fixed during the period of one correlation time τ_c, i.e.,

$$\omega_0 \tau_c << 1 \quad . \tag{154}$$

It should be noted that these relations do not imply anything about the relative magnitudes of ω_p and ω_0, or of ω_0 and the relaxation rate, although a sufficiently strong perturbation will of course mask any resonance effect.

The unperturbed density matrix in the S''' frame at $t = 0$, i.e., $\rho'''(0)$, is diagonal in an m-representation whose z axis is the $\underset{\sim}{k}_1$ axis. If the perturbation $\mathcal{H}_R$ can be taken as spherically symmetrical, then $\rho'''(t)$ will remain diagonal along $\underset{\sim}{K}(t)$ and its time-evolution may be expressed in terms of only its diagonal elements along the $\underset{\sim}{K}(t)$ axis, $\rho_m = \langle m|\rho|m \rangle$. In first-order perturbation theory, Eq. (152) yields rate equations which can be written

$$\dot{\rho}_m(t) = \sum_{m'} F_{mm'} \rho_{m'}(t) \quad . \tag{155}$$

In the transition matrix F, sums on rows or columns are zero. The general solution of Eq. (155) is

$$\rho_m(t) = \rho_m(eq) + \sum_{i=0}^{2I} S_{mi}\, \zeta_i(0)\, e^{-k_i t} \quad . \tag{156}$$

Here $\rho_m(eq)$ denotes the equilibrium value of $\rho_m(t)$ that is approached as $t \to \infty$. The set of exponential coefficients $\{-k_i\}$ are the eigenvalues of F. (They should not be confused with the propagation vectors $\underset{\sim}{k}_1$ and $\underset{\sim}{k}_2$.) The quantities $\zeta_i(0)$ give the initial values of the eigenvectors of F: they are determined by the initial conditions. The transformation S connects the ρ_m basis set with the eigenvectors and diagonalizes F, i.e.,

$$\rho_m(t) - \rho_m(eq) = \sum_{i=0}^{2I} S_{mi}\, \zeta_i(t)$$

$$F_{diag} = S^{-1} F S \quad . \tag{157}$$

The statistical tensors along $\underset{\sim}{K}(t)$, $(\rho_q^\lambda)_{\underset{\sim}{K}(t)}$, which are constructed from the diagonal elements of the density matrix in the m-representation, ρ_m, are nonzero only if q = 0 (Eq. (1)). The time-evolution of these tensors is governed by the same set of exponents $\{k_i\}$:

$$(\rho_0^\lambda(t))_{\underset{\sim}{K}(t)} = \sum_{i=0}^{2I} R_{\lambda i}\, e^{-k_i t} \quad . \tag{158}$$

From Eqs. (1), (156), and (158), and the boundary conditions

$$\rho_0^\lambda(eq) = 0 \qquad \lambda > 0$$

$\rho_0^0 = 1$, independent of time,

we can write, for $\lambda = 0$,

$$R_{0i} = \delta_{0i} \quad . \tag{159}$$

The constancy of ρ_0^0 also requires $k_0 = 0$. For $\lambda > 0$,

$$R_{\lambda i} = \zeta_i(0) \sum_m (-1)^{I+m} S_{mi} \langle I-m\ Im | \lambda\ 0 \rangle \quad , \tag{160}$$

and $\rho_0^\lambda(t)$ decays to zero as a sum of exponentials, for $\lambda > 0$. Substitution of $(\rho_0^\lambda(t))_{\underset{\sim}{K}(t)}$ for $(\rho_0^\lambda)^*_{\underset{\sim}{k}_1}$ in Eq. (91) gives

$$W(\underset{\sim}{k}_1, \underset{\sim}{k}_2, t) = \sum_{\lambda,i}^{*} R_{\lambda i}\, e^{-k_i t}\, A_\lambda P_\lambda[\cos \eta(t)] \quad . \tag{161}$$

For the specific case of relaxation in metals via isotropic magnetic hyperfine interaction with conduction electrons, the perturbation $\mathcal{H}_R$ takes the form

$$\mathcal{H}_A = A\, \underset{\sim}{I}\cdot\underset{\sim}{S} = A\, I_z S_z + \frac{1}{2}[I_+ S_- + I_- S_+] \quad .$$

We note that this interaction is also isotropic in the S''' frame. The $\omega_0\tau_c$ condition is easily met: at the Fermi energy the conduction electrons have $\tau_c \sim 10^{-12}$ sec, while even for very large hyperfine fields ω_0 is only in the 10^9 - 10^{10} sec^{-1} range. The condition $\omega_p\tau_c \ll 1$ is also satisfied, but by

a smaller margin, because the instantaneous hyperfine interaction with a conduction electron exceeds the time-average interaction that is manifest as a hyperfine field or (especially) as a Knight shift. Abragam and Pound[12] showed that the A $\underset{\sim}{I}\cdot\underset{\sim}{S}$ interaction leads to a single-exponential decay of their quantity III^{00}_{kk}, which is proportional to our G^{00}, or, in the S''' frame, to $(\rho_0^\lambda(t))_{\underset{\sim}{K}(t)}$. This is a consequence of the fact that each ρ_0^λ is itself an eigenvector ζ_i of F. This requires that

$$S_{mi} = (-1)^{I+m} \langle I-m\ Im | i\ 0 \rangle \quad . \tag{162}$$

The orthogonality of the Clebsch-Gordan coefficients then gives, from Eqs. (160) and (162),

$$R_{\lambda i} = \zeta_i(0)\ \delta_{i\lambda} \quad . \tag{163}$$

Abragam and Pound gave the decay constants explicitly. In our notation their result has the form

$$k_{\lambda A}(\text{free atom}) = -\frac{2}{3}\tau_{cA}\left(\frac{A}{\hbar}\right)^2 I(I+1)\ S(S+1)\ [1 - (2I+1)W(II\lambda I;II)] \quad .$$

Here the subscript A denotes the A $\underset{\sim}{I}\cdot\underset{\sim}{S}$ interaction. After evaluation of the Racah coefficient this reduces to

$$k_{\lambda A}(\text{free atom}) = -\frac{2}{3}\tau_{cA}\left(\frac{A}{\hbar}\right)^2 S(S+1)\ \lambda\ (\lambda+1) \quad . \tag{164}$$

Now this result is directly applicable to isolated paramagnetic atoms. In a solid or liquid metal this expression for $k_{\lambda A}$ would require multiplication by

a proportionality factor to account for conduction-electron statistics. The relaxation constant $k_{\lambda A}$ for either a free atom or a metal varies with λ as $\lambda(\lambda+1)$ and for $\lambda = 1$ the value of k_{1A} is just $1/T_{1A}$, where T_{1A} is the spin-lattice relaxation time. The subscript A denotes the $A\,\underset{\sim}{I}\cdot\underset{\sim}{S}$ mechanism. Thus we can write

$$k_{1A} = 1/T_{1A} \quad ,$$

$$k_{\lambda A} = \frac{\lambda(\lambda+1)}{2T_{1A}} \quad . \tag{165}$$

Accordingly, Eq. (161) becomes

$$W(\underset{\sim}{k}_1,\underset{\sim}{k}_2,t) = \sum_{\lambda} \rho_0^{\lambda}(0)_{\underset{\sim}{k}_1} e^{-\frac{\lambda(\lambda+1)}{2T_{1A}}t} A_\lambda P_\lambda[\cos\eta(t)] \quad . \tag{166}$$

In time-integral studies the response functions are obtained by multiplying the appropriate time-differential functions by $\frac{1}{\tau} e^{-t/\tau}$, where τ is the nuclear lifetime and integrating on dt. Comparisons of Eqs. (91) and (166), however, show that the effect of considering relaxation is simply to multiply each response function $\Gamma_\lambda(t)$ by

$$e^{-\frac{\lambda(\lambda+1)t}{2T_{1A}}} \quad .$$

Combining this with the factor $\frac{1}{\tau} e^{-t/\tau}$, we have the factor $\frac{1}{\tau} e^{-t/\tau'}$, where the effective lifetime τ' is defined by

$$\frac{1}{\tau'} = \frac{1}{\tau} + \frac{\lambda(\lambda+1)}{2T_{1A}} \quad . \tag{167}$$

Now the integrals

$$\hat{\Gamma}_\lambda = \frac{1}{\tau} \int_0^\infty \Gamma_\lambda(t)\, e^{-t/\tau'}\, dt \quad , \tag{168}$$

all have the same functional dependence on τ' that the corresponding integrals in the absence of relaxation had on the true nuclear lifetime τ, except that the integral response functions are all attenuated by the factors

$$\frac{1 + (\lambda\omega\tau)^2}{1 + (\lambda\omega\tau')^2} \quad .$$

Thus relaxation reduces the relative magnitude of the resonant effect as well as broadening the line. It is necessary, in the presence of relaxation, to increase the rf field amplitude by a ratio τ/τ' in order that $\omega_1\tau'$ should attain a given value.

These considerations are easily generalized to include also the effects of quadrupole relaxation caused by randomly fluctuating electric field gradients. The Hamiltonian governing this interaction, $\mathcal{H}_Q$, is invariant to a coordinate transformation into the S''' frame where it can also be treated using first-order perturbation theory. Taken alone, $\mathcal{H}_Q$ would cause $(\rho_0^\lambda)_{\underset{\sim}{K}(t)}$ to decay as

$$(\rho_0^\lambda(t))_{\underset{\sim}{K}(t)} = (\rho_0^\lambda(0))_{\underset{\sim}{k}_1}\, e^{-k_{\lambda Q} t} \quad , \tag{169}$$

where[12,36]

$$k_{\lambda Q} = \frac{3}{80} \frac{\tau_{cQ}}{\hbar^2} (eQ)^2 \overline{\overline{V_{zz}^2}} \frac{\lambda(\lambda+1)[4I(I+1)-\lambda(\lambda+1)-1]}{I^2(2I-1)^2} \quad . \tag{170}$$

Here $(eQ)^2 \overline{\overline{V_{zz}^2}}$ is the ensemble-averaged square of a fluctuating, axially-symmetric electric field gradient that causes relaxation, while τ_{cQ} is its correlation time. Defining

$$K = \frac{3}{80} \frac{\tau_{cQ}}{\hbar^2} (eQ)^2 \overline{\overline{V_{zz}^2}} \quad ,$$

we can write

$$k_{1Q} = \frac{1}{T_{1Q}} = K \frac{2[4I(I+1)-3]}{I^2(2I-1)^2} \quad . \tag{171}$$

Since both the $A\ \underset{\sim}{I}\cdot\underset{\sim}{S}$ and quadrupole relaxation mechanisms are treated as first-order perturbations, the effective spin-lattice relaxation constant is given by

$$\frac{1}{T_1'} = \frac{1}{T_{1A}} + \frac{1}{T_{1Q}} \quad . \tag{172}$$

The λ-dependence of $k_{\lambda Q}$ is different from that of $k_{\lambda A}$, however: from Eqs. (170) and (171),

$$k_{\lambda Q} = \frac{\lambda(\lambda+1)}{2T_{1Q}} \left[1 - \frac{\lambda(\lambda+1)-2}{4I(I+1)-3}\right] \quad . \tag{173}$$

Thus the effective nuclear lifetime is given by

$$\frac{1}{\tau'} = \frac{1}{\tau} + k_{\lambda A} + k_{\lambda Q}$$

$$= \frac{1}{\tau} + \frac{\lambda(\lambda+1)}{2}\left\{\frac{1}{T_{1A}} + \frac{1}{T_{1Q}}\left[1 - \frac{\lambda(\lambda+1)-2}{4I(I+1)-3}\right]\right\} \quad . \tag{174}$$

This τ' can be used in Eq. (168) as before.

The above discussion of spin-lattice relaxation applies to solids, liquids, and gases. It is, within the assumptions that $\mathcal{H}_R$ is isotropic and that $\mathcal{H}_Q$ is both random and axially symmetric, a rather complete treatment of relaxation effects in NMR/RD. In any magnetic resonance experiment the question of transverse relaxation (T_2) must be considered. Since it is known that angular correlation patterns in perpendicular geometries are sensitive to T_2,[45] it might be expected that our equation should contain T_2 explicitly. However, relaxation that arises from $\mathcal{H}_A$ can be described by a single parameter (A) and thus by a single relaxation time (T_{1A}), and similarly for $\mathcal{H}_Q$. In a general discussion of relaxation effects the coefficients k_λ are functionally dependent on both T_1 and T_2. For example, Gabriel[45] gave (in our notation)

$$k_\lambda^{(q)} = \lambda(\lambda+1)/2T_1 + q^2\left(\frac{1}{T_2} - \frac{1}{T_1}\right) \quad , \tag{175}$$

for isotropic magnetic hyperfine interactions. However when the criterion $\omega_0\tau_c << 1$ is met, he pointed out that $T_1 = T_2$, and the $k_\lambda^{(q)}$ become independent of q. We have avoided this problem altogether by working in the S''' frame where there is no transverse relaxation.

Of course this discussion applies only to T_2 effects that arise from $\mathcal{H}_A$ and $\mathcal{H}_Q$. The high dilution of NMR/RD samples precludes T_2 effects from interactions with like spins, however, except possibly in NMR/ON experiments on very long-lived states. The remaining T_2-like effect, namely inhomogeneous broadening, is well-known in both NMR/NR[4] and NMR/ON[3] experiments.

REFERENCES

1. E. Matthias, D. A. Shirley, M. P. Klein, and N. Edelstein, Phys. Rev. Letters 16, 974 (1966).
2. E. Matthias and R. J. Holliday, Phys. Rev. Letters 17, 897 (1966).
3. J. E. Templeton and D. A. Shirley, Phys. Rev. Letters 18, 240 (1967).
4. K. Sugimoto, K. Nakai, K. Matuda, and T. Minamisono, Phys. Letters 25B, 130 (1967), and J. Phys. Soc. Japan 25, 1258 (1968).
5. H. J. Besch, N. Köpf, and E. W. Otten, Phys. Letters 25B, 120 (1967).
   H. J. Besch, U. Köpf, E. W. Otten, and Ch. v. Platen, Phys. Letters 26B, 721 (1968).
   U. Köpf, H. J. Besch, E. W. Otten, and Ch. v. Platen, Zeitschr. Physik 226, 297 (1969).
6. D. Quitmann, J. M. Jaklevic, and D. A. Shirley, Phys. Letters 30B, 329 (1969).
7. H. Ackermann, D. Dubbers, J. Mertens, A. Winnacker, and P. v. Blanckenhagen, Phys. Letters 29B, 485 (1969).
8. M. Deutsch and S. C. Brown, Phys. Rev. 85, 1047 (1952).
9. J. Brossel and F. Bitter, Phys. Rev. 86, 308 (1952).
10. M. Guichon, J. E. Blamont, and J. Brossel, Compt. Rend. 243, 1859 (1956); J. Phys. Radium 18, 99 (1957). See also A. Kastler, Physics Today, September 1967, p. 34.
11. N. Bloembergen and G. R. Temmer, Phys. Rev. 89, 883 (1953).
12. A. Abragam and R. V. Pound, Phys. Rev. 92, 943 (1953).

13. Unsuccessful attempts at NMR/ON were made, using paramagnetic salts (G. R. Temmer, private communication). The major problem in these efforts, and one that seemed insuperable in both NMR/PAC and NMR/ON work, was the heating effect of the very large rf fields that appeared necessary. "Hyperfine enhancement" of the rf field circumvented this.

14. G. J. Perlow, Allerton Park Conference Report, University of Illinois, June 1960 (unpublished).

15. D. Connor, Phys. Rev. Letters 3, 429 (1959).

16. D. Connor and Tung Tsang, Phys. Rev. 126, 1506 (1962).
Tung Tsang and D. Connor, Phys. Rev. 132, 1141 (1963).

17. F. M. Pipkin and J. W. Culvahouse, Phys. Rev. 106, 1102 (1957), and Phys. Rev. 109, 1423 (1958).

18. K. Ziock, V. W. Hughes, R. Prepost, J. Baily, and W. Cleland, Phys. Rev. Letters 8, 103 (1962).

19. E. D. Commins and D. A. Dobson, Phys. Rev. Letters 10, 347 (1963).

20. K. Sugimoto, A. Mizobuchi, N. Nakai, and K. Matuda, Phys. Letters 18, 38 (1965), and J. Phys. Soc. Japan 21, 213 (1966).

21. E. Matthias, D. A. Shirley, N. Edelstein, H. J. Körner, and B. A. Olsen, Hyperfine Interactions and Nuclear Radiation, ed. by E. Matthias and D. A. Shirley (North-Holland Publishing Company, Amsterdam, 1968) p. 878.

22. N. Niesen, J. Lubbers, and W. J. Huiskamp, p. 894, ibid.

23. J. A. Barclay, W. D. Brewer, E. Matthias, and D. A. Shirley, p. 902, ibid.

24. W. D. Brewer, D. A. Shirley, and J. E. Templeton, Phys. Letters 27A, 81 (1968).

25. J. A. Barclay, Lawrence Radiation Laboratory, Berkeley (unpublished).

26. A. D. Gulko, S. S. Trostin, and A. Hudoklin, Soviet Physics, JETP 25 998 (1967).

27. E. Matthias, Hyperfine Structure and Nuclear Radiations, ed. by E. Matthias and D. A. Shirley (North-Holland Publishing Company, Amsterdam, 1968), p. 815.

28. D. A. Shirley, p. 843, ibid.

29. B. A. Olsen, E. Matthias, and R. M. Steffen, University of Uppsala, Institute of Physics Report UUIP-583, April 1968.

30. F. P. Khaimovich, Soviet Physics JETP 27, 156 (1968).

31. J. Christiansen, H. -E. Mahnke, E. Recknagel, D. Riegel, G. Weyer, and W. Witthuhn, Phys. Rev. Letters 21, 554 (1968).

32. U. Fano, Rev. Mod. Phys. 29, 74 (1957).

33. D. M. Brink and G. R. Satchler, Angular Momentum (Clarendon Press, Oxford, 1962).

34. R. J. Blin - Stoyle and M. A. Grace, Encyclopedia of Physics, Vol. XLII (Springer Verlag, Berlin, 1957), p. 555.

35. T - P. Gray and G. R. Satchler, Proc. Phys. Soc. (London) A 68, 349 (1955).

36. H. Frauenfelder and R. M. Steffen, "Angular Correlations," Chapter XIX A, in Alpha- Beta- Gamma-Ray Spectroscopy, ed. by K. Siegbahn (North-Holland Publishing Company, Amsterdam, 1965).

37. C. P. Slichter, Principles of Magnetic Resonance, Harper's Physics Series (Harper and Row, New York, 1963).

38. R. R. Lewis, Phys. Rev. 186, 352 (1969).

39. I. I. Rabi, N. F. Ramsey, and J. Schwinger, Rev. Mod. Phys. 26, 167 (1954).

40. A. R. Edmonds, Angular Momentum in Quantum Mechanics, Second Ed. (Princeton University Press, 1957), Eq. (4.1.26), p. 59.

41. For further references see also A. Kastler, Physics Today, September 1967, p. 34.

42. A. G. Redfield, Phys. Rev. 98, 1787 (1955).

43. M. Lee and W. I. Goldburg, Phys. Rev. 140, A1261 (1965).

44. J. S. Waugh, L. M. Huber, and U. Haeberlen, Phys. Rev. Letters 20, 180 (1968).

45. H. Gabriel, Phys. Rev. 181, 506 (1969).

Table I. The Response Function $\Gamma_1(t) = \underset{\sim}{K}(t)\cdot\underset{\sim}{k}_2$ for Selected Geometries.

No.	θ_1	ϕ_1	θ_2	ϕ_2	$\Gamma_1(t) = \underset{\sim}{K}(t)\cdot\underset{\sim}{k}_2$
1	0°	0°	180°	0°	$-G_{11}^{00} = -\cos^2\beta - \sin^2\beta\ \cos\omega_e t$
1'	0°	0°	0°	0°	$G_{11}^{00} = \cos^2\beta + \sin^2\beta\ \cos\omega_e t$
2	0°	0°	90°	90°	$-\frac{i}{\sqrt{2}}[G_{11}^{01} + G_{11}^{0-1}] = \sin\beta\ \cos\beta\ \sin(\omega t+\Delta)[1 - \cos\omega_e t] - \sin\beta\ \cos(\omega t+\Delta)\sin\omega_e t$
3	0°	0°	90°	0°	$\frac{1}{\sqrt{2}}[-G_{11}^{01} + G_{11}^{0-1}] = \sin\beta\ \cos\beta\ \cos(\omega t+\Delta)[1 - \cos\omega_e t] + \sin\beta\ \sin(\omega t+\Delta)\sin\omega_e t$
4	0°	0°	90°	45°	$\frac{1}{2}[-G_{11}^{01} + G_{11}^{0-1} - iG_{11}^{01} - iG_{11}^{0-1}] = \sin\beta\ \cos\beta[1 - \cos\omega_e t]\sin(\omega t + \Delta + \frac{\pi}{4}) - \sin\beta\ \sin\omega_e t\ \cos(\omega t + \Delta + \frac{\pi}{4})$
5	90°	45°	0°	0°	$\frac{1}{2}[-G_{11}^{10} + G_{11}^{-10} + iG_{11}^{10} + iG_{11}^{-10}] = \sin\beta\ \sin\omega_e t\ \cos(\Delta + \frac{\pi}{4}) + \sin\beta\ \cos\beta[1 - \cos\omega_e t]\sin(\Delta + \frac{\pi}{4})$
6	90°	135°	0°	0°	$\frac{1}{2}[G_{11}^{10} - G_{11}^{-10} + iG_{11}^{10} + iG_{11}^{-10}] = \sin\beta\ \sin\omega_e t\ \sin(\Delta + \frac{\pi}{2}) - \sin\beta\ \cos\beta[1 - \cos\omega_e t]\cos(\Delta + \frac{\pi}{4})$
7	0°	0°	135°	90°	$-\frac{1}{\sqrt{2}}G_{11}^{00} - \frac{i}{2}[G_{11}^{01} + G_{11}^{0-1}] = \frac{1}{\sqrt{2}}\{\sin\beta\ \cos\beta\ \sin(\omega t+\Delta)[1 - \cos\omega_e t] - \sin\beta\ \cos(\omega t+\Delta)\sin\omega_e t - \cos^2\beta - \sin^2\beta\ \cos\omega_e t\}$
8	45°	90°	0°	0°	$\frac{1}{\sqrt{2}}G_{11}^{00} + \frac{i}{2}[G_{11}^{10} + G_{11}^{-10}] = \frac{1}{\sqrt{2}}\{\sin\beta\ \sin\omega_e t\ \cos\Delta + \cos^2\beta + \sin^2\beta\ \cos\omega_e t + \sin\beta\ \cos\beta[1 - \cos\omega_e t]\sin\Delta\}$

(continued)

Table I. (Continued)

No.	θ_1	ϕ_1	θ_2	ϕ_2	$\Gamma_1(t) = \underset{\sim}{K}(t)\cdot\underset{\sim}{k}_2$
9	90°	0°	90°	180°	$\frac{1}{2}[-G_{11}^{11} + G_{11}^{1-1} + G_{11}^{-11} - G_{11}^{-1-1}] = \cos\beta \sin\omega_e t \sin\omega t$ $-\sin(\omega t+\Delta) \cos\omega_e t \sin\Delta + [\cos^2\beta \cos\omega_e t - \sin^2\beta]\cos(\omega t+\Delta)\cos\Delta$
10	90°	0°	90°	135°	$\frac{\sqrt{2}}{4}[-G_{11}^{11} + G_{11}^{1-1} + G_{11}^{-11} - G_{11}^{-1-1} + iG_{11}^{11} + iG_{11}^{1-1} - iG_{11}^{-11} - iG_{11}^{-1-1}]$ $= \cos\beta \sin\omega_e t \sin(\omega t + \frac{\pi}{4}) - \cos\omega_e t \sin(\omega t + \Delta + \frac{\pi}{4})\sin\Delta$ $- [\sin^2\beta + \cos^2\beta \cos\omega_e t]\cos(\omega t + \Delta + \frac{\pi}{4})\cos\Delta$
11	90°	45°	90°	135°	$\frac{1}{2}[G_{11}^{1-1} + G_{11}^{-11} + iG_{11}^{11} - iG_{11}^{-1-1}] = \cos\beta \cos\omega t \sin\omega_e t$ $+ \cos\omega_e t \sin(\omega t + \Delta + \frac{\pi}{4})\cos(\Delta + \frac{\pi}{4})$ $- [\sin^2\beta + \cos^2\beta \cos\omega_e t]\cos(\omega t + \Delta + \frac{\pi}{4})\sin(\Delta + \frac{\pi}{4})$
12	90°	45°	90°	0°	$\frac{\sqrt{2}}{4}[G_{11}^{11} - G_{11}^{1-1} - G_{11}^{-11} + G_{11}^{-1-1} - iG_{11}^{11} + iG_{11}^{1-1} - iG_{11}^{-11} + iG_{11}^{-1-1}]$ $= -\cos\beta \sin\omega_e t \sin(\omega t + \frac{\pi}{4}) - \sin(\omega t+\Delta) \cos\omega_e t \cos(\Delta + \frac{\pi}{4})$ $+ [\sin^2\beta + \cos^2\beta \cos\omega_e t] \cos(\omega t+\Delta)\sin(\Delta + \frac{\pi}{4})$
13	90°	90°	90°	45°	$\frac{\sqrt{2}}{4}[G_{11}^{11} + G_{11}^{1-1} + G_{11}^{-11} + G_{11}^{-1-1} - iG_{11}^{11} + iG_{11}^{1-1} - iG_{11}^{-11} + iG_{11}^{-1-1}]$ $= -\cos\beta \sin\omega_e t \sin(\omega t + \frac{\pi}{4}) + \cos\omega_e t \cos\Delta \cos(\omega t + \Delta + \frac{\pi}{4})$ $+ [\sin^2\beta + \cos^2\beta \cos\omega_e t] \sin(\omega t + \Delta + \frac{\pi}{4})\sin\Delta$

UCRL-18413

Table II. The Response Function $\Gamma_2(t)$ for Various Geometries. The angles refer to Fig. 3.

No.	θ_1	ϕ_1	θ_2	ϕ_2	$\Gamma_2(t) = \frac{3}{2}(\underset{\sim}{K}(t)\cdot\underset{\sim}{k}_2)^2 - \frac{1}{2}$
1	0°	0°	180°	0°	G_{22}^{00}
2	0°	0°	90°	90°	$-\frac{1}{2}G_{22}^{00} - \sqrt{\frac{3}{8}}(G_{22}^{02} + G_{22}^{0-2})$
3	0°	0°	90°	0°	$-\frac{1}{2}G_{22}^{00} + \sqrt{\frac{3}{8}}(G_{22}^{02} + G_{22}^{0-2})$
4	0°	0°	90°	45°	$-\frac{1}{2}G_{22}^{00} + i\sqrt{\frac{3}{8}}(G_{22}^{02} - G_{22}^{0-2})$
5	90°	45°	0°	0°	$-\frac{1}{2}G_{22}^{00} + i\sqrt{\frac{3}{8}}(G_{22}^{-20} - G_{22}^{20})$
6	90°	135°	0°	0°	$-\frac{1}{2}G_{22}^{00} + i\sqrt{\frac{3}{8}}(G_{22}^{20} - G_{22}^{-20})$
7	0°	0°	135°	90°	$\frac{1}{4}G_{22}^{00} + i\sqrt{\frac{3}{8}}(G_{22}^{01} + G_{22}^{0-1}) - \sqrt{\frac{3}{32}}(G_{22}^{02} + G_{22}^{0-2})$
8	45°	90°	0°	0°	$\frac{1}{4}G_{22}^{00} + i\sqrt{\frac{3}{8}}(G_{22}^{10} + G_{22}^{-10}) - \sqrt{\frac{3}{32}}(G_{22}^{20} + G_{22}^{-20})$
9	90°	0°	90°	180°	$\frac{1}{4}G_{22}^{00} - \sqrt{\frac{3}{32}}(G_{22}^{20} + G_{22}^{-20} + G_{22}^{0-2} + G_{22}^{02}) + \frac{3}{8}(G_{22}^{22} + G_{22}^{2-2} + G_{22}^{-22} + G_{22}^{-2-2})$
10	90°	0°	90°	135°	$\frac{1}{4}G_{22}^{00} - \sqrt{\frac{3}{32}}(G_{22}^{20} + G_{22}^{-20} + iG_{22}^{0-2} - iG_{22}^{02}) + i\frac{3}{8}(-G_{22}^{22} + G_{22}^{2-2} - G_{22}^{-22} + G_{22}^{-2-2})$
11	90°	45°	90°	135°	$\frac{1}{4}G_{22}^{00} - i\sqrt{\frac{3}{32}}(-G_{22}^{20} + G_{22}^{-20} + G_{22}^{0-2} - G_{22}^{02}) - \frac{3}{8}(G_{22}^{22} - G_{22}^{2-2} - G_{22}^{-22} + G_{22}^{-2-2})$
12	90°	45°	90°	0°	$\frac{1}{4}G_{22}^{00} - \sqrt{\frac{3}{32}}(-iG_{22}^{20} + iG_{22}^{-20} + G_{22}^{0-2} + G_{22}^{02}) + i\frac{3}{8}(-G_{22}^{22} - G_{22}^{2-2} + G_{22}^{-22} + G_{22}^{-2-2})$
13	90°	90°	90°	45°	$\frac{1}{4}G_{22}^{00} + \sqrt{\frac{3}{32}}(G_{22}^{20} + G_{22}^{-20} + iG_{22}^{0-2} - iG_{22}^{02}) - i\frac{3}{8}(G_{22}^{22} - G_{22}^{2-2} + G_{22}^{-22} - G_{22}^{-2-2})$

UCRL-18413

Table III. The response function $\Gamma_4(t)$ for several selected geometries. The angles refer to Fig. 3. The corresponding formulas for random phase can be obtained by omitting all terms with $q - \bar{q}$.

No.	Θ_1	ϕ_1	Θ_2	ϕ_2	$\Gamma_4(t) = \frac{35}{8}(\underset{\sim}{K}(t)\cdot\underset{\sim}{k}_2)^4 - \frac{15}{4}(\underset{\sim}{K}(t)\cdot\underset{\sim}{k}_2)^2 + \frac{3}{8}$
1	0°	0°	180°	0°	G_{44}^{00}
5	90°	45°	0°	0°	$\frac{3}{8}G_{44}^{00} + \frac{\sqrt{10}}{8}i[G_{44}^{20} - G_{44}^{-20}] - \frac{\sqrt{70}}{16}[G_{44}^{40} + G_{44}^{-40}]$
6	90°	135°	0°	0°	$\frac{3}{8}G_{44}^{00} - \frac{\sqrt{10}}{8}i[G_{44}^{20} - G_{44}^{-20}] - \frac{\sqrt{70}}{16}[G_{44}^{40} + G_{44}^{-40}]$
8	45°	90°	0°	0°	$-\frac{13}{32}G_{44}^{00} + \frac{\sqrt{5}}{16}i[G_{44}^{10} - G_{44}^{-10}] - \frac{5\sqrt{10}}{32}[G_{44}^{20} + G_{44}^{-20}] - \frac{\sqrt{35}}{16}i[G_{44}^{30} - G_{44}^{-30}]$ $+ \frac{\sqrt{70}}{64}[G_{44}^{40} + G_{44}^{-40}]$
9	90°	0°	90°	180°	$\frac{9}{64}G_{44}^{00} - \frac{3\sqrt{10}}{64}[G_{44}^{20} + G_{44}^{-20} + G_{44}^{0-2} + G_{44}^{02}] + \frac{5}{32}[G_{44}^{22} + G_{44}^{2-2} + G_{44}^{-22} + G_{44}^{-2-2}]$ $+ \frac{3\sqrt{70}}{128}[G_{44}^{40} + G_{44}^{-40} + G_{44}^{0-4} + G_{44}^{04}] - \frac{5\sqrt{7}}{64}[G_{44}^{42} + G_{44}^{4-2} + G_{44}^{-4-2} + G_{44}^{-42} + G_{44}^{2-4}$ $+ G_{44}^{-2-4} + G_{44}^{-24} + G_{44}^{24}] + \frac{35}{128}[G_{44}^{44} + G_{44}^{4-4} + G_{44}^{-44} + G_{44}^{-4-4}]$
11	90°	45°	90°	135°	$\frac{9}{64}G_{44}^{00} + \frac{3\sqrt{10}}{64}i[G_{44}^{20} - G_{44}^{-20} - G_{44}^{0-2} + G_{44}^{02}] - \frac{5}{32}[G_{44}^{22} - G_{44}^{2-2} - G_{44}^{-22} + G_{44}^{-2-2}]$ $- \frac{3\sqrt{70}}{128}[G_{44}^{40} + G_{44}^{-40} + G_{44}^{0-4} + G_{44}^{04}] - \frac{5\sqrt{7}}{64}i[G_{44}^{42} - G_{44}^{4-2} + G_{44}^{-42} - G_{44}^{-4-2} - G_{44}^{-2-4}$ $+ G_{44}^{2-4} - G_{44}^{-24} + G_{44}^{24}] + \frac{35}{128}[G_{44}^{44} + G_{44}^{4-4} + G_{44}^{-44} + G_{44}^{-4-4}]$
13	90°	90°	90°	45°	$\frac{9}{64}G_{44}^{00} + \frac{3\sqrt{10}}{64}[G_{44}^{20} + G_{44}^{-20} + iG_{44}^{0-2} - iG_{44}^{02}] - \frac{5}{32}i[G_{44}^{22} - G_{44}^{2-2} + G_{44}^{-22} - G_{44}^{-2-2}]$ $+ \frac{3\sqrt{70}}{128}[G_{44}^{40} + G_{44}^{-40} - G_{44}^{0-4} - G_{44}^{04}] - \frac{5\sqrt{7}}{64}[iG_{44}^{42} - iG_{44}^{4-2} + iG_{44}^{-42} - iG_{44}^{-4-2}$ $+ G_{44}^{-2-4} + G_{44}^{2-4} + G_{44}^{-24} + G_{44}^{24}] - \frac{35}{128}[G_{44}^{44} + G_{44}^{4-4} + G_{44}^{-44} + G_{44}^{-4-4}]$

FIGURE CAPTIONS

Fig. 1. The transformation from the laboratory frame S into the rotating frame S'(t).

Fig. 2. The transformations (a) from the S' frame into the S" frame, with $\underset{\sim}{H}_e$ as the z" axis, and (b) into S''', a second rotating frame. The S" → S''' transformation transforms $\underset{\sim}{H}_e$ to zero in the S''' frame.

Fig. 3. The unit vectors $\underset{\sim}{k}_1$ and $\underset{\sim}{k}_2$ in the laboratory frame.

Fig. 4. Illustration of the way in which line shape follows from geometry, for the case $\lambda = 2$, $\omega_1\tau \to \infty$. Both $\underset{\sim}{k}_1$ and $\underset{\sim}{k}_2$ are taken along the z (z') axis, and diagrams at left are in the S' frame. $\hat{\Gamma}_2$ is evaluated by integrating $e^{-t/\tau} P_2 [\cos\eta(t)] d\eta$ around a circle described by $\underset{\sim}{K}(t)$. In case (a), for $(\omega-\omega_0) \ll \omega_1$, $\eta(t)$ is always small, P_2 is near unity, and $\hat{\Gamma}_2$ is thus also near unity (heavy portion of line on right). For frequencies nearer ω_0, the form of P_2 leads to minima and a hard-core value, as shown in (b) and (c).

Fig. 5. Slow component of $\Gamma_\lambda(t)$ for three geometries, with $\omega = \omega_0$. For geometries 1 and 5 only the slow component (precession about H_1) is observable, while the fast component of Γ_2 appears in geometry 13. The curves shown are for $\omega_0 = 12\omega_1$. In this case the envelope for random Δ, indicated by dashed curves, ranges from +1 to -1/2, while the <u>mean</u> value varies from +1/4 to -1/8.

Fig. 6. $\Gamma_\lambda(t)$ near $t = 0$ for $\lambda = 2, 4$, for geometries 9 and 11. Only the phase is different for the two geometries.

Fig. 7. $\Gamma_\lambda(t)$ for $\lambda = 2, 4$ in the time region $\omega_1 t \sim 1$, where the oscillations have been substantially affected by precession about $\underset{\sim}{H}_1$. The curves have been calculated for geometry 9 at resonance (b) and close to resonance (a and c).

Fig. 8. Power dependence of $\hat{\Gamma}_\lambda$ at resonance for geometry 1, showing hard-core behavior for even λ.

Fig. 9. Line shapes for geometry 1, showing multipole structure and saturation behavior.

Fig. 10. Line shapes in the saturation limit $\omega_1\tau \to \infty$, with $\underset{\sim}{k}_2$ along z and $\underset{\sim}{k}_1$ along x with $\Delta = 0$, along y with $\Delta = 0$, in the x-y plane with Δ random, and along z.

Fig. 11. The approach to saturation for geometry 5, with $\Delta = 0$. Note sensitivity to sign of $\omega_1\tau$ which vanishes, for all λ, as $|\omega_1\tau| \to \infty$.

Fig. 12. Response function $\hat{\Gamma}_2$ for geometry 8, with $\Delta = 0$. Note sensitivity to sign of $\omega_1\tau$, which disappears as $\omega_1\tau \to \infty$. For $\omega = \omega_0$ this geometry, is equivalent to the usual method of determining gH_0 by spin rotation, but in the rotating frame S'.

Fig. 13. Response function $\hat{\Gamma}_4$ for a geometry similar to 5, and $\Delta = 0$, but with θ_1 reduced to $\pi/8$ in order to enhance the sensitivity of $\hat{\Gamma}_4$ to the sign of $\omega_1\tau$.

Fig. 14. Response function $\hat{\Gamma}_1$ for a geometry similar to 5, and $\Delta = 0$, but with θ_1 increased to $\pi/2$ in order to enhance the sensitivity of the sign of $\omega_1\tau$.

Fig. 15. Response functions for geometry 9, with $\Delta = 0$, and $\lambda = 2, 4$. For odd λ and $\omega_0 >> \omega_1$, $\hat{\Gamma}_\lambda \cong 0$.

Fig. 16. Response functions for geometry 11, with $\Delta = 0$, and $\lambda = 2, 4$, and $\omega_1 > 0$. For odd values of λ, and $\omega_0 >> \omega_1$, $\hat{\Gamma}_\lambda \cong 0$. Curves for $\omega_1 < 0$ may be obtained by reflection through $\omega = \omega_0$.

Fig. 17. Response functions for geometry 13, with $\Delta = 0$ and $\lambda = 2, 4$. For odd λ, $\hat{\Gamma}_\lambda \cong 0$ if $\omega_0 >> \omega_1$.

Fig. 18. Summary of the "on-off" effects to be expected for several perpendicular geometries.

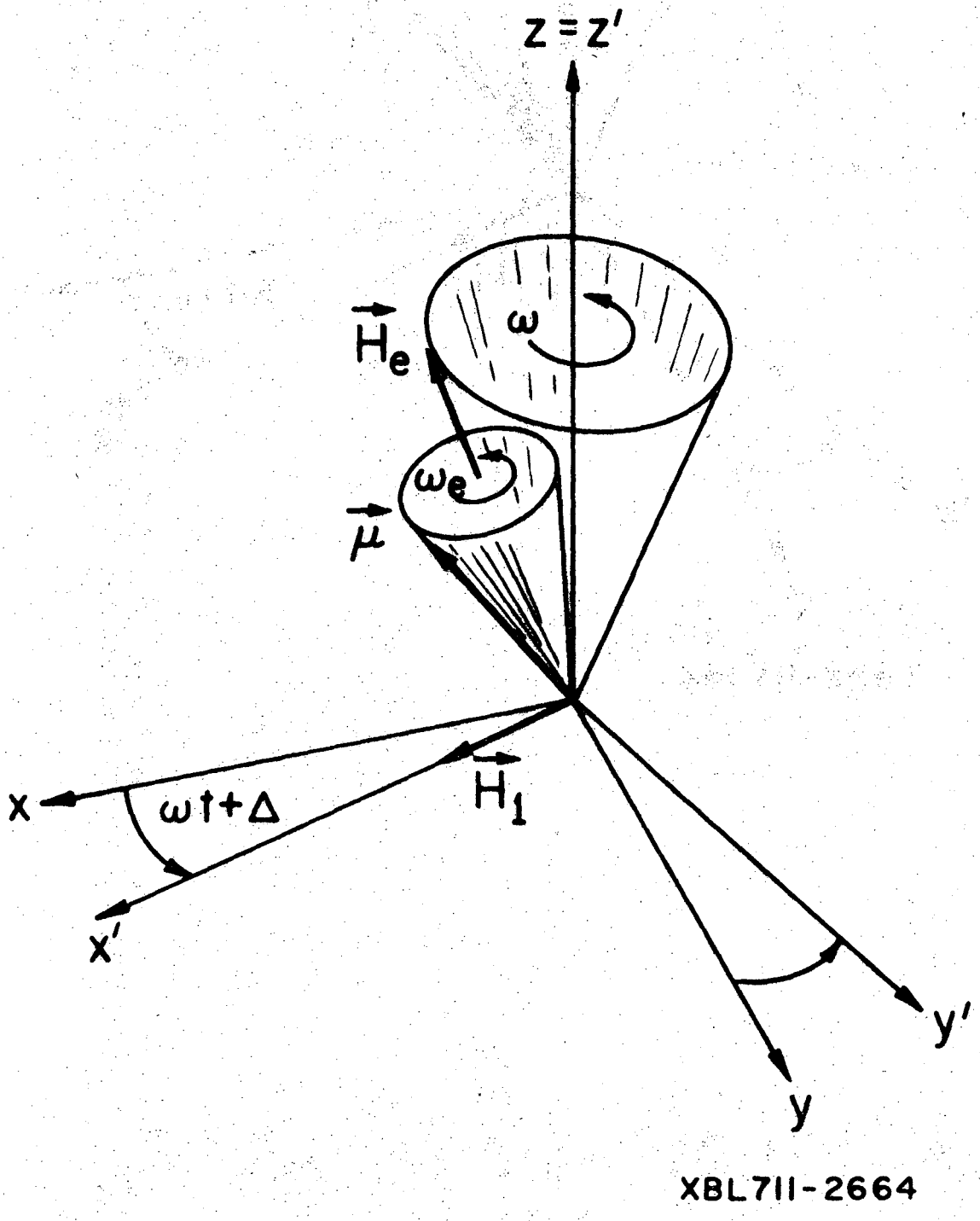

Fig. 1

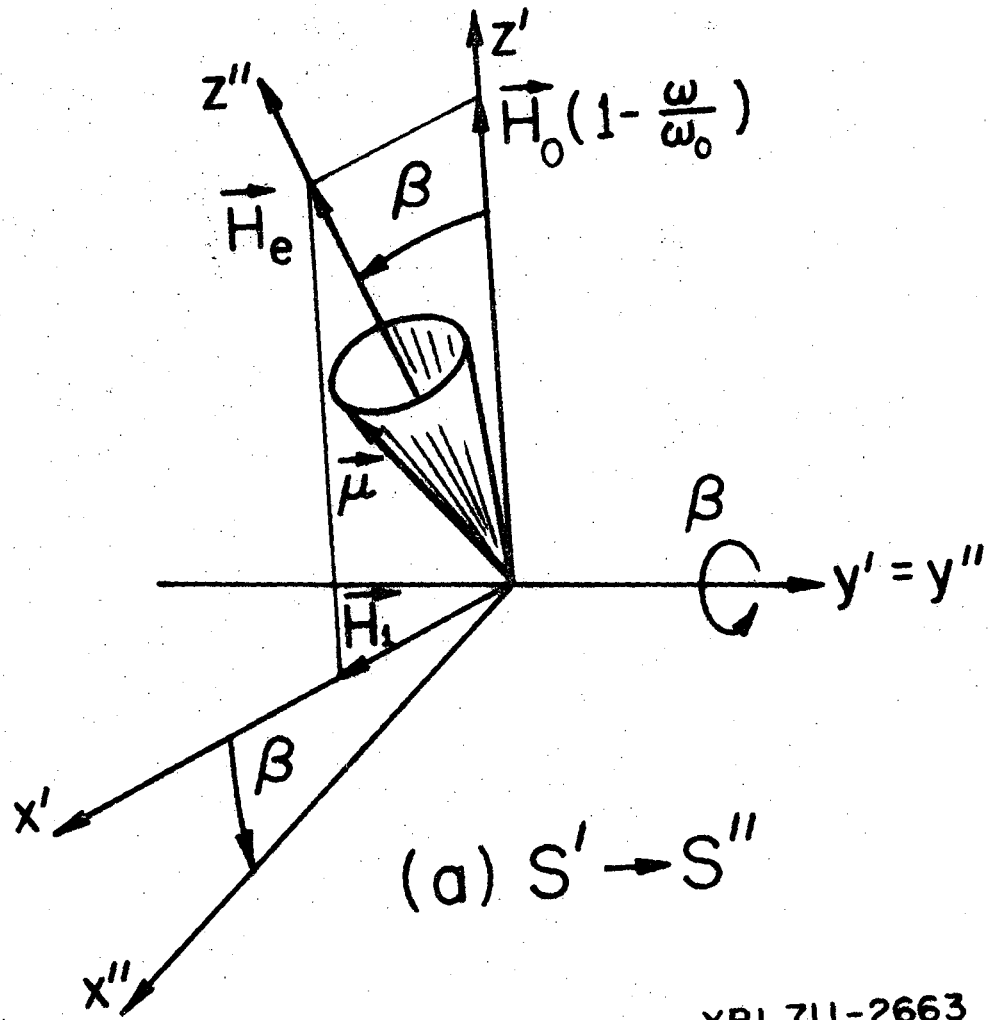
z'
z''
$\vec{H}_0(1-\frac{\omega}{\omega_0})$
$\vec{H}_e$
β
$\vec{\mu}$
β
y' = y''
$\vec{H}_1$
β
x'
x''
(a) S' → S''
XBL711-2663

Fig. 2a

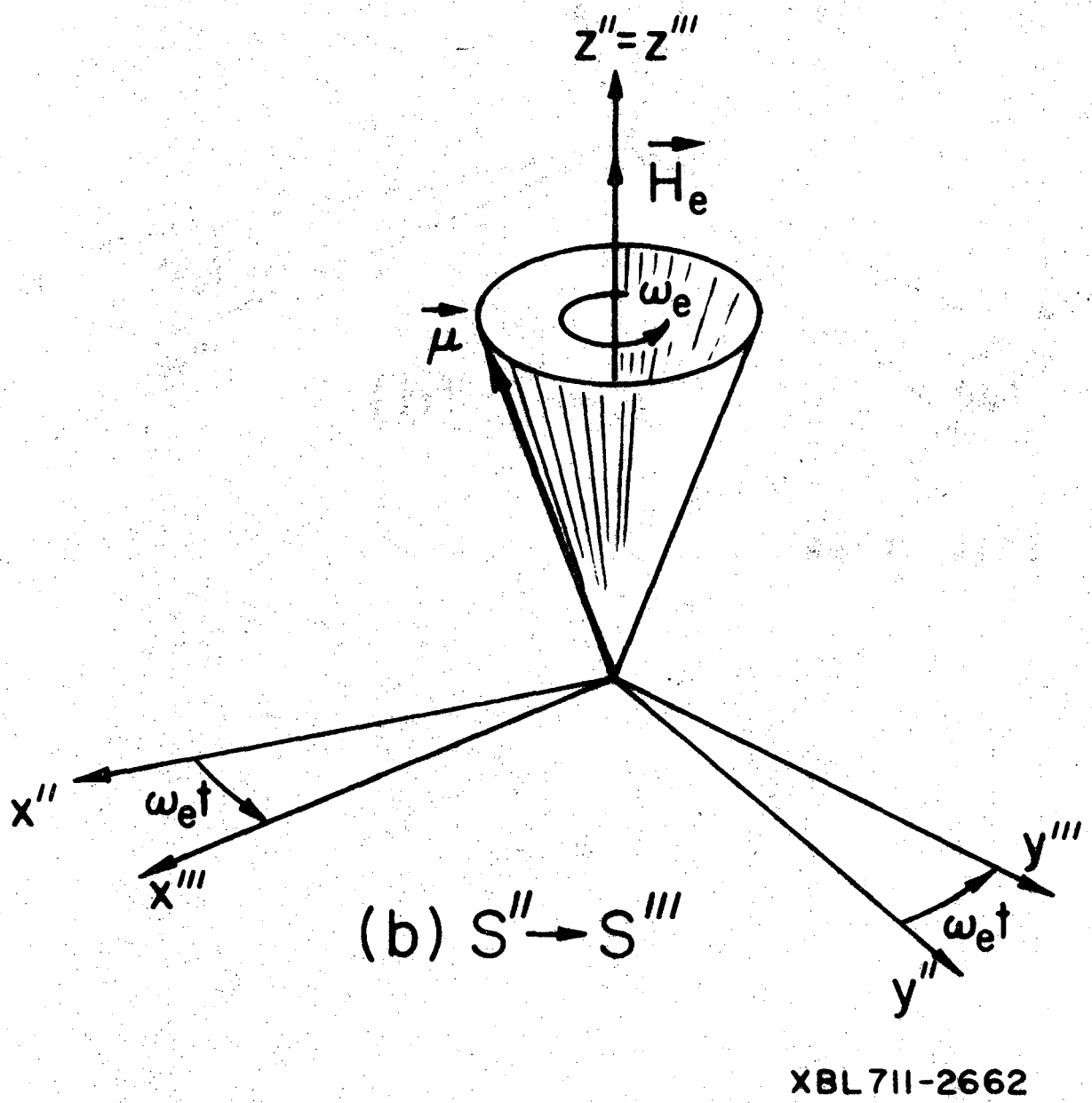

Fig. 2b

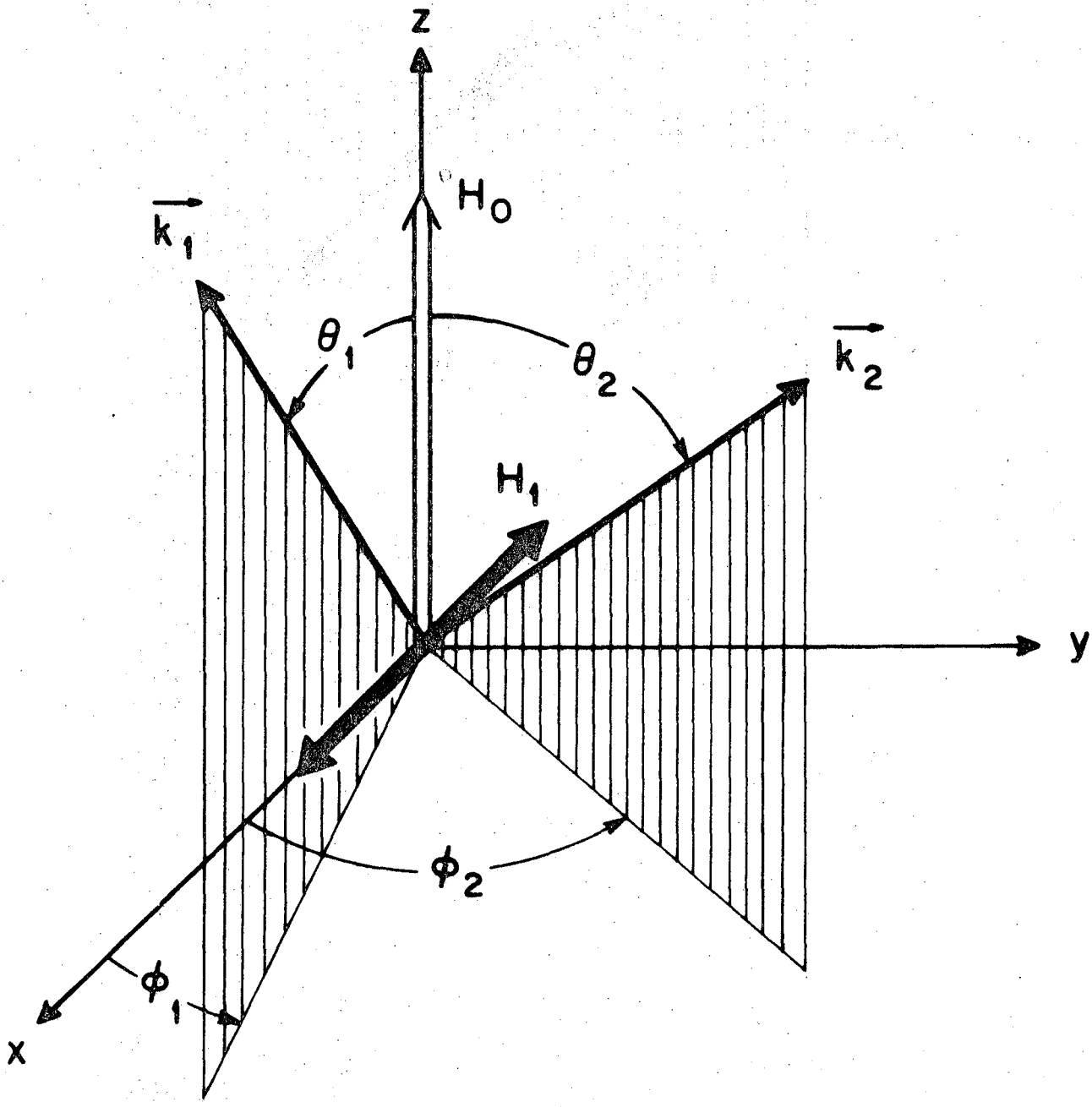

XBL678-3906

Fig. 3

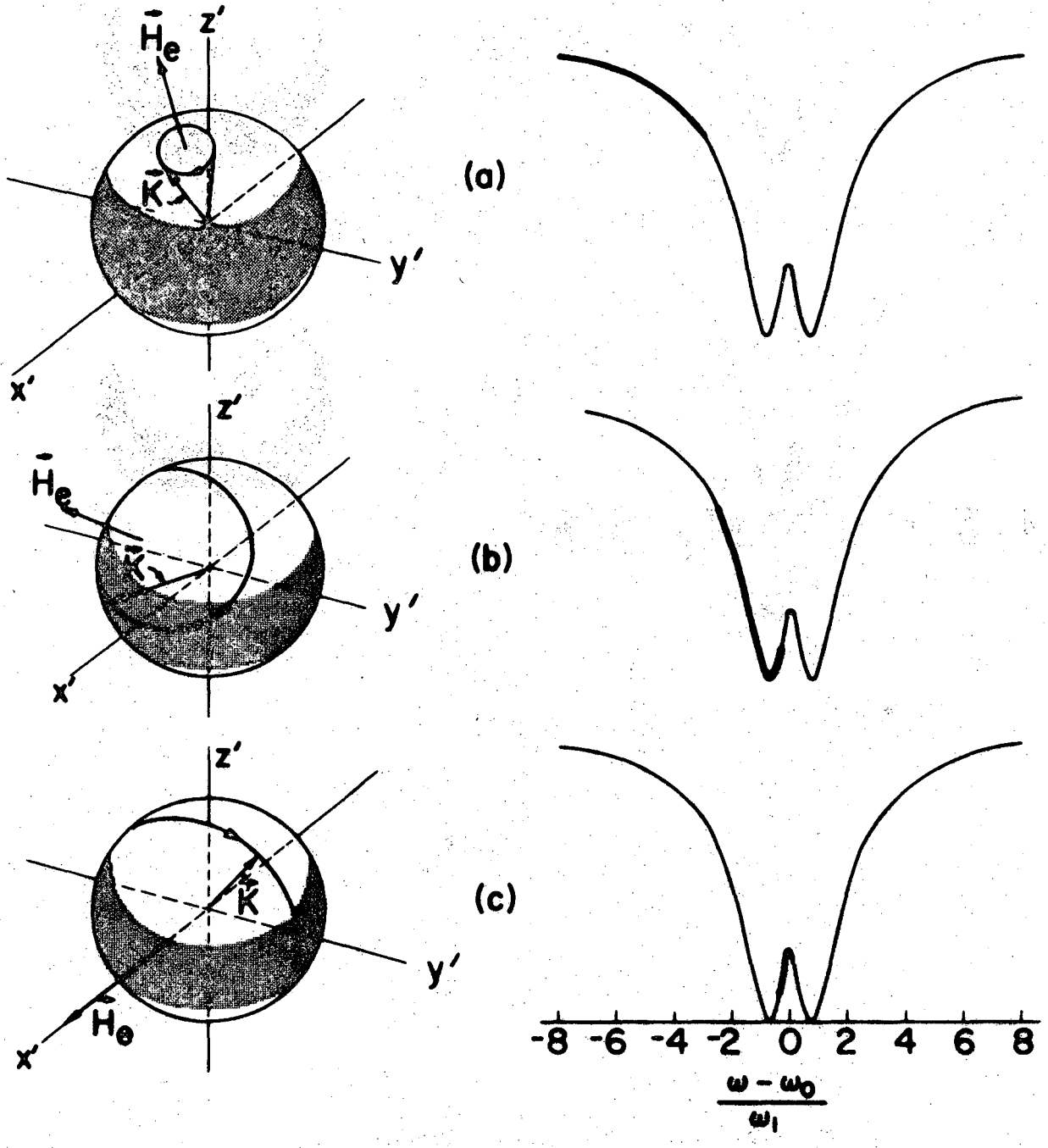
$\bar{H}_e$
z′
$\bar{K}$
y′
x′
(a)
(b)
(c)
-8 -6 -4 -2 0 2 4 6 8
$\frac{\omega - \omega_0}{\omega_1}$
XBL 687 - 3459

Fig. 4

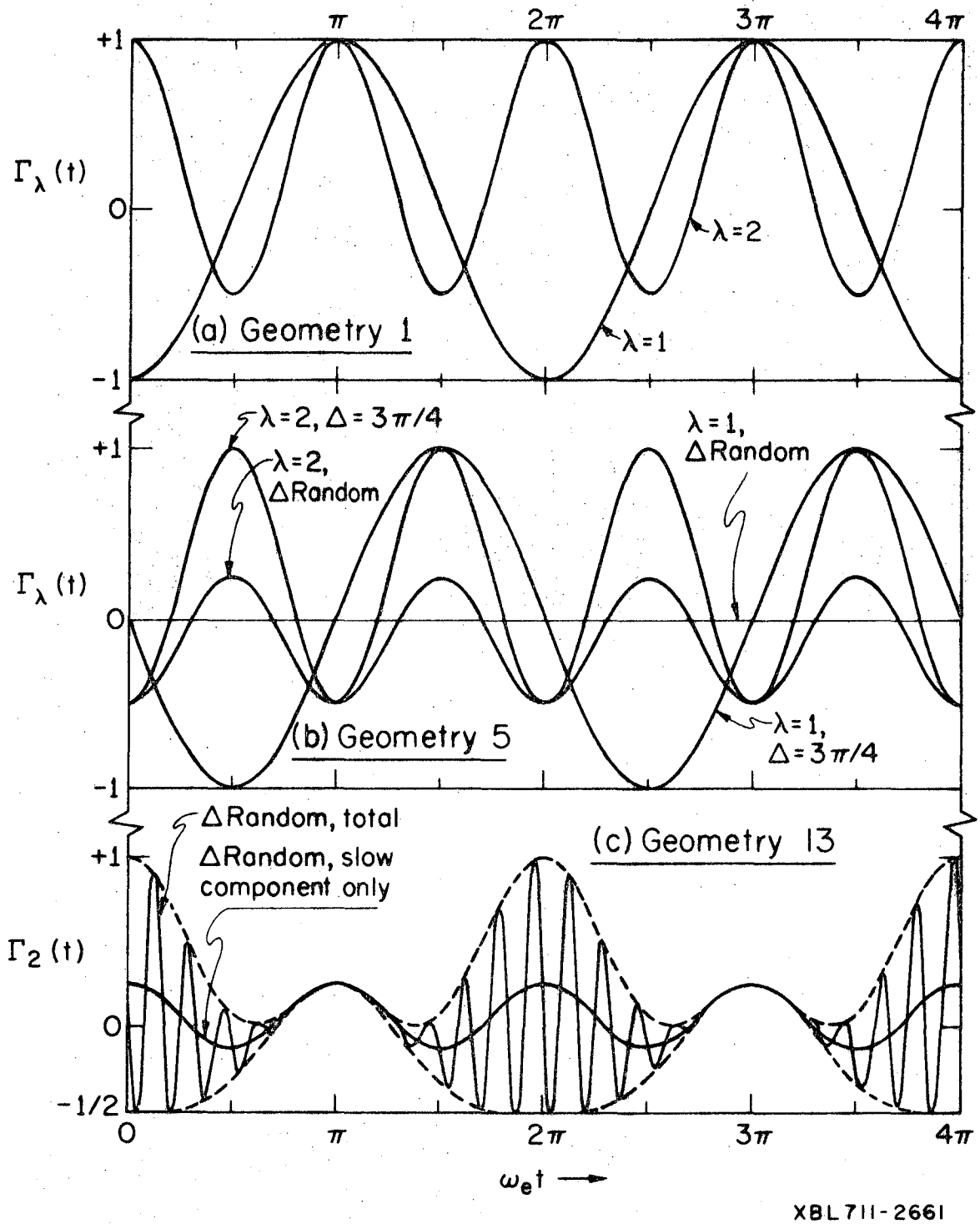
π
2π
3π
4π
+1
0
-1
$\Gamma_\lambda(t)$
λ=2
λ=1
(a) Geometry 1
λ=2, Δ=3π/4
λ=2, ΔRandom
λ=1, ΔRandom
λ=1, Δ=3π/4
(b) Geometry 5
ΔRandom, total
ΔRandom, slow component only
(c) Geometry 13
$\Gamma_2(t)$
-1/2
$\omega_e t$ ⟶
XBL711-2661

Fig. 5

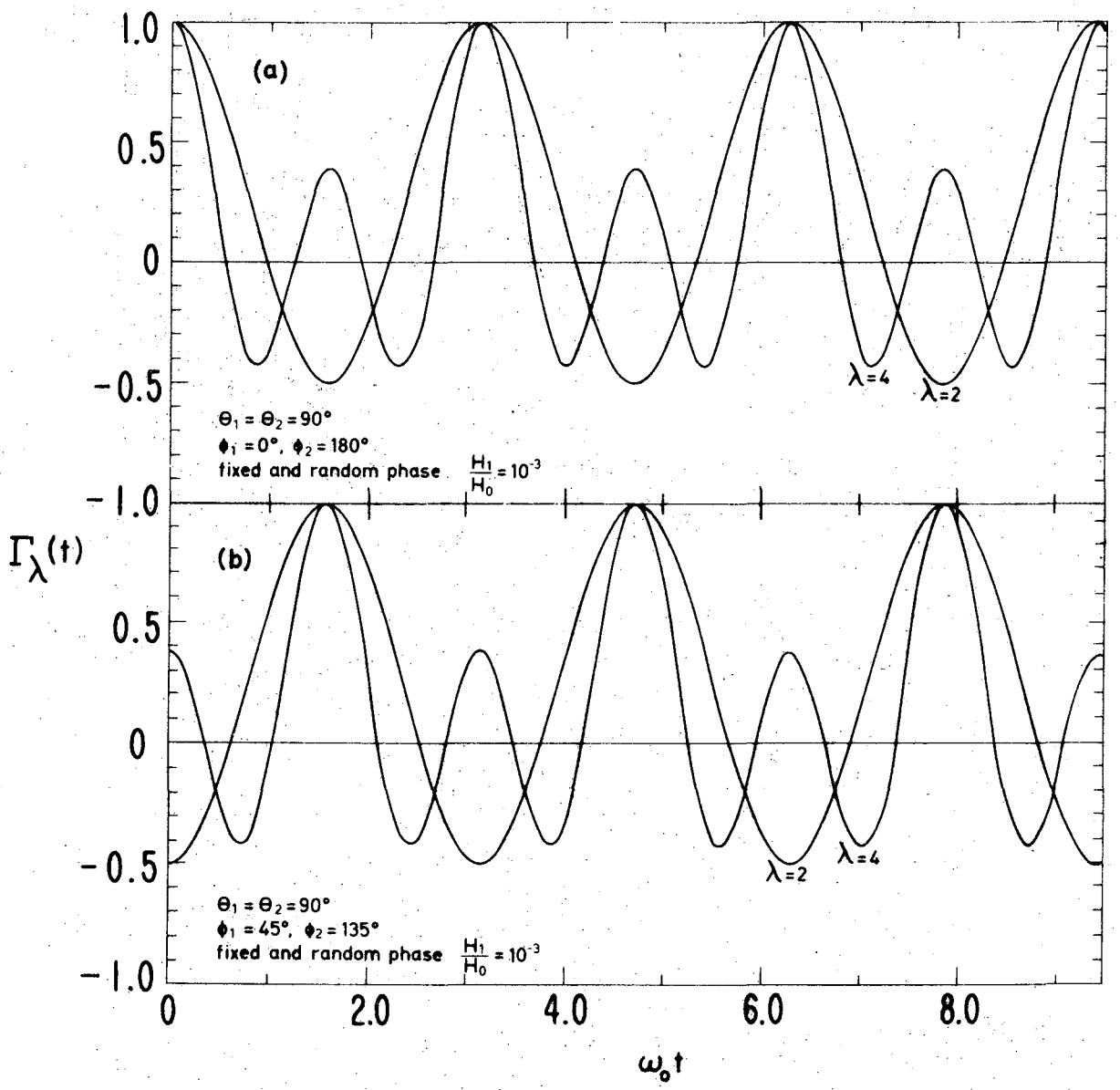
1.0
0.5
0
-0.5
-1.0
(a)
λ=4
λ=2
Θ1 = Θ2 = 90°
φ1 = 0°, φ2 = 180°
fixed and random phase
H1/H0 = 10^-3
Γλ(t)
(b)
λ=2
λ=4
Θ1 = Θ2 = 90°
φ1 = 45°, φ2 = 135°
fixed and random phase
H1/H0 = 10^-3
0
2.0
4.0
6.0
8.0
ω0t
XBL704-2644

Fig. 6

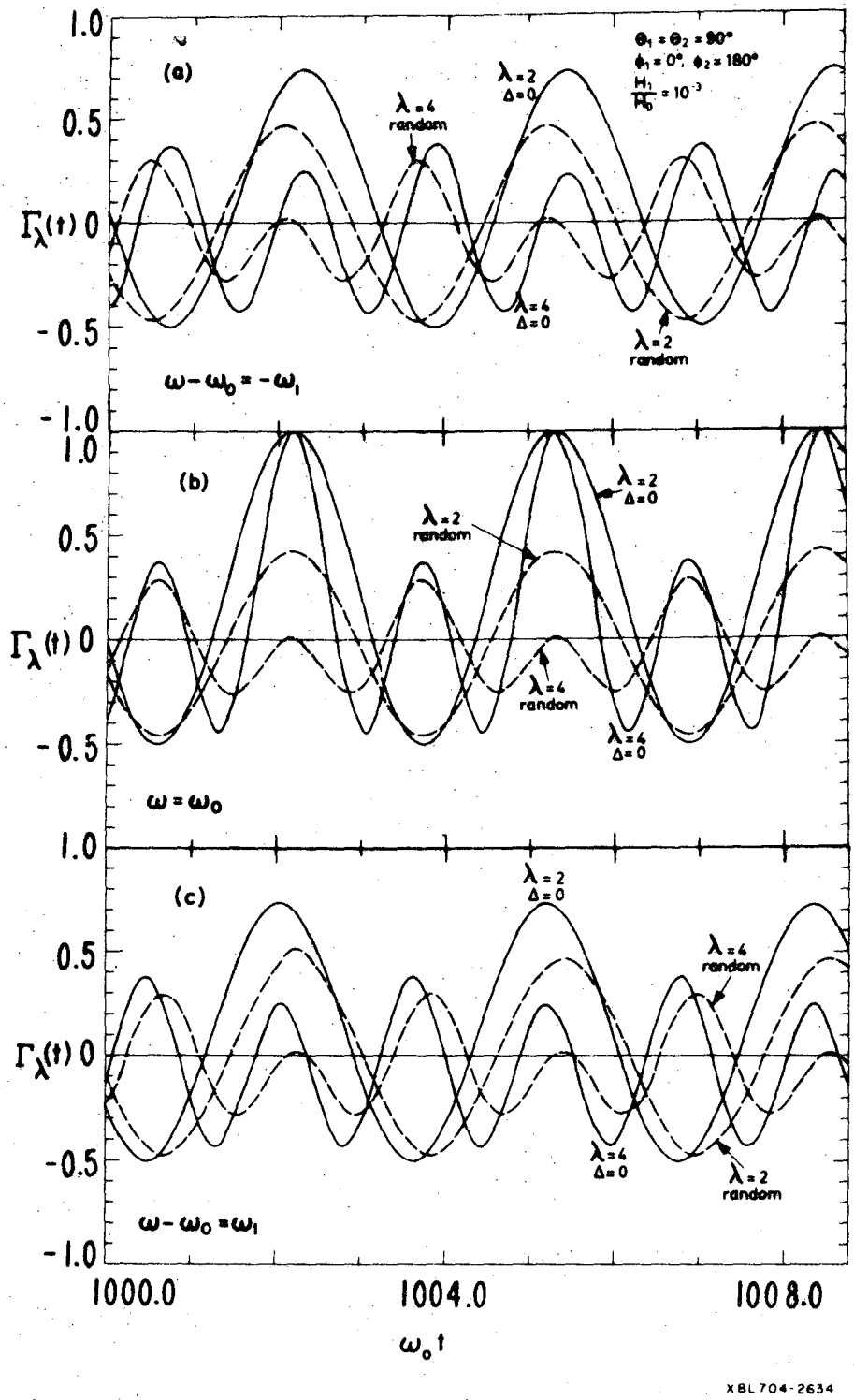
(a)
$\theta_1 = \theta_2 = 90°$
$\phi_1 = 0°$, $\phi_2 = 180°$
$\frac{H_1}{H_0} = 10^{-3}$
$\lambda = 2$ $\Delta = 0$
$\lambda = 4$ random
$\lambda = 4$ $\Delta = 0$
$\lambda = 2$ random
$\omega - \omega_0 = -\omega_1$
(b)
$\lambda = 2$ $\Delta = 0$
$\lambda = 2$ random
$\lambda = 4$ random
$\lambda = 4$ $\Delta = 0$
$\omega = \omega_0$
(c)
$\lambda = 2$ $\Delta = 0$
$\lambda = 4$ random
$\lambda = 4$ $\Delta = 0$
$\lambda = 2$ random
$\omega - \omega_0 = \omega_1$
$\Gamma_\lambda(t)$
1.0
0.5
0
-0.5
-1.0
1000.0
1004.0
1008.0
$\omega_0 t$
XBL704-2634

Fig. 7

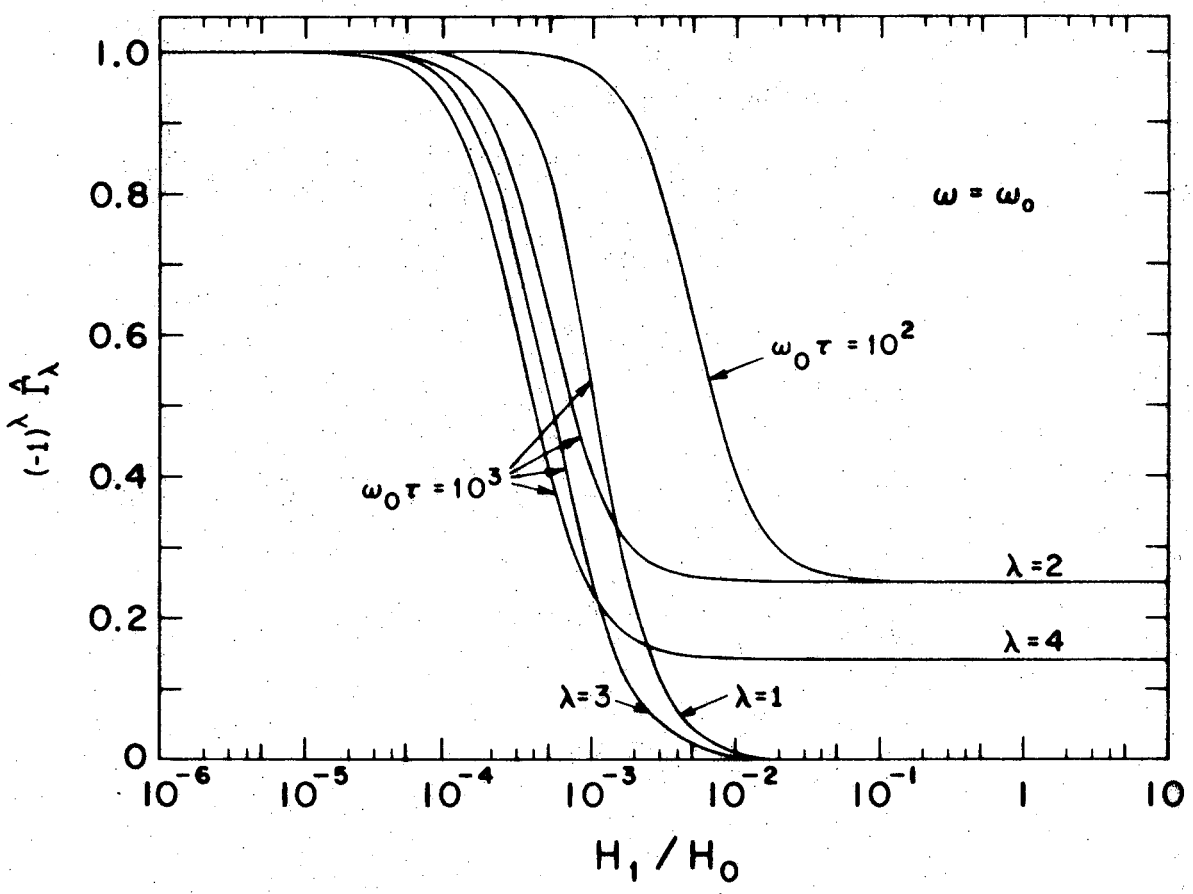
1.0
0.8
0.6
0.4
0.2
0
$(-1)^{\lambda} F_{\lambda}$
$\omega = \omega_0$
$\omega_0\tau = 10^2$
$\omega_0\tau = 10^3$
$\lambda=2$
$\lambda=4$
$\lambda=3$
$\lambda=1$
10^{-6}
10^{-5}
10^{-4}
10^{-3}
10^{-2}
10^{-1}
1
10
H_1 / H_0
XBL677-3499

Fig. 8

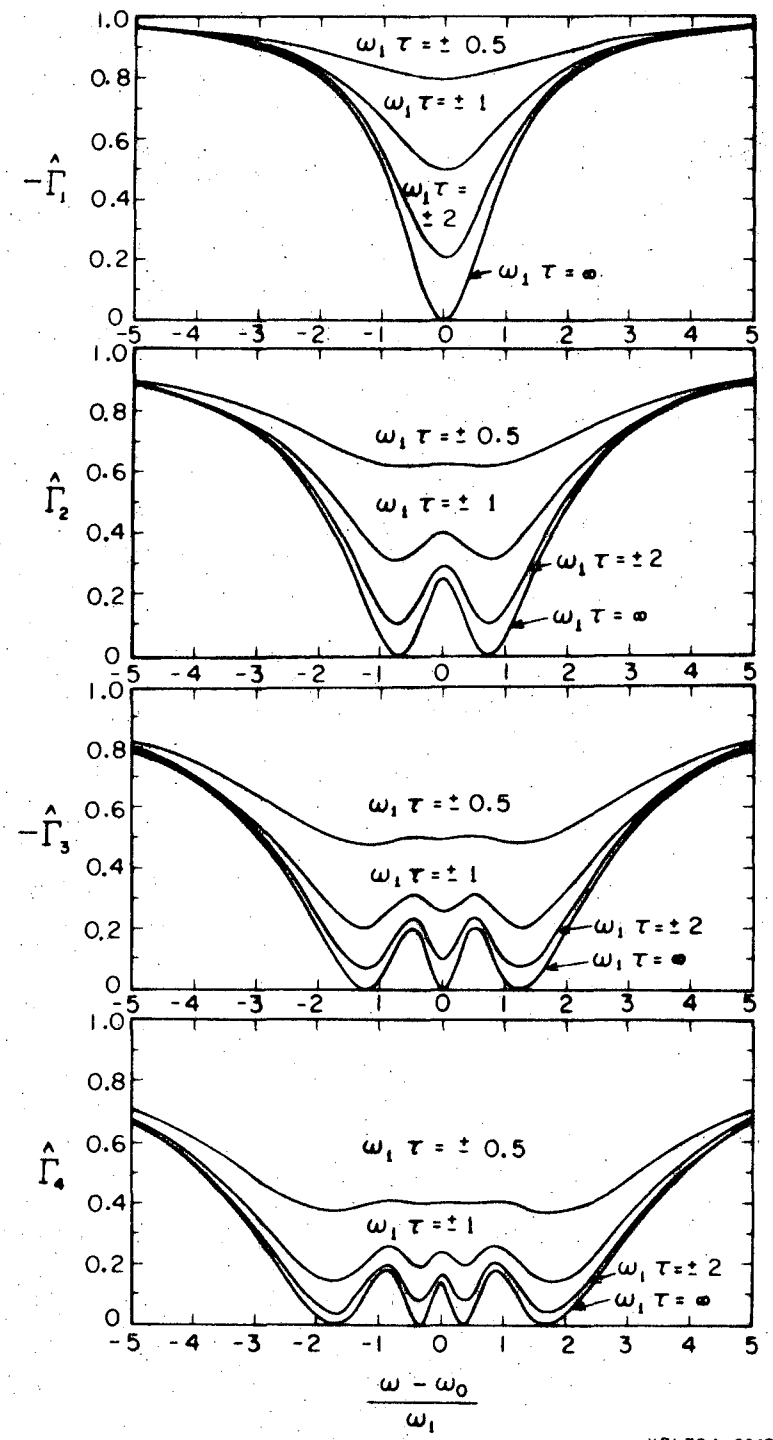
$-\hat{\Gamma}_1$
$\omega_1\tau = \pm 0.5$
$\omega_1\tau = \pm 1$
$\omega_1\tau = \pm 2$
$\omega_1\tau = \infty$
$\hat{\Gamma}_2$
$\omega_1\tau = \pm 0.5$
$\omega_1\tau = \pm 1$
$\omega_1\tau = \pm 2$
$\omega_1\tau = \infty$
$-\hat{\Gamma}_3$
$\omega_1\tau = \pm 0.5$
$\omega_1\tau = \pm 1$
$\omega_1\tau = \pm 2$
$\omega_1\tau = \infty$
$\hat{\Gamma}_4$
$\omega_1\tau = \pm 0.5$
$\omega_1\tau = \pm 1$
$\omega_1\tau = \pm 2$
$\omega_1\tau = \infty$
$\frac{\omega - \omega_0}{\omega_1}$
XBL704-2642

Fig. 9

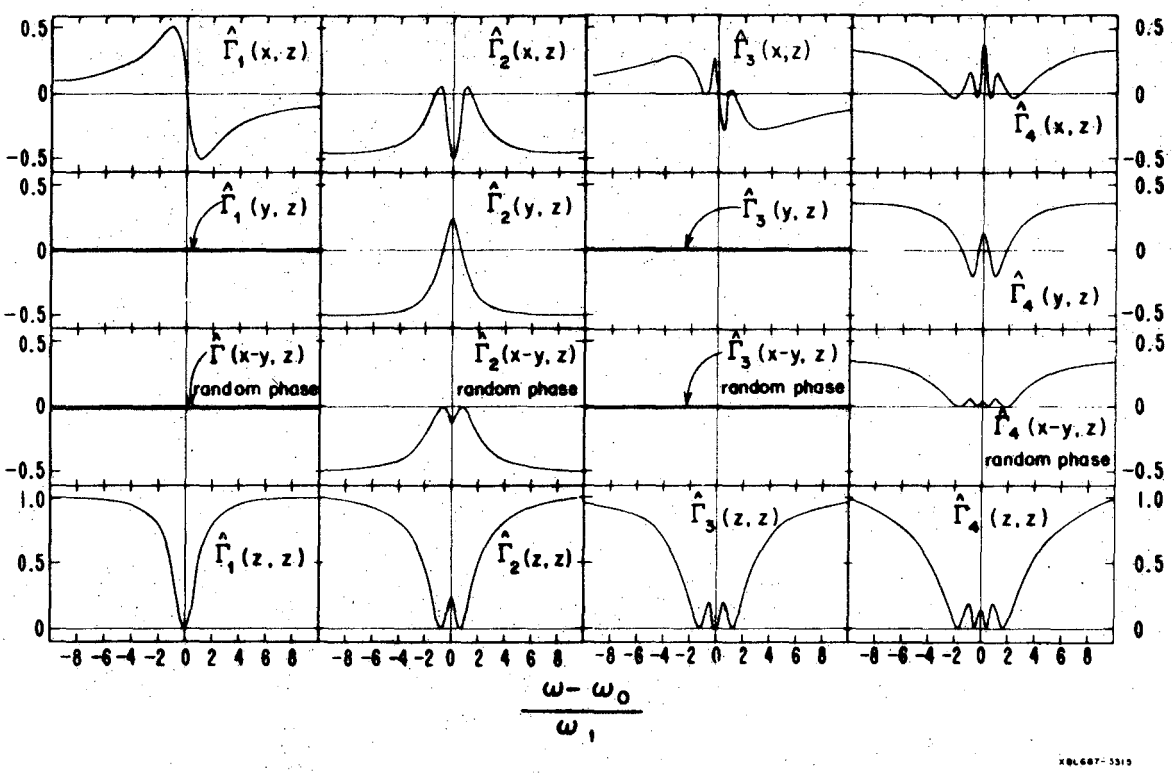
$\hat{\Gamma}_1(x,z)$
$\hat{\Gamma}_2(x,z)$
$\hat{\Gamma}_3(x,z)$
$\hat{\Gamma}_4(x,z)$
$\hat{\Gamma}_1(y,z)$
$\hat{\Gamma}_2(y,z)$
$\hat{\Gamma}_3(y,z)$
$\hat{\Gamma}_4(y,z)$
$\hat{\Gamma}(x-y,z)$ random phase
$\hat{\Gamma}_2(x-y,z)$ random phase
$\hat{\Gamma}_3(x-y,z)$ random phase
$\hat{\Gamma}_4(x-y,z)$ random phase
$\hat{\Gamma}_1(z,z)$
$\hat{\Gamma}_2(z,z)$
$\hat{\Gamma}_3(z,z)$
$\hat{\Gamma}_4(z,z)$
$\frac{\omega-\omega_0}{\omega_1}$

Fig. 10

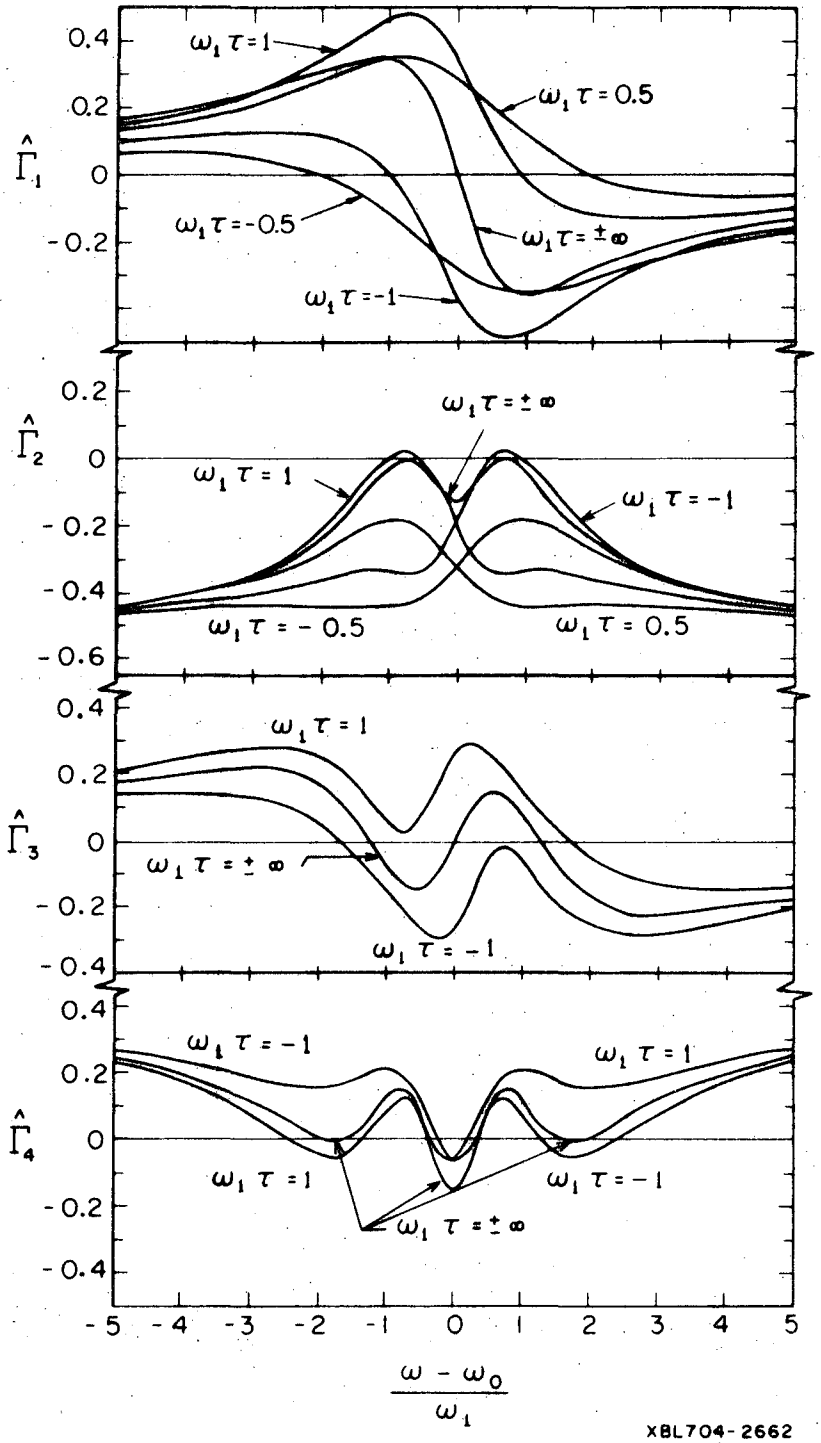
$\hat{\Gamma}_1$
$\omega_1\tau = 1$
$\omega_1\tau = 0.5$
$\omega_1\tau = -0.5$
$\omega_1\tau = \pm\infty$
$\omega_1\tau = -1$
$\hat{\Gamma}_2$
$\omega_1\tau = \pm\infty$
$\omega_1\tau = 1$
$\omega_1\tau = -1$
$\omega_1\tau = -0.5$
$\omega_1\tau = 0.5$
$\hat{\Gamma}_3$
$\omega_1\tau = 1$
$\omega_1\tau = \pm\infty$
$\omega_1\tau = -1$
$\hat{\Gamma}_4$
$\omega_1\tau = -1$
$\omega_1\tau = 1$
$\omega_1\tau = 1$
$\omega_1\tau = -1$
$\omega_1\tau = \pm\infty$
$\frac{\omega - \omega_0}{\omega_1}$
XBL704-2662

Fig. 11

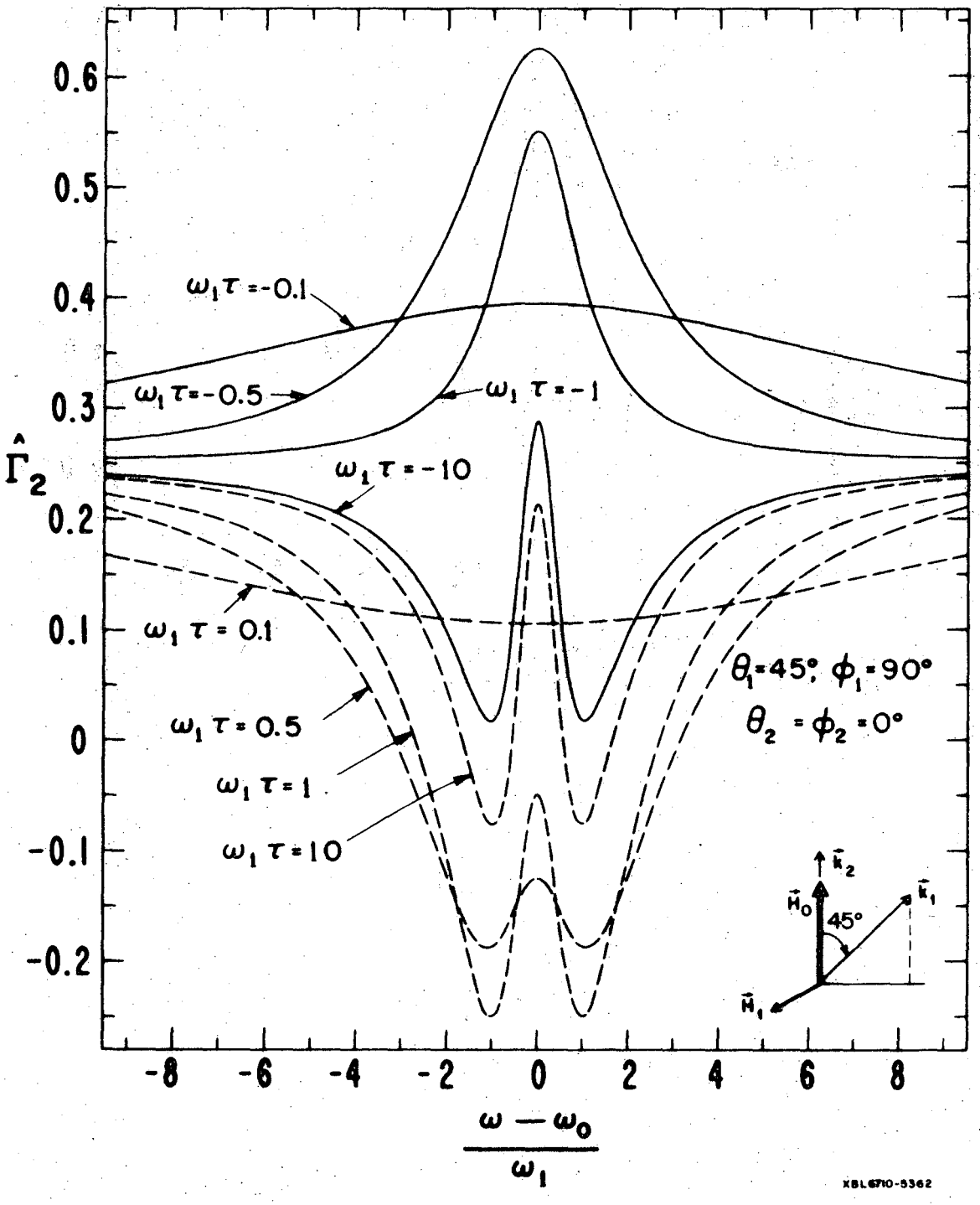
0.6
0.5
0.4
0.3
0.2
0.1
0
-0.1
-0.2
$\hat{\Gamma}_2$
$\omega_1\tau = -0.1$
$\omega_1\tau = -0.5$
$\omega_1\tau = -1$
$\omega_1\tau = -10$
$\omega_1\tau = 0.1$
$\omega_1\tau = 0.5$
$\omega_1\tau = 1$
$\omega_1\tau = 10$
$\theta_1 = 45°$, $\phi_1 = 90°$
$\theta_2 = \phi_2 = 0°$
$\vec{k}_2$
$\vec{H}_0$
45°
$\vec{k}_1$
$\vec{H}_1$
-8 -6 -4 -2 0 2 4 6 8
$\frac{\omega - \omega_0}{\omega_1}$
XBL6710-5362

Fig. 12

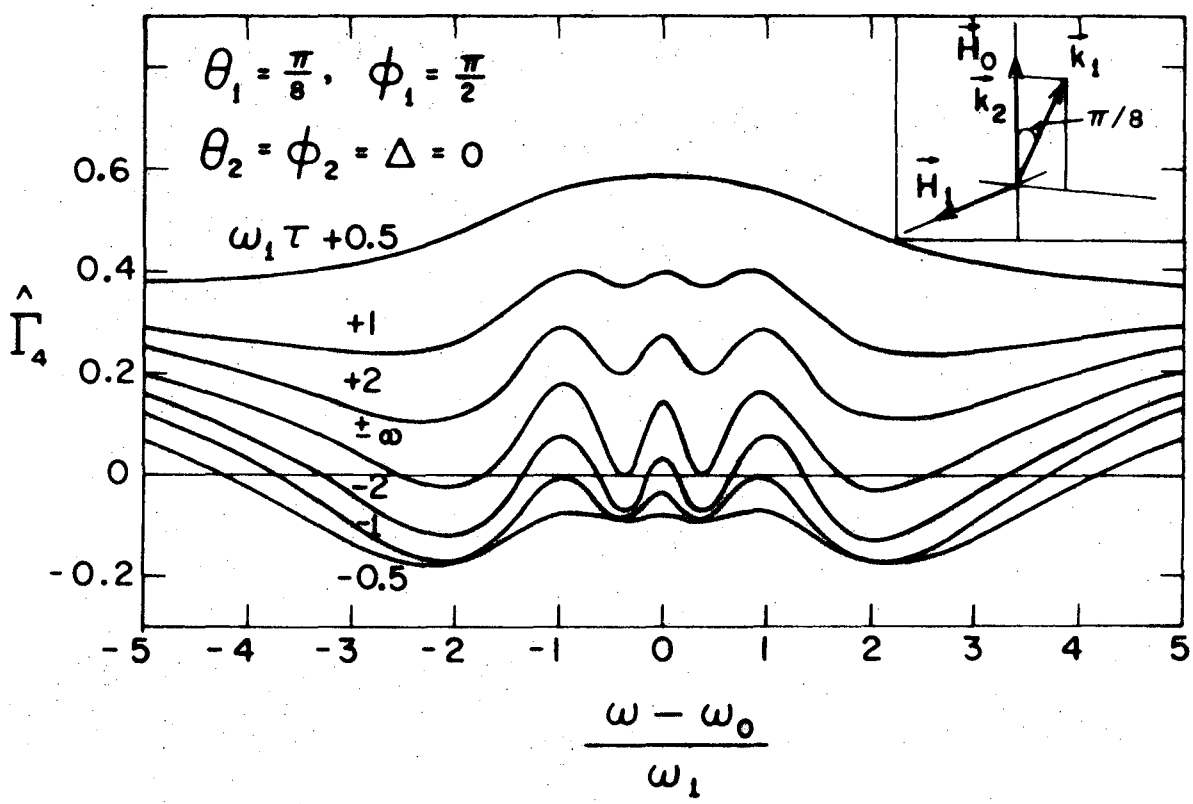

XBL704-2639

Fig. 13

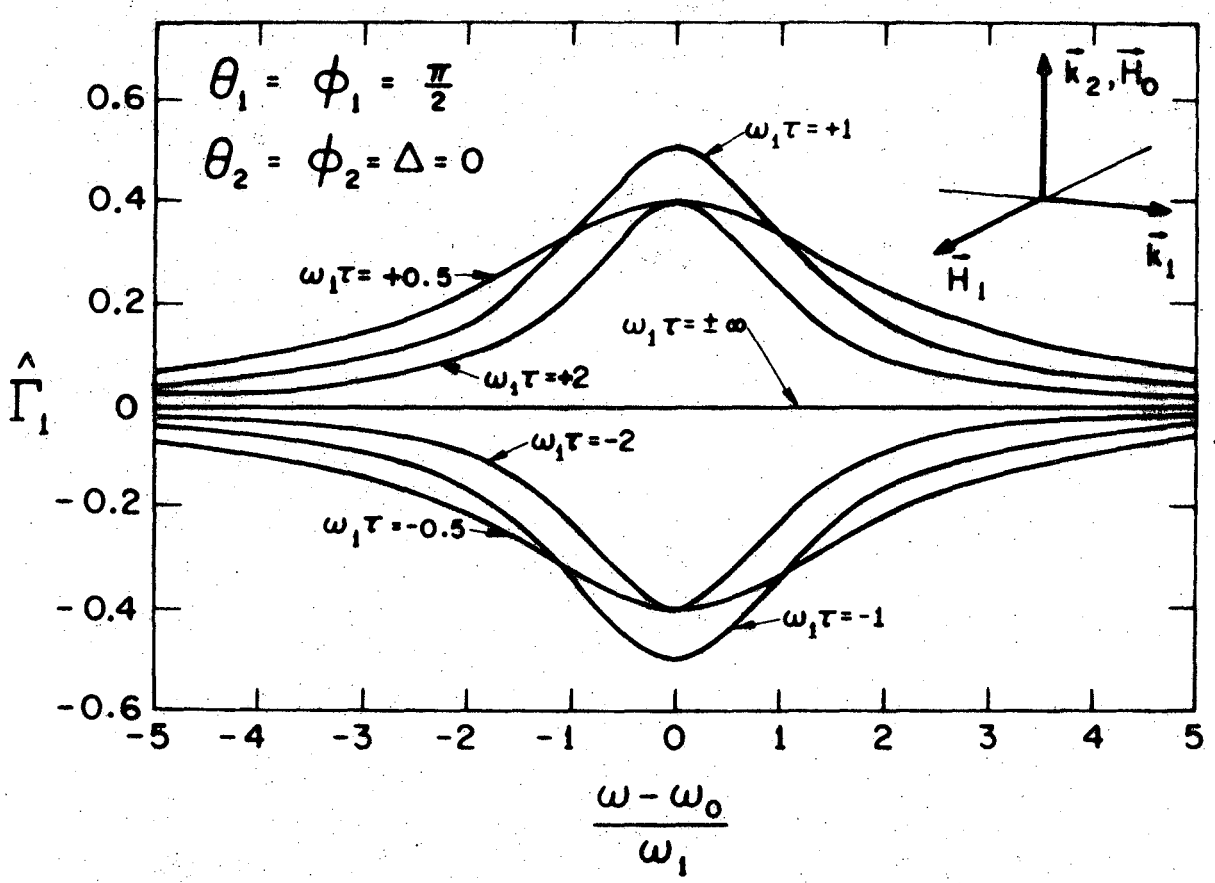

XBL 704-2640

Fig. 14

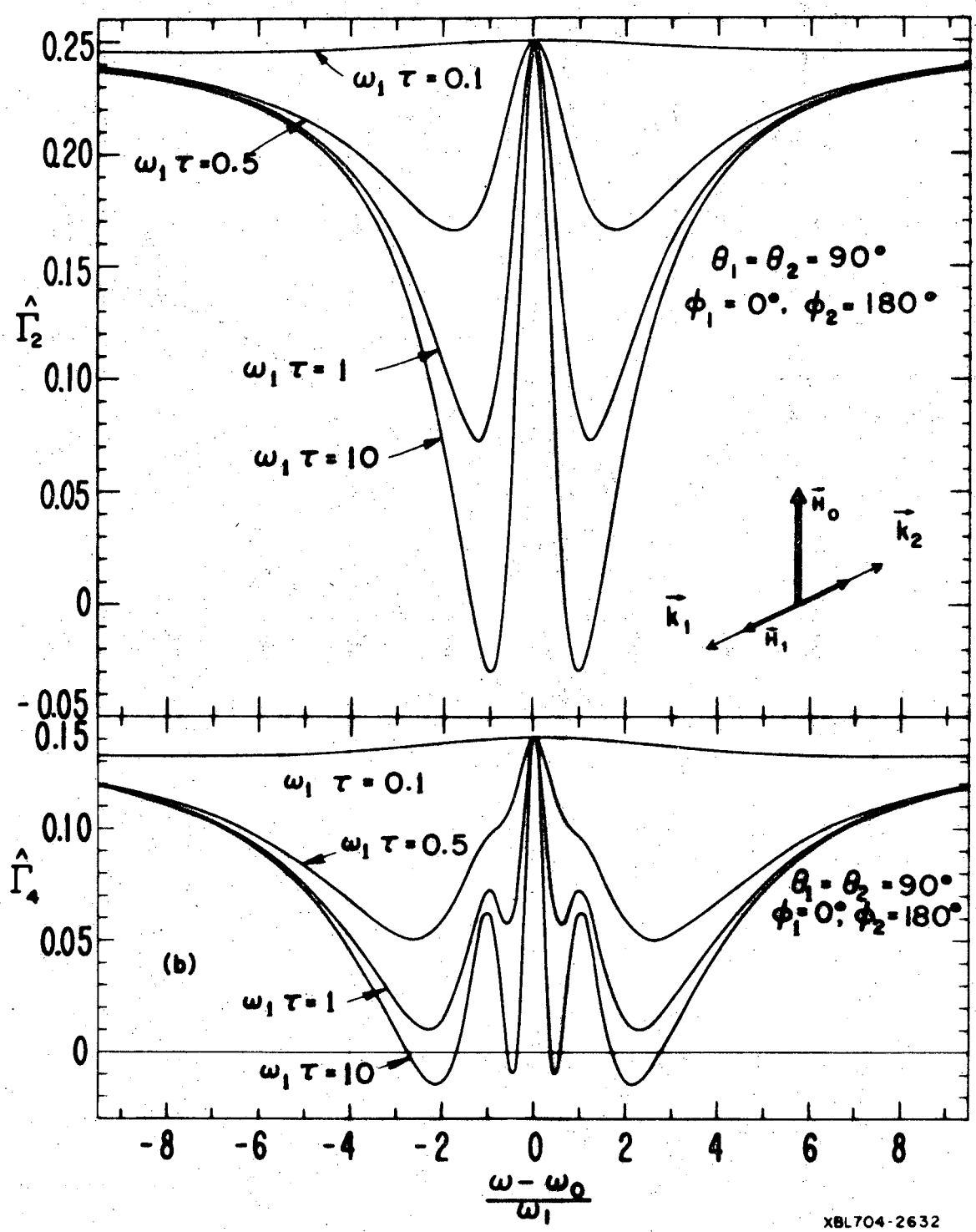
0.25
0.20
0.15
0.10
0.05
0
-0.05
$\hat{\Gamma}_2$
$\omega_1 \tau = 0.1$
$\omega_1 \tau = 0.5$
$\omega_1 \tau = 1$
$\omega_1 \tau = 10$
$\theta_1 = \theta_2 = 90°$
$\phi_1 = 0°, \phi_2 = 180°$
$\vec{H}_0$
$\vec{k}_2$
$\vec{k}_1$
$\vec{H}_1$
0.15
0.10
0.05
0
$\hat{\Gamma}_4$
$\omega_1 \tau = 0.1$
$\omega_1 \tau = 0.5$
$\omega_1 \tau = 1$
$\omega_1 \tau = 10$
$\theta_1 = \theta_2 = 90°$
$\phi_1 = 0°, \phi_2 = 180°$
(b)
-8
-6
-4
-2
0
2
4
6
8
$\frac{\omega - \omega_0}{\omega_1}$
XBL704-2632

Fig. 15

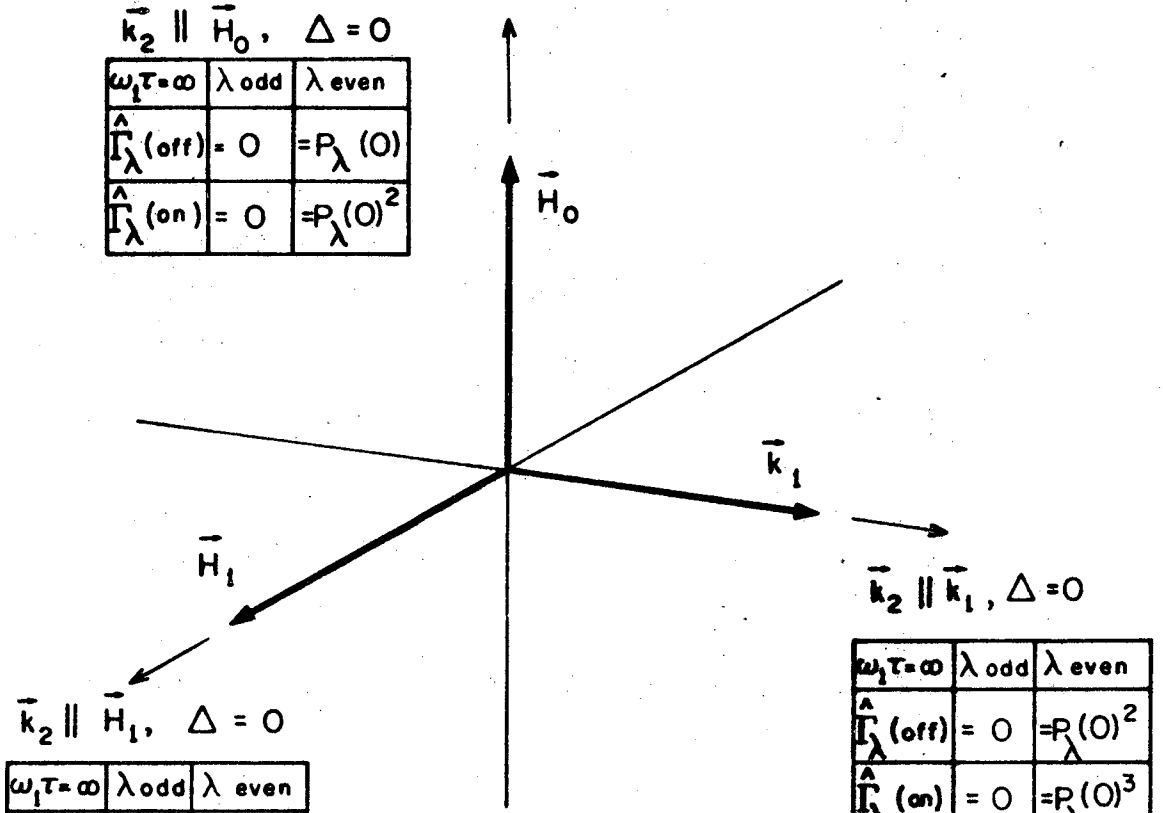

$\omega_1\tau = \infty$	λ odd	λ even
$\hat{\Gamma}_\lambda$ (off)	= 0	$= P_\lambda(0)$
$\hat{\Gamma}_\lambda$ (on)	= 0	$= P_\lambda(0)^2$

$\omega_1\tau = \infty$	λ odd	λ even
$\hat{\Gamma}_\lambda$ (off)	= 0	$= P_\lambda(0)^2$
$\hat{\Gamma}_\lambda$ (on)	= 0	$= P_\lambda(0)^3$

$\omega_1\tau = \infty$	λ odd	λ even
$\hat{\Gamma}_\lambda$ (off)	= 0	$= P_\lambda(0)^2$
$\hat{\Gamma}_\lambda$ (on)	= 0	$= P_\lambda(0)^3$

XBL 704 – 2636

Fig. 18

TECHNICAL INFORMATION DIVISION
LAWRENCE RADIATION LABORATORY
UNIVERSITY OF CALIFORNIA
BERKELEY, CALIFORNIA 94720